Modifying Tin Dioxide surfaces to Achieve Chemical Stability and Electronic Functionality

A thesis submitted in partial fulfilment of

the requirements for the degree of

Master of Science in Chemistry

Joel Schuurman

University of Canterbury

Christchurch

2018

Acknowledgements

I Would first and foremost like to thank Professor Alison Downard who without a doubt has made all this possible. Without out her help, encouragement, support, and constructive feedback I would have struggled to even get off the ground you have been nothing less than a mentor and inspiration to me over the last two years. Truly I am very grateful for to you for all you have done. Thank you also to Associate Professor Martin Allen for your help support and knowledge on this project along with your undeniable enthusiasm. A huge thank you to Alex McNeill aka the captain of team Schneill and warrior on the frontlines of metal oxide research. Thank you for the yarns, laughs and almost single handedly showing me how to postgrad. Thank you to Rodigo Gazoni and Jonty Scott for the sublime surfaces you produced for me to science with along with being a wealth of knowledge of all things physics. To the Chemistry Department and support staff, thank you for all the support during this project while also making the last two years as enjoyable as they whereby being the fantastic extended loving nerdy family that you were. To Helen Devereux and Gary Turner thank you for all the training and assistance with all things nano. Without your ongoing assistance I would never have learnt the kind of patience required for research that can only come from long hours sitting in front of the AFM.

Mum and Dad thank you for EVERYTHING you have done up to this point and will no doubt continue to do for the rest of my life. Thank you for having the foresight to plant the seed of curiosity and your patience, love and support which has no doubt grown that seed into the full fledge passion for science that I have now. Joe, Ben and the Poppets thank you for being the stable home I got to come back to every night to relax and unwind. Thank you for not just tolerating but understanding and accepting what no doubt has been a very tired, grumpy temperamental Joel at times. Thank you for being a quite joyful space that I could look forward to coming home to. Thank you also to my dear sweet Opa who is at the very start of all of this. Thank you for your love, support, prayers and encouragement. Truly I have appreciated all our discussions over the last two years (both scientific and religious) and the interest you have taken in my research giving me the opportunity to boar your ears off with my excitement for surface modification and transparent conductors. Because of you, and in addition to many other things, I now finally know what swatting is and have a 100+ page document to prove it. Thank you also to the rest of my friends and family for your support

and just being who you are to me I may never say it as much as I should but these relationships are the foundation on which I choose to do the things I do.

And finally thank you to the Downard Dream Team for being the Downard Dream Team. Never did I imagine working within such an amazing group of outstanding individuals that provided the right amount of feedback, support, encouragement and distraction. It has truly been a pleasure working with you all and the memories I've made in the group will never be forgotten. What is it that makes the Dream Team so awsome… its most defiantly the repport.

Table of Contents

Abbreviations

ACN	Acetonitrile
AFM	Atomic Force Microscopy
ATR	Attenuated Total Reflection
BE	Binding Energy
CA	Water Contact Angle
CF3BD	Trifluoromethyl Benzene Diazonium Tetrafluoroborate
CV	Cyclic Voltammetry
CVD	Chemical Vapour Deposition
DCM	Dichloromethane
DFT	Density Functional Theory
EtOH	Ethanol
F13OPA	Tridecafluorooctadecyl Phosphonic Acid
FWHM	Full Width Half Maximum
IPA	Isopropyl Alcohol
IR	Infrared Spectroscopy
ITO	Indium Tin Oxide
MBE	Molecular Beam Epitaxy
NBD	Nitrobenzene Diazonium Tetrafluoroborate
NP	Nitrophenyl
ODPA	Octadecyl Phosphonic Acid
PFBPA	Benzene Pentafluoro Phosphonic Acid
PPC	Persistent Photoconductivity
Ra	Average Roughness

RSF	Relative sensitivity factors
SAM	Self-assembled monolayer
SCE	Saturated Calomel Electrode
STM	Scanning Tunnelling Microscopy
THF	Tetrahydrofuran
XPS	X-ray Photoelectron Spectroscopy

Abstract

This research has investigated the surface modification and tunability of surface electrical properties of thin films of SnO_2. SnO_2 thin films were successfully modified with trifluoromethyl benzene diazonium tetrafluoroborate (CF3BD) and nitrobenzene diazonium tetrafluoroborate (NBD) modifiers via spontaneous self-assembly or electrochemical pathways and tridecafluorooctadecyl phosphonic acid (F13OPA), octadecylphosphonic acid (ODPA) and benzene pentafluoro phosphonic acid (PFBPA). The SnO_2 substrates were mist chemical vapour deposition (CVD) and molecular beam epitaxy (MBE) grown, and were either un-doped or doped with Sb. Surfaces were characterised using both a laboratory based and Australian Synchrotron X-ray photoelectron spectroscopy (XPS) along with water contact angles (CA) and atomic force microscopy (AFM).

Results from CA measurements revealed little change to surface wettability after modification but AFM measurements show an increase in the SnO_2 surface roughness after modification. Furthermore, AFM in contact mode was used to scratch away a section of the modifying layer at the SnO_2 surface allowing the layer thickness to be measured. The thickness was consistent with a multilayer for surfaces modified with aryl diazonium salts. XPS results revealed the presence of covalently bond aryl moieties and phosphonic acids at the SnO_2 surface confirming successful surface modification by both class of modifiers. XPS was also used to measure changes to the low energy band edge of SnO_2 surface after modification. From these spectra, changes in band bending were calculated. In most cases, no change or decrease in the downwards band bending for surfaces modified using aryl diazonium salts was observed and phosphonic acids gave an increase in downwards band bending. Further XPS analysis revealed that electrochemically initiated modification using CF3BD resulted in a higher surface concentration of modifiers than did spontaneous reaction. Additionally, the Sb dopant at SnO_2 surfaces increased the apparent surface concentration of phosphonic acid modifiers over that at the un-doped surfaces. Doping also appeared to influence the grafting pathway for aryldiazonium ions and decreased the presence of azo links at modified surfaces.

Chapter 1. Introduction

1.1. Metal Oxides

Material science has had a profound influence on the world with the discovery of new materials such as plastics and synthetic rubber which have given a flexibility and ease of engineering and new lightweight products. The scientific understanding of electron flow through materials has led to the development of products like transistors which brought an age of computers. The impact of these examples highlights the importance of the physical sciences, along with showing the need to better develop an understanding of the material world at a fundamental level.

Metal oxides are a broad group of materials that can be considered as having a positively charged metal core surrounded by negatively charged oxygens and in general the bonding is considered ionic. This definition however is oversimplified which is evident in the complications that arise when studying them.[1] Their unique properties along with a wide range of different compositions and structures has meant that they have been found to have uses in electronics, often as conductors, while their optical properties have placed them in dye sensitized solar cells and flat panel displays. Despite their thermodynamic stability,[2] the surfaces of most metal oxides are usually reactive and so they are also used as catalysts, catalyst supports and sensors.[3, 4, 5] The reactivity of the surface is considered that of Lewis acid base interactions and rely heavily on surface hydroxyl groups along with the coordination of elements at the surface.[6] Although there are wide variations between different metal oxides, in general they are divided into three groups: transition metal oxides, and pre- and post- non-transition metal oxides.

Each group has its own unique trends; this research is focused on tin dioxide a post non-transition metal oxide. A reason for the difficulty of studying metal oxides is that there is no one comprehensive theory that completely satisfactorily describes the structure and electronic properties. Two models are used at different times to limited effectiveness. The semi-empirical ionic model which places electrons in oxygen orbitals, has been found to be a reasonable first principle approach. The band theory model which is based around hybridization best describes the electrical properties of the material. Other computational methods such as ab initio and density functional theory (DFT) have been used to study interactions at the surface to a good effect.[7] One study by Oviedo et al.[8] used DFT

calculations to study the adsorption of O_2 on SnO_2 surfaces. Results showed that reduction of the SnO_2 surface would offer different binding environments to adsorbates and as such assist in the absorption of gas phase species.

The crystal structure of metal oxides, and in turn the surface structure, are very complex, depending on the coordination number of the ions along with the stoichiometry. Defects in the bulk material are exacerbated at the surface where other defects are also present such as step edges and point defects like oxygen vacancies.[9] These defects give rise to varying reactivity of the surface and limited reproducibility of material preparation and products, making the surface of metal oxides hard to characterise. Small changes in factors like surface wettability or presence of adventitious C have been shown to affect the surface chemistry of metal oxides. A study by Tsikritzis et al.[10] looked into the effects of surface pre-treatments of ITO, such as chemical cleaning and argon sputtering, before surface modification with nickel phthalocyanine. Results showed that without removal of adventitious C by surface pre-treatment, any dipole introduced at the surface as a result of surface modification was neutralised by the presence of adventitious C and thus expected shifts in ITO surface energetics were also neutralised. Adding to the difficulties, metal oxide surfaces have the tendency to reorganise to lower their coordination number and to lower the surface energy.[11]

The fickle nature of a metal oxide surface means a slight deviation in crystal formation and experimental preparation can cause a major change in nanoscopic properties. Batzill et al.[12] studied the morphology of SnO_2 surface before and after heating, using surface characterisation techniques such as Scanning Tunnelling Microscopy (STM), Ion Scattering Spectroscopy and Low Energy Electron Diffraction. Results revealed that the SnO_2 surface structure consisted of terraces with a large number of defects and periodic step edges. Surface defects were found to result from misalignment of SnO_2 with the supporting substrate during growth. These misalignments would stack with the thickness of the epitaxial growth causing exaggerated defects at the surface. As a result, areas of higher concentration of Sn were found throughout the SnO_2 substrate.

Experimentally there are a wide and varied range of techniques that are used to build up an understanding of metal oxides. Well characterised thin films are selected and controlled by use of the supporting substrate used to grow the film by methods such as molecular beam epitaxy (MBE) which is discussed later in section 1.2.2. Batzill et al.[13] were able to grow (101) SnO_2 by plasma assisted-MBE on r-plane sapphire. The growth method and use of the

supporting substrate meant that defects typically experienced during growth of SnO_2 thin films could be partially compensated for by antiphase domain boundaries introduced within the growth. Because of the fore mentioned complications, surface studies, were possible, are ideally conducted under ultra-high vacuum. Infra-red spectroscopic (IR) methods is on technique commonly used in a variety of forms along with microscopic methods like STM.[14, 15] Other methods are water contact angles for a measure of wettability and X-ray photoelectron spectroscopy (XPS) which uses X-rays to eject core orbital electrons at the surface of a material. Measuring the energy of the ejected electron gives information about the composition and chemical environments of that surface.[16]

Indium doped tin oxide (ITO) is one metal oxide that is in use globally as a transparent conductor. Its properties make ITO an ideal material for use in modern optoelectronic devices which require UV/visible transparency along with good conductivity. Thin films of ITO are applied to surfaces for applications such as flat panel displays or aeroplane windscreens to solve problems like ice formation or to provide interactive functionality to computing. Indium however is a limited resource thus requiring an alternative material that is stable and has the same properties as ITO and can be implemented into technology.

1.2. Tin Dioxide

To find an effective alternative for ITO the replacement material needs to match the optical transparency in the UV/visible region, and have similar electronic properties such as size of the band gap.[17] In terms of practicality the replacement material also needs to be suitable for manufacturing processes, and needs to remain stable under atmospheric conditions. For these reasons SnO_2 is a material of interest.[14, 18] Although it has been identified as a potential candidate to replace ITO, research conducted on SnO_2 in this area is limited. It has a high conductivity and optimal transparency and has already been identified for potential use as a gas sensor, catalyst and transparent conductor. Already several attempts have been made to turn SnO_2 materials into sensor devices with some success highlighting SnO_2 materials for use in future devices. The work by Matsubura et al.[19] and Hyodo et al.,[20] SnO_2 was modified with silanes specifically designed to target analytes of interest to increase the sensitivity of SnO_2 to gaseous CO, H_2 and CH_4 and invoke an electrical response. Additionally, Nardis et al.[21] used a mixed Co porphyrin SnO_2 sol-gel surface to detect the presence of methanol vapour.

The major problem that is identified with SnO_2 as a replacement for ITO is that it has a reactive surface. This surface is susceptible to changes under an oxygen environment. These changes have a great influence on the band bending which is crucial in maintaining consistent conductivity.[1] Present research on SnO_2 is for its use as a gas sensor or a catalyst where a measurable surface change is a desirable feature. This has meant that experimental studies are in relation to gas sensing and the issues of stability of specific stoichiometric surfaces of SnO_2 are not directly addressed. It was found that its stability as a gas sensor can be increased by incorporation of dopants such as fluorine or antimony or by having amorphous multilayers of ZnO and SnO_2.[22] An investigation into mixed metal oxide gas sensors by Vaezi et al.[22] grew a stacked alumina, ZnO and SnO_2 material (in that order). Analysis with Field Emission Scanning Electron Microscopy, X-ray Diffraction and Electron Dispersive Elemental analysis found that while the sensitivity of the device to analytes of interest was reduced, the stability of the device, measured by changes in material resistance over time, was better than that of isolated ZnO or SnO_2 materials.

Other studies have used computational methods to investigate the surface stability of SnO_2 to environmental conditions finding a sensitivity of the surface to oxygen partial pressures. Xu et al.[23] investigated the surface energies of SnO_2 (110), (101), (100), and (001) faces in response to O_2 partial pressure and temperature using DFT calculations. It was revealed that, while temperature dependant, the SnO_2 (110) face was the most stable to O_2 at a wide range of pressures while the SnO_2 (001) face was the least stable. Bulk and surface properties of SnO_2 are very different in that the surface of SnO_2 is heavily influenced by the Sn dual valence of either +II or +IV whereas the bulk Sn(IV) is considerably more stable. The SnO_2 crystal structure is seen in figure 1.1 with the shaded plane showing the (110) surface that grows naturally and has been well studied. However due to the dual valence of Sn, this surface along with other surfaces such as the (101) surface can be readily reduced making it very difficult to get a non-defective surface.[12]

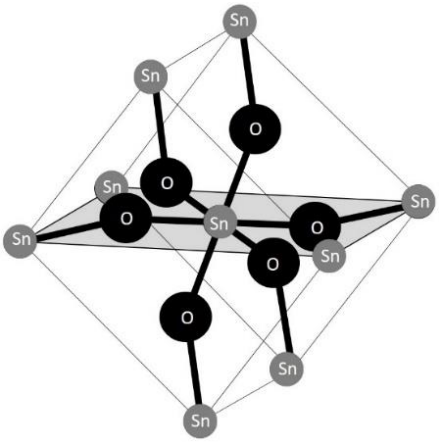

Figure 1.1. *Crystal structure of SnO_2 with the grey shaded plane the (110) surface which is the fastest growing face.*

One method for altering the electronic properties of SnO_2 is to alter the SnO_2 surface. For metal oxides this is usually done by exploiting hydroxyl groups naturally found on the surface by reacting them with other selected modifiers to form self-assembled monolayers (SAMs).[2] These SAMs may be useful for three purposes: the first is to prevent reorganisation of the surface to maintain the properties of interest, the second is to protect the surface from unwanted contaminants that may react with the surface and thirdly to alter the degree of band bending at the surface. To date modifications of SnO_2 have only been done on powders or have been investigated computationally. While Wada et al.[24] and Golovanov et al.[25] have investigated surface modification of SnO_2 surface with silane there are only a few reports on surface modification of SnO_2 with phosphonic acids which will be discussed in a later section.

Addition of molecular species anchored through surface atoms to SnO_2 is expected to have an effect on the band structure of the material at the surface, bending the bands towards or away from the Fermi level and altering the conductivity. For example, downwards bending of the valence band below the Fermi level will create an electron well at the surface giving the surface metallic properties. A measure of change in band bending can be obtained through XPS valence band spectra.[1, 5] Another consideration is that reactivity and bonding are expected to be different over the surface because of defects. These defects are readily formed both in the preparation of SnO_2 thin films and also develop over time. However, growth methods such as MBE help reduce these effects by producing highly ordered surfaces.

There are two main forms of tin oxides: stannous, SnO and stannic, SnO_2. Stannic oxide is the more abundant, thermodynamically stable and the most studied of the two oxides while

also having the larger band gap.[1] SnO_2 can be further classified as either stoichiometric or non-stoichiometric materials which have different properties. Stoichiometric SnO_2 is a good insulator while non-stoichiometric SnO_2, due to its oxygen vacancies, is a good conductor.[17] Although the bulk material will generally be either SnO or SnO_2, at the surface both oxidation states may be present due to redox processes that occur. Most notably as seen in figure 1.2 the SnO_2 (101) surface is able to be reduced whereby it loses its outermost row of surface oxygens greatly altering the surface topology.[26] Surface reduction of the SnO_2 (101) face is of particular interest with the MBE grown SnO_2 surface under investigation in this work also consisting of the (101) face. Electronically the difference between the Sn(II) and Sn(IV) states is the difference between having the Sn 5s orbital filled or unfilled and although this has a minor effect in the chemical shifts of Sn core levels by XPS, distinctions can be made between Sn(II) and Sn(IV) by either comparing their XPS valence band spectra or by measuring the energy separation between Sn4d 5/2 peak and the low energy edge of the valence band.[1] This adjustable oxygen surface means that the surface work function can be tuned by approximately 1 eV. It is also important point to note that its ability to change between oxidation states has a great influence on the stability, geometry and defective nature of the SnO_2 surface. It is difficult to reproducibly prepare surfaces and therefore to obtain high reproducibility of results for experiments based on the surface.[5]

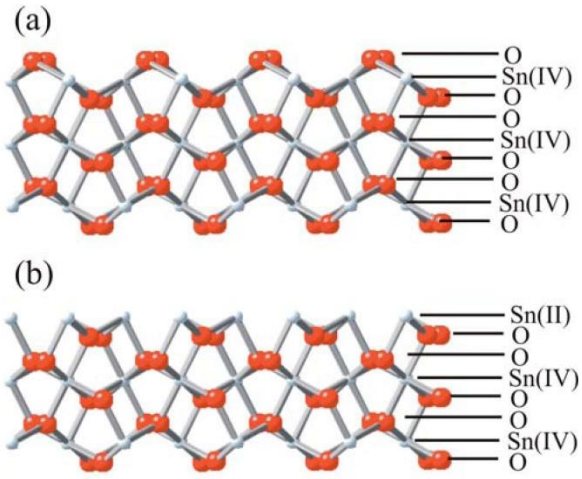

Figure 1.2. *A ball and stick model of the SnO_2 (101) surface highlighting the differences in reduced and oxidized surface. (a) is (101) with outermost surface oxygens present, (b) reduced surface with outermost surface oxygens removed. Figure taken from reference 26.*[26]

All these factors have a great effect on the oxide's reactivity giving rise to varied surface structures of differing degrees of reactivity along with altering the band structure (Figure 1.3)

and the conductivity. It is found that the excitation between states from the UV/visible region are disallowed which is what gives SnO_2 its optical transparency in this region along with a large fundamental band gap.[1] The derived states of the reduced surface also lie only just above the bulk valence band meaning that even with the reduced surface a large band gap is still maintained.

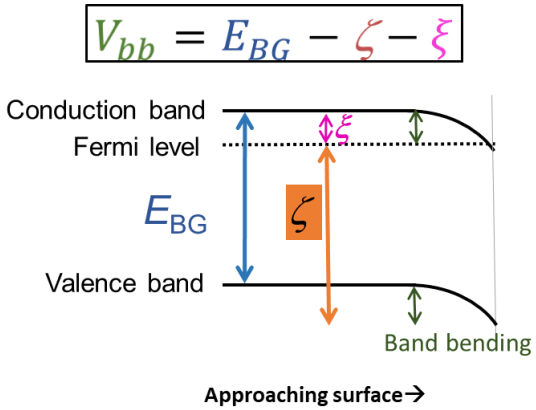

Figure 1.3. *Representation of band bending at a near surface region of a semi-conductor with conduction and valence bands bending below the Fermi level as the bands approach the surface due to crystal cleaving and surface hydroxylation. The valence band bending (V_{bb}) is determined by the band gap energy (E_{BG}) and the displacement of the bands from the Fermi level depicted by ζ and ξ.*

1.2.1. Chemical Vapour Deposition

Metal oxide chemical vapour deposition is a method for producing highly quality robust epitaxial thin films. These films are commonly grown within industry to efficiently produce surfaces with specific electrical properties for use in devices. Somewhat volatile precursor solutions are heated in a vacuum producing a mist that is then funnelled over a substrate and on decomposition or reactions of the precursor, elements are deposited onto the supporting substrate.[27] Although this technique is quick and reliable it produces surfaces that are amorphous and rougher than its MBE counterpart. For this reason, CVD-grown SnO_2 has limited use as a model system for studying interactions between SnO_2 and a surface modifier. This work investigates the modification of the amorphous SnO_2 thin film grown on r-plane sapphire by mist-CVD.

1.2.2. Molecular Beam Epitaxy

Molecular beam epitaxy produces the highest quality material giving a high degree of control for surface orientation and film thickness. However, the growth method is time consuming and expensive making the use of this method less practical for wide scale production of bulk materials. MBE films are grown under ultra-high vacuum and temperatures, whereby elements are heated into their gaseous phase and directed onto a supporting substrate. The slow nature of this growth method allows for atoms at the surface of the substrate to find a position that is an energetic minimum and at which the epitaxial surface can grow off.[27] This means that surfaces are very smooth with a specific crystal orientation that matches the underlying substrate. SnO_2 surface grown by MBE are highly robust and given their uniformity are ideal for use as a model surface for studying surface modifications. This work investigates the modification of the (101) face of SnO_2 thin films grown by MBE on r-plane sapphire.

1.3. Surface Chemistry

An investigation of the surface modification of materials is assisted by an understanding of the surface properties such as surface morphology and surface electronic properties. The aim of surface modification is to modify the surface in some way either to optimise already existing properties, to change surface properties or to add functionality for further chemical reactions. These modifications are often done with the addition of monolayers, by reacting surface functional groups with modifiers making a single molecular layer that covers the surface.[2] The general principles of surface modification lead to a great diversity and flexibility for chemists to work with and provide practical solutions to problems such as making a surface anti stick, hydrophobic or hydrophilic, as a base for biological growth or anti-corrosive.[28, 29, 30, 31] An example of this is by Chockalingam et al.[32] were an ITO surface was modified with organophosphates in a step wise fashion building up a film. The film was then terminated with a bio-recognition molecule used to adhere cells to the ITO surface. Investigation of the surfaces ability to hold cells in place found that the ITO modified surface performed just as well as similar devices made using an Au substrate.

Depending on the modifier, modifications can be carried out using different methods, such as solution reactions to less common vapour phase deposition. Different methods for surface

modification is shown by Tsud et al.[33] for the addition of benzyl phosphonic acids on Al surface using a vacuum vapour phase method, or by Maat et al.[34] for the addition of alkenes onto Si surfaces using a photochemical method. Modifiers can be selected for their surface reactivity where silanes, for example, give rapid covalent bond formation and crosslink with themselves at the surface while catechol for example can react with a wide variety of surfaces and have extremely strong bonding.[35, 36, 37, 38]

Surface modifiers are made up of several basic components that contribute to the overall properties of the SAM.[39] A reactive head group interacts with the surface and a tail group, which is usually involved in van der Waal's interactions, contributes to the packing of the SAM. In general, for metal oxides, the modifier is first physiosorbed to the surface before covalently reacting with one or several hydroxyl groups on the surface. Bulk properties of SAMs can be easily studied, for example, Nie et al.[40] used AFM to distinguish monolayers from multi layers for a Si surface modified with octadecyl phosphonic acid. However detailed analysis of the makeup of the SAM is more problematic. Brodard-Severac et al.[41] using Highfield O Magnetic Angle Spinning Nuclear Magnetic Resonance spectroscopy, investigated the binding of ^{17}O enriched phosphonic acids to titanium oxide surfaces. The authors found phosphonic acid reaction with the surface formed Ti-O-P bonds via various binding modes, evidenced by the presence of residual P=O and P-OH bonds. Figure 1.4 shows the range of bonding modes that have been proposed for phosphonic acids.

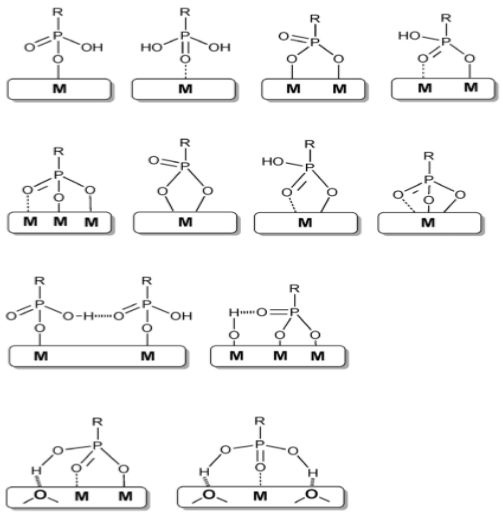

Figure 1.4. *Various binding modes of phosphonic acids at a metal oxide.*[41, 42, 43] *Figure taken from reference 2.*[2]

The nature of modifier-surface interactions relies on the alignment of the modifier head group to the surface hydroxyls along with along with the tendency for reactivity between the two often governed by Lewis acid base interactions. These interactions mean that reactions are very dependent on conditions such as pH, solvent and concentration. This was demonstrated by Chen et al.[44] who investigated the effect of different solvent on phosphonic acid SAM formation on ITO. SAMs were characterised using cyclic voltammetry, XPS and STM, which showed that SAMs were more dense and stable when formed in solvents with low di-electric constants that were inert to ITO. The stability of the monolayer and its longevity is reliant on its density and packing and also on the bonding to the surface for example, for phosphonic acids many modes may be possible (figure 1.4). Most modifications involve an annealing step were it is found that through tail-tail interactions monolayers will reorganise to form dense and organised packing arrangements to reduce the overall energy of the surface.

Phosphonic acids, carboxylic acids and silanes are an example of modifiers that will react with surface hydroxyl groups. Surface hydroxyl groups form naturally on some metal oxides on exposure to air, and can be generated or increased in concentration via wet or dry etching or plasma activation making the surface more susceptible to modification and generally increasing the coverage of the modifier. These modifications normally proceed via condensation reactions with the loss of water. A study conducted by Raman et al.[45] investigated the interactions between long chain organic acids and native metal oxides. Given the results of the investigation it was proposed that for carboxylic and phosphonic acids, the reaction normally starts via attraction between the surface hydroxyl group with the modifier double bonded oxygen group followed by reaction between the modifier hydroxyl group and the surface hydroxyl group. As water is lost during the reaction it has been noted that water has a great influence on how well organised a SAM will be. Water disrupts the packing of the modifier tails creating a more disordered less smooth SAM.[44] This may not be desirable and so vapour methods for SAM preparation may be favoured. The organisation of a SAM is also improved by having a longer tail attached to the head group. This gives stronger lateral van der Waal's interactions helping to order the SAM.[46]

1.4. Phosphonic Acids

Phosphonic acids are one modifier that is of interest for surface modification. Like its surface chemistry counterparts such as silanes and carboxylic acid modifiers, phosphonic acids

readily undergo condensation reactions with surface hydroxyl groups forming layers of laterally ordered modifiers. Chockalingam et al.[32] has shown that ITO surface in the presence of a mixture of phosphonic and carboxylic acids will react preferentially with the phosphonic acid. Phosphonic acids are proven to form particularly stable and well defined monolayers on ITO[47, 48, 49] and ZnO[50] and so are of particular interest for this work.[39] One study by Hotchkiss et al.[51] was able to tune the work function of ITO by 1.2 eV my modifying the surface with a fluorinated benzyl phosphonic acid. A wide variety of phosphonic acid modifiers are commercially available.

There are few reports of the modification of SnO_2 using phosphonic acid modifiers: Ferri et al.[52] attached mixed valence ruthenium complexes to a SnO_2 electrode by using either a phosphonic acid or carboxylic acid head group attached to a ligand. These complexes are known to be electrochromic where under different electrical potentials the complex will absorb different wavelengths of light. This has applications in switchable mirrors and windows and optical information storage. After addition of the ruthenium complexes the electrode was characterised by absorption spectroscopy and cyclic voltammetry where the voltage was cycled between -0.5 V and 0.5 V for 20,000 cycles changing the valency of the ruthenium complex and its absorptive characteristics. Surfaces modified with carboxylic acids were found to lose optical density after only 12,000 cycles while surfaces modified with phosphonic acids started losing optical density after 20,000 cycles showing the superior stability of the phosphonic acid linkage to SnO_2.

Additional studies by Gheonea et al.[53] and Holland et al.[54] have investigated phosphonic acid modification on nanoparticle of SnO_2 using a wide range of techniques including IR and NMR. Gheonea et al.[53] modified SnO_2 nanoparticles with a phenyl and vinyl phosphonic acid. Results from IR confirmed successful modification of SnO_2 with phosphonic acid detecting the presence of a Sn-O-P bond with a greater degree of modification being attributed to the phenyl phosphonic acid. Additionally, TGA was used to investigate the thermal stability of the modification finding that SnO_2 bound phosphonic acid was stable up to 200 °C. Holland et al.[54] investigated the modification of SnO_2 nanoparticle with a carboxyethane and phenyl phosphonic acid. Results found that nanoparticles modified with the carboxyethane phosphonic acid became water soluble while the phenyl phosphonic acid modified nanoparticles were not. Additional analysis of the modification with NMR also revealed the presence of Sn-O-P bound on phosphonic acid modified SnO_2 nanoparticles. This analysis also found a for bi or tridentate bonding for both phosphonic acids used.

1.5. Aryl Diazonium Salts

Aryldiazonium ions are another modifier of potential interest for metal oxides. An aryldiazonium ion can be reduced creating an aryl radical that is able to bond to a surface.[55]

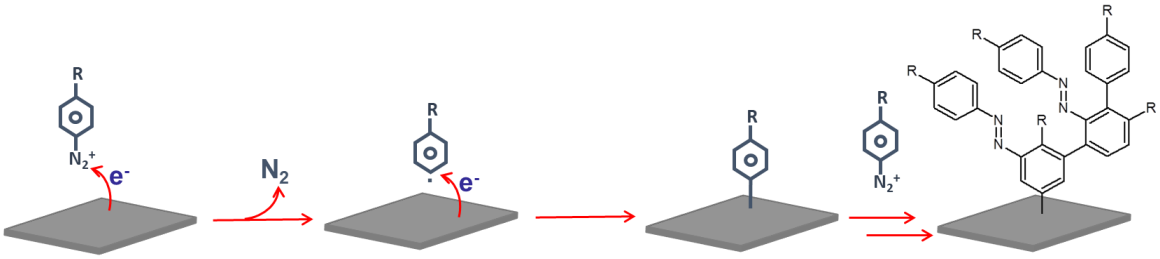

Figure 1.5. *Proposed mechanism for the formation of aryl diazonium multilayer via production of an aryl diazonium radical intermediate*

As seen in figure 1.5 the aryl diazonium is reduced producing an aryl radical which then forms bonds at a surface with the formation of multilayers either by attack of already formed aryl layers with radicle intermediates forming covalent C-C bonds between layers or by electrophilic substitution or aryl layers with the diazo groups forming azo linkages between layers. The radical nature of this mechanism allows for attachment to a wide range of surfaces opening additional avenues for SnO_2 surface modification. The choice of diazonium ion derivative used leads to layers with a range of functionality.[56] This modification method is known to give layers with strong bonds to a surface which is of interest in regards to longevity of surface modifications. Commonly, electrochemical methods are used to reduce the diazonium ion producing the radical. This places a dependency on conductivity however spontaneous methods of surface grafting have been demonstrated.[57, 58] Research by Mesnage et al.[59] and Maldonado et al.[60] have found that layers of aryl groups can be grafted to metal oxides such as TiO_2 and ITO however there is only one report on their use on SnO_2.[61] In that work SnO_2 surfaces grown by CVD, at different temperatures and vapour injection frequencies, were modified using carboxybenzene diazonium salt via an electrochemical pathway. Modified and unmodified SnO_2 films were characterised predominantly using XPS. Investigation of the C1s narrow scan revealed the presence of carboxy groups at the surface along with other C environments pertaining to the carboxyphenyl film however no evidence was found for direct attachment of the modifier to the SnO_2 surface via Sn indicating attachment was most likely via Sn-O-C bonds. While no detailed analysis of the feature seen O1s narrows scan was conducted, this feature was seen to shift to higher binding energies

(BE) after modification. While the electrical properties of the SnO_2 film were not investigated, results revealed that all CVD grown surfaces were successfully modified with the aryl diazonium ion with SnO_2 surfaces grown at lower temperatures showing a higher yield of surface moieties.

1.6. Characterisation

Characterisation of sub-5 nm layers on surfaces is challenging. General surface characteristics such as topography and surface wettability can be measured easily with techniques such as Atomic force microscopy (AFM) and water contact angle (CA) measurements however a more detailed analysis of a surface and the chemical interactions involved in the modifying layer are difficult due to the very small amount of material. For a surface modified with a thin film, interactions of interest such as bonding and packing occur predominantly over a 3 nm range. This small layer thickness coupled with the broad spectrum of interactions that may be occurring: physisorption, mono, bi and tri-dentate bonding (for example for phosphonic acids) hydrogen bonding etc make it difficult to obtain quantitative data against a background of atmospheric and bulk material effects. Transmission mode and attenuated total reflection (ATR) mode IR are other methods that allow for identification of functionality at the surface however these are limited by requiring a substrate that is non-absorbing in the region of interest for transmission mode, or a surface that is very smooth to make good contact with the ATR crystal making IR a difficult to implement technique for extremely thin surface layers.

Despite difficulties in characterisation as mentioned above, a combination of techniques is helpful to piece together a detailed picture of the surface. Beyond AFM topographical imaging and CA measurements, AFM can be used in contact mode to scratch away the modifying layer, at the surface allowing for post scratch imaging showing the depth of the modification layer at the surface. Primarily however XPS is the characterisation technique of choice for surface chemistry whereby X-rays are used to eject electrons from a material. These electrons and their kinetic energy are then picked up on a detector. Given the quantized state of electrons, specific electrons of specific elements will always be found at the same energy. This technique is good at probing mainly the surface of a material, (typical penetration depth for laboratory based XPS is approximately 10 nm) identifying the

material's elemental composition and detecting changes to the environment of atoms making XPS a very important technique for surface characterisation.

1.7. Aims

The overarching focus of this work is to develop a replacement material for ITO for use in opto-electrical devices. This thesis begins work towards this goal by exploring the potential use of SnO_2 for this application. As a starting point, it is necessary to establish a controllable method for surface modification of SnO_2 so that its properties can be optimised for device application. Therefore, the aims of this thesis were:

- Aim One
  To controllably modify the SnO_2 surface by attaching a thin layer of chemical modifiers

- Aim Two
  To tune the electrical properties by controllably changing the band bending at the surface

Chapter 2. Experimental Methods

2.1. Chemicals

Acetone (HPLC grade, RCl Labscan), methanol (HPLC grade, Loda Chemie), isopropanol (IPA; HPLC grade, Sigma Aldrich), acetonitrile (ACN; HPLC grade, Sigma Aldrich, ≥ 99%), diethyl ether (Sigma Aldrich, Reagent grade), tetrahydrofuran (THF; HPLC grade, Sigma Aldrich), octadecylphosphonic acid (Sigma Aldrich, 97%), 3,3,4,4,5,5,6,6,7,7,8,8,9,9,9-tridecafluorooctadecylphosphonic acid (Sigma Aldrich, ≥ 95%), 2,3,4,5,6-pentafluoro-benzylphosphonic acid (Sigma Aldrich, 97%), 4-(trifluoromethyl)aniline (Sigma Aldrich, 99%), p-nitroaniline (B.D.H Laboratory Chemical Divisions, Reagent), tetrafluoroboric acid solution (Sigma Aldrich, 48% wt in water), tetrabutylammonium hydroxide solution (Sigma Aldrich, 40% wt in water), dichloromethane (DCM; HPLC grade, Fisher Scientific), potassium chloride (reagent grade, Sigma Aldrich) and potassium ferricyanide (analytical grade, Analar, 99%) were used as supplied. Milli-Q water (resistivity > 18 MΩ cm) was used for all aqueous solutions and washing All other reagents were standard laboratory grade.

2.1.1. Synthesis of Nitrobenzene Diazonium Tetrafluoroborate (NBD) and Trifluoromethylbenzene Diazonium Tetrafluoroborate (CF3BD)

Aryldiazonium salts were synthesised using a literature method.[62] Briefly, the amine derivative (5 mmol) was dissolved in 4 mL of 25% HBF_4, the mixture was cooled in an acetone-salt-ice bath and sodium nitrite ($NaNO_2$, 5 mmol), dissolved in small amount of water, was added dropwise to the cold mixture with stirring. The precipitate formed was filtered under suction. The crude product was then purified by dissolving in a minimum amount of ACN and cooling the solution in an ice bath with gradual addition of diethyl ether to re-precipitate the product. The product was filtered and washed with cold water and diethyl ether. The purified product was dried under vacuum and stored in the freezer in the dark

2.1.2. Preparation of Tetrabutylammonium Tetrafluoroborate

Tetrabutylammonium tetrafluoroborate ($[Bu_4N]BF_4$) electrolyte was prepared from tetrabutylammonium hydroxide ($[Bu_4N]OH$, 40%) and tetrafluoroboric acid (HBF_4, 48%).

HBF_4 (5mL) was diluted to 25 mL with water and added, with stirring, to diluted TBAOH (20 mL diluted to 100 mL with water). The white precipitate was washed with water and filtered under vacuum. The $[Bu_4N]BF_4$ electrolyte was dried for 3 days in an oven at 60 °C and then for 2 days under vacuum at 80 °C. The electrolyte was stored in a desiccator.

2.2. Substrates

2.2.1. Indium Tin Oxide

Indium tin oxide coated glass (ITO; 25×25 mm^2 8-12 Ω,) was purchased from SPI Supplies and was diced into 12.5×12.5 mm^2 sections by local technicians as required.

2.2.2. Tin Dioxide

2.2.2.1. Chemical Vapour Deposition

Epitaxial SnO_2 thin films were produced locally on r-plane sapphire by mist chemical vapour deposition producing a polycrystalline SnO_2 surface. Films were grown by Jonty Scott at the University of Canterbury in the Department of Physics and Astronomy.

2.2.2.2. Molecular Beam Epitaxy

Epitaxial SnO_2 thin films were produced locally on r-plane sapphire by molecular beam epitaxy producing highly ordered (101) SnO_2 surfaces. Films were grown by Rodrigo Gazoni at the University of Canterbury in the Department of Physics and Astronomy.

2.2.3. Glassy Carbon (GC)

GC disk electrodes were fabricated in the Mechanical Workshop of the Department of Chemistry at the University of Canterbury. GC plugs were cut into 5 mm lengths from a cylindrical GC rod with a 3 mm diameter. The plug was then connected to a brass rod and encased in Teflon leaving exposed at one end the face of the GC plug while having the brass

rod protruding from the Teflon at the other end to be used as the electrical contact for the electrode. The Teflon ensures only the face of the GC disk is in contact with the solution. GC electrodes were cleaned by hand polishing with a slurry of 1 µm alumina powder (Leco Corporation) on a piece of lecloth (Leco Corporation) until there were no visible markings or scratches. After polishing, the electrodes were sonicated in Milli-Q water for 5 min to ensure elimination of the alumina from the surface. This procedure was repeated after each set of experiments

2.3. Modification Methods

All metal oxide surfaces to be modified were cleaned using the same procedure independent of the type of modification that was going to be undertaken, first by soaking in each of HPLC grade acetone with gentle wiping with a cotton bud followed by 10 min sonication in HPLC grade DCM, methanol and IPA with a rinse in Milli-Q water between methanol and IPA and after IPA. Cleaned surfaces were blown dry under nitrogen.

2.3.1. Surface Modification with Aryl Diazonium Salts (Spontaneous Grafting)

Cleaned SnO_2 samples were modified spontaneously with recrystalized trifluoromethyl benzene diazonium tetraflouroborate (CF3BD) by placing in a 50 mM solution of the diazonium salt in Milli-Q water and covering with aluminium foil for 8 h. After 8 h the samples were removed from solution and sonicated for 4 min in Milli-Q water and then blow dried under nitrogen before being stored under vacuum.

2.3.2. Surface Modification with Aryl Diazonium Salts (Electrochemical Grafting)

Electrochemical modification of SnO_2 surfaces with CF3BD used a solution of 0.1 M $[Bu_4N]BF_4$ and 10 mM recrystallized diazonium salt in ACN. The sample to be grafted was set up by first taping a small piece of copper wire to a gold contact sputtered onto the edge of the surface followed by placing an inner and outer O-ring on the surface with the

electrochemical cell (with a hole in the base) placed on top. The cell was held in place by springs attached to a stand. The cell was filled with the modification solution (≈ 10 ml) to approximately 1/3 full. The solution was degassed by flushing with nitrogen for 10 min followed by addition of the Saturated Calomel Electrode (SCE) reference and Pt wire counter electrodes. Electrografting was carried out using a Eco Chemie Autolab PGSTAT302 or PGSTAT302N potentiostat/galvanostat running Autolab NOVA version 1.9-1.11. Two cyclic scans were performed between 0.6 and -0.3 V (initial potential was 0.6 v) at a scan rate of 0.2 V/s.

After grafting, the sample was sonicated for 4 min in the supporting electrolyte solution free of the diazonium ion, blow dried with nitrogen and stored under vacuum.

2.3.3. Surface Modification with Phosphonic Acids

For the optimised standard procedure, cleaned ITO and SnO_2 samples were modified with phosphonic acids by soaking for 6 h in a Teflon beaker containing a 5 mM solution of the phosphonic acid in HPLC grade THF. Samples were rinsed in fresh THF and left to anneal on a hot plate at 150 °C for 24 h under a nitrogen stream. After annealing, modified samples were sonicated in fresh THF for 4 min, blow dried with nitrogen and stored under vacuum to await characterisation.

2.4. Experimental Methods

2.4.1. Water Contact Angles (CA)

Changes in surface wettability were measured using water contact angles. Samples were placed horizontally on a stage and 1 – 2 µL droplets of Milli-Q water were placed on the surface. At least 3 photographs of the surface and droplet were taken using an Edmund Scientific camera with a macrolens. Images were processed using ImageJ V1.48 software (NIH, Bethesda, MD) with a drop analysis plug in.

2.4.2. Cyclic Voltammograms (CV)

A solution of 1 mM $K_3[Fe(CN)_6]$ was made up in 0.1 M KCl in Milli-Q water and added to an electrochemical cell (setup as described in 2.3.3) and degassed by passing nitrogen through the solution for 10 min. Cyclic voltammetry was carried out using an Eco Chemie Autolab PGSTAT302 or PGSTAT302N potentiostat/galvanostat running Autolab NOVA version 1.9-1.11. A single cyclic scan was run between 0.0 and 0.4 V at a scan rate of 0.1 V/s.

2.4.3. Atomic Force Microscopy (AFM)

A Dimension 3100 AFM with Nanoscope IIIa controller (Digital Instruments, Veeco, Plainview, NY) was used for all AFM studies. For surface topographical measurements images were collected in tapping mode using silicon cantilevers (Tap300AlG, Budget Sensors, Bulgaria) with resonant frequencies between 200-400 kHz. Scan parameters including scan rate and feedback control settings were optimised for each image.

To measure film thickness, AFM in contact mode using a carbon cantilevers ((Tap300DLC, Budget Sensors, Bulgaria) with an applied voltage of 0.3 V was used followed by a topographical scan of the same area with

Image analysis was conducted using Nanoscope Analysis software (Bruker) 2010, version 1.2. The data reported, where possible, was the average of three or more measurements made over multiple samples or multiple locations on the one sample with errors corresponding to the standard deviation of those averages.

2.4.4. X-ray Photoelectron Spectroscopy (XPS)

2.4.4.1. Laboratory Based XPS

XPS spectra were recorded by Dr Colin Doyle, Department of Chemical and Materials Engineering, The University of Auckland. XPS data were obtained using a Kratos Axis Ultra DLD spectrometer with a monochromatic Al Kα source (1486.7 eV).

2.4.4.2. Synchrotron XPS

Surface sensitive variable photon energy (1486 – 150 eV) XPS was performed on CVD and MBE grown SnO_2 samples at the soft X-ray beamline of the Australian Synchrotron. Data were obtained by Martin Allen, Roger Reeves, Rodrigo Gazoni, Alexandra McNeill and Jonty Scott of the University of Canterbury. XPS measurements were carried out at room temperature at a base pressure of 2×10^{-10} mbar and without the use of an electron flood gun. Photoemission spectra were collected using a Specs Phoibos 150 hemispherical electron energy analyser with the detector axis arranged in the direction normal to the sample surface. To insure a consistent sampling depth (≈ 10 nm) for XPS narrow scans a photon energy of 150 eV above that of the expected elemental emission was used.

2.4.4.2.1. Analysis of XPS Spectra

All XPS data analysis was carried out in CasaXPS Ltd software 1999 – 2017 version 2.3.18. Quantitative elemental analysis of samples was carried out on XPS survey scans obtained using the laboratory XPS instrument by applying relative sensitivity factors. Narrow scans were analysed manually by fitting either a linear, Tougaard or Shirley background and fitting peaks with the minimum number of components. Additional peaks were added to improve the fit with adjustment of fit parameters such as Gaussian:Lorentzian ratios and full width half maxima. All peak fits were constrained to have a full width half maximum to be less than 2 with O1s bulk oxygen fits being constrained to the same values as found in an unmodified reference sample. The Sb3d 5/2 peaks were constrained to be identical to the Sb3d 3/2 peak seen in the same scan.

All spectra were normalised for comparison of scans obtained from different samples. F1s, N1s, C1s and P2p narrow scans were all normalised to the Sn3d 5/2 of that sample obtained in the survey scan (diazonium modified surfaces) or the Sn3d narrow scan (phosphonic acid modified surfaces). O1s narrow scans were normalised to the peak assigned to surface O (diazonium modified surfaces) or the peak assigned to bulk O (phosphonic acid modified surfaces) of the O1s narrow scan of that sample.

For results obtained from the Australian Synchrotron, no direct comparison of peak areas can be made between elements obtained from different scans because the relative sensitivity factor (RSF) of each element is unknown. Comparisons can be made between the amount of

an element present in different samples after the peaks of each sample have been normalised as described above.

Chapter 3. Aryl Diazonium Salts Surface Modification

3.1. Introduction

Aryl diazoniums salts were investigated as modifiers for SnO_2 with the 4-trifluoromethyl benzene diazonium tetrafluoroborate (CF3BD) and the 4-nitrobenzene diazonium tetrafluoroborate (NBD) of particular interest. As described in chapter 1, aryl diazonium ions are widely used for surface modification and have the key advantage of giving strongly bound, stable layers on a range of materials including metal oxides.[63, 64, 65]

For the present work with the goal of tuning the electrical properties of the surface, the conjugated structure of the benzene ring should assist in donating or withdrawing electron density from the surface.[66, 67] For CF3BD and NBD with electron withdrawing CF_3 and NO_2 groups respectively, grafting of aryl groups was expected to decrease the downwards band bending. Very recently, Mc Neill et al.[68] showed that ZnO surfaces experienced upwards band bending after electrochemical grafting of NBD and CF3BD diazonium salts. Both modifiers are also convenient to characterise because F and N on the modifier act as markers for identification by XPS confirming successful surface modification.

The grafting from diazonium ions can be either driven electrochemically, if the surface is conducting enough, or the reduction reaction can occur spontaneously by placing a surface in a solution of the modifier and leaving for an extended amount of time. The latter approach relies on the substrate having sufficient reducing power to reduce the diazonium ion. Although the precise pathway by which the grafting occurs at hydroxylated surfaces is unknown, figure 3.1 shows a proposed mechanism whereby two aryl diazoniums ions are reduced followed by abstraction of a surface hydrogen by one aryl radical followed by attack at the same site by a second aryl radical.[69]

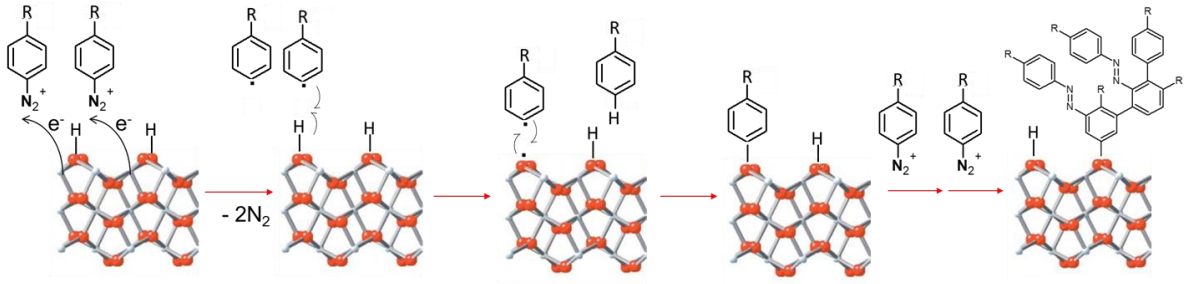

Figure 3.1. *Possible mechanism for the grafting of metal oxides with aryl diazonium salts based on the mechanism proposed at Si surfaces.[69] In this work R=CF_3 or NO_2 for CF3BD and NBD diazonium salts respectively.*

As mentioned in chapter 1 there is only one report of the use of aryl diazoniums ions to modify un-doped SnO_2 films.[61] This thesis work expands the range of diazoniums used for this purpose and focuses on detailed analysis of the resulting surface structures. Both spontaneous and electrochemically-driven grafting are examined at two types of substrates: moderately- and highly-doped (with Sb) SnO_2 grown by MBE.

3.2. Method Development at Glassy Carbon

Electrochemical grafting of NBD to a GC disk was briefly examined to establish the correct potential range for the reduction of NBD. GC was used for these experiments because GC electrodes can be reused (after cleaning), whereas SnO_2 samples are single-use because it is not possible to reproducibly regenerate identical clean surfaces.

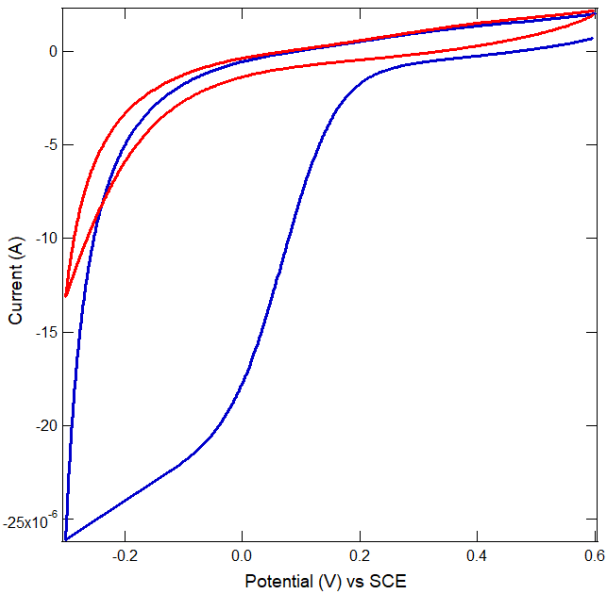

Figure 3.2. *Two repeat CVs of 10 mM NBD in 0.1 M [Bu$_4$N]BF$_4$ in ACN obtained at a GC disk electrode at 0.2 V/s. First scan: blue, second scan: red.*

Figure 3.2 shows repeat CVs of NBD at GC. For the first scan (blue) there is a large reduction peak between 0.1 to -0.3 V attributed to the reduction of NBD. This produces aryl radicals, some of which form a nitrophenyl (NP) layer on the surface. In the follow-up scan run immediately after the first scan, there is no reduction peak because build-up of the modification layer on the surface of the GC working electrode blocks the transfer of the electrons to aryl diazonium salts in solution. This is a strong indication that modification has taken place at the GC working electrode.

To validate the presence of a film at the GC working electrode CVs of $Fe(CN)_6^{3-}$ were recorded before and after modification of the electrode. The CVs in figure 3.3 show clear evidence for the presence of a modifying layer. After modification, there is no redox response from the $Fe(CN)_6^{3-}$, consistent with an insulating surface layer that blocks electron transfer by increasing the distance between the electrode surface and redox probe.

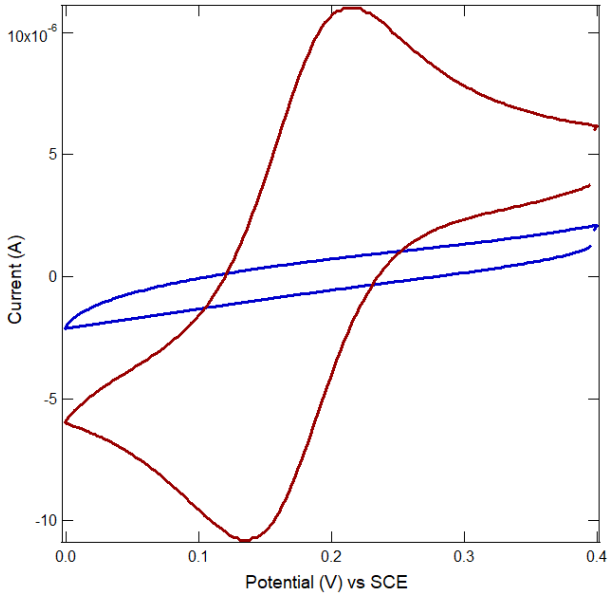

Figure 3.3. *CVs obtained at bare (red) and NP modified (blue) GC disk of 1 mM $K_3[Fe(CN)_6]$ in 0.1 M KCl with a scan rate of 0.1 V/s.*

3.3. Moderately and Highly Doped Molecular Beam Epitaxy SnO_2 Surfaces Spontaneously Modified via Nitrobenzene Tetrafluoroborate and Trifluoromethyl Benzene Tetrafluoroborate Diazonium Salts

The surface layers formed on MBE grown SnO_2 after spontaneous grafting with NBD, and spontaneous and electrochemical grafting with CF3BD were characterised by water contact angle (CA) measurements, AFM roughness and film thickness measurements and soft X-ray XPS analysis carried out at the Australian synchrotron. For each sample, the analysis order was first XPS then CA then AFM.

3.3.1. Spontaneous Grafting of NBD on Moderately and Highly Doped MBE SnO_2 Surfaces

SnO_2 grown by MBE and doped with ≈ 0.02 and 0.2 % Sb for moderately doped and highly doped surfaces respectively as detailed in section 2.2.2.2., were spontaneously modified with NBD following the procedure in section 2.3.2.

3.3.1.1. Water Contact Angles and Atomic Force Microscopy Measurements on Spontaneously NBD Modified MBE SnO_2 surfaces

Surface wettability was expected to increase upon successful surface modification due to the presence of attached NP groups rendering a more hydrophilic surface. Given the smooth nature of the MBE-grown SnO_2, surface modification was also expected to increase the surface roughness. Film thickness measurements were made as detailed in section 2.4.3. In brief, a section of film was removed by scratching with an AFM tip, and then the depth of the scratch was measured by topographical imaging. The SnO_2 surface is sufficiently hard that no underlying substrate was removed during the scratching. The results of water CA measurements and AFM film thickness and roughness measurements are listed in table 3.1. Figure 3.4 shows topographical images and line profiles of the NP modified surface after scratching.

Table 3.1. *Summary of results for CA and AFM surface roughness and modification layer thickness for moderately and highly doped unmodified and NP modified SnO_2 sample.*

Sample	CA (°)	Literature CA (°)	Roughness (nm)	Thickness (nm)
Moderately doped SnO_2 reference	99 ± 2	≈96[a]	0.3 ± 0.1	-
Moderately doped SnO_2 spontaneously modified with NBD	91 ± 1	87[b]	0.8 ± 0.1	1.3 ± 0.5
Highly doped SnO_2 reference	90 ± 3	≈96[a]	0.2 ± 0.1	-
Highly doped SnO_2 spontaneously modified with NBD	87 ± 4	87[b]	0.9 ± 0.1	1.6 ± 0.6

[a] reference 70[70]; [b] reference 71.[71] The CA was measured for a NP film on Au.

For moderately doped SnO_2 surfaces, table 3.1 shows a good comparison between literature and experimental CA with an increase in surface wettability from bare to modified surfaces. The presence of a modification layer is further supported by a change in surface roughness

from 0.3 to 0.8 nm from bare SnO_2 to modified SnO_2. The thickness of the modifying layer was 1.3 ± 0.5 nm. The molecular length of the NP moiety is ≈ 0.6 nm and therefore the film most likely has a multilayer structure.

Highly doped SnO_2 surfaces show no significant change in wettability after modification. The CA of the NP modified surface matches that reported for NP films however the CA for the unmodified sample is lower than expected. This may be due to an order of magnitude difference of Sb content between the moderately and highly doped samples. The measured film thickness for the NP layer is 1.6 ± 0.6 nm which is not significantly different to the thickness of the film on the moderately doped sample. The modified highly doped surface appears patchy with possible SnO_2 surface features being visible through the modification layer (figure 3.4) while the moderately doped surface appears more uniform. The apparent scratches on the modified highly doped sample may be due to damage during prior handling on polishing of the sapphire substrates. In summary CA and AFM measurements give evidence for successful surface modification for both moderately and highly doped SnO_2 surfaces. More detailed information was obtained from the XPS measurements.

(a)

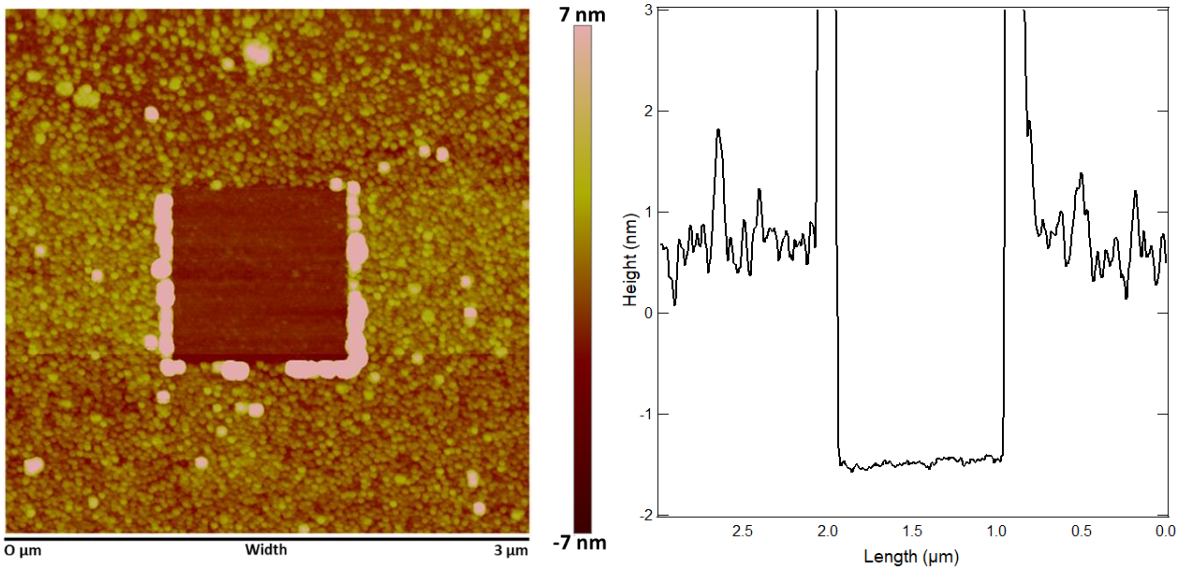

(b)

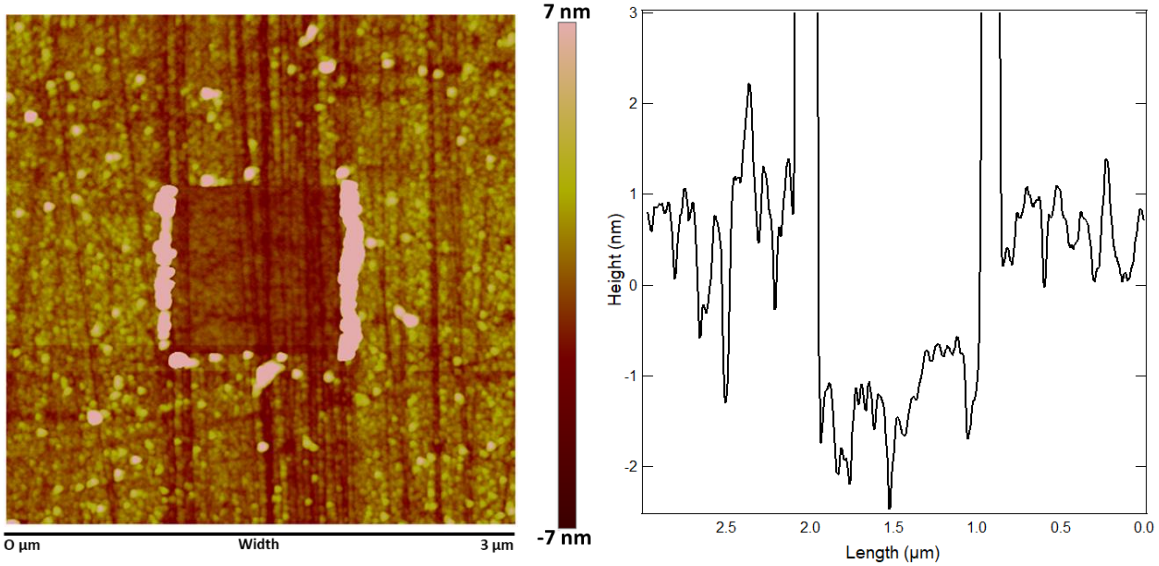

Figure 3.4. *Surface topography measurements taken by AFM showing the modified surfaces after the NP layer has been removed in a central area. The corresponding depth profiles of the surfaces are also shown. (a) Moderately doped SnO_2 and (b) highly doped SnO_2. Note: the clear scratch lines on the topographical image in (b) are attributed to sample damage during prior handling.*

3.3.1.2. X-ray Photoelectron Spectroscopy Measurements on Spontaneously NBD Modified MBE SnO_2 surfaces

XPS analyses of surfaces modified with NP layers were expected to show the presence of N from nitro groups and possible azo linkages. Investigation of the O1s narrow scan was expected to reveal a decrease in the relative amount of O from the bulk SnO_2 in relation to surface O due to attenuation of ejected electrons as a modification layer is built up. Tables 3.2 a - c list the binding energy (BE) of all peaks observed in the O, N and C regions, and gives the corresponding assignments based on literature data. Table 3.3 gives the ratio of intensities of peaks to the Sn3d 5/2 peak as obtained from the spectra. Spectra are shown in figure 3.5.

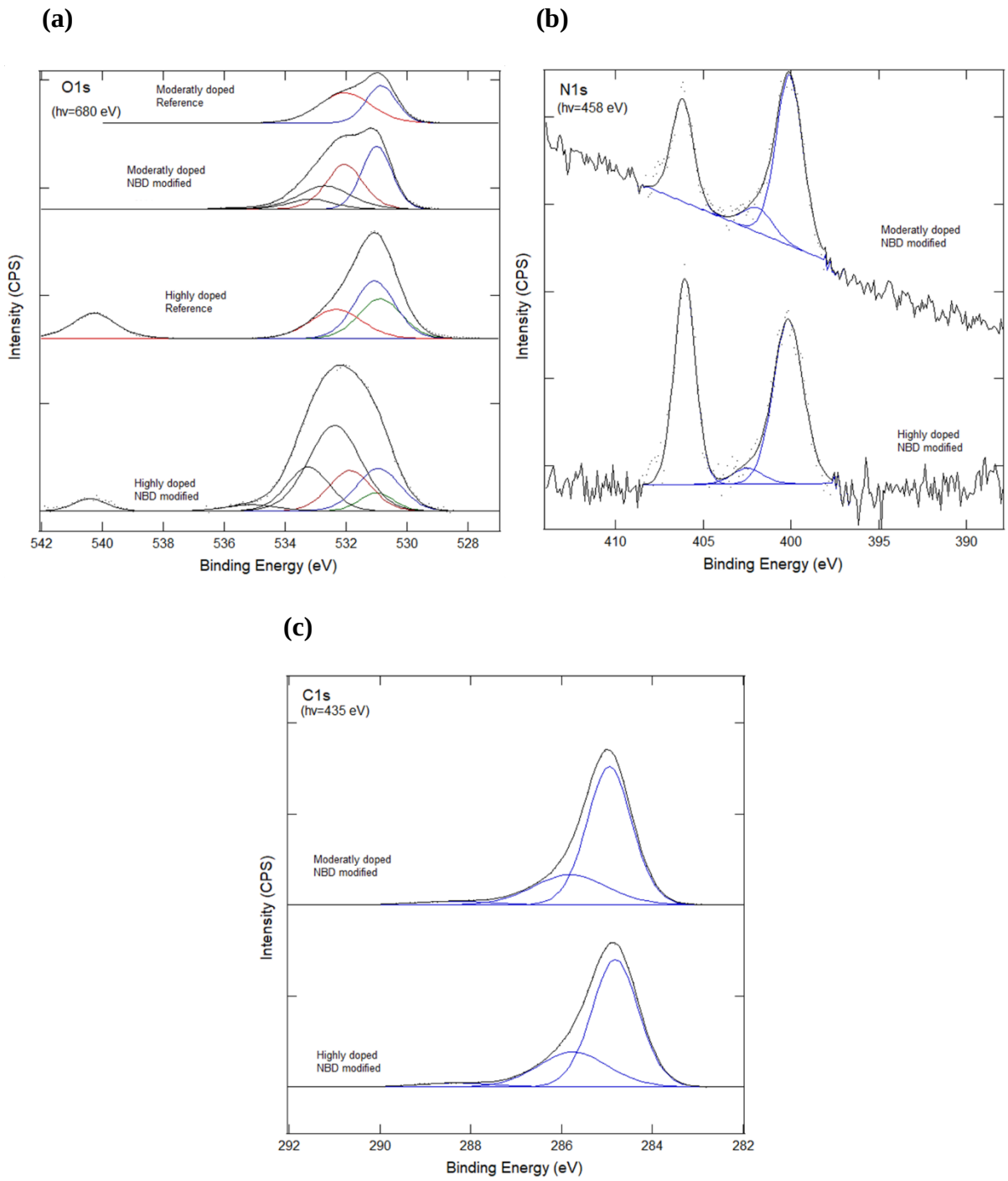

Figure 3.5. *XPS O1s, N1s and C1s narrow scans, (a), (b) and (c) respectively, of SnO_2 surfaces spontaneously modified with NBD and their reference sample. (a) Spectrum normalised to the O1s surface oxygen peak with surface oxygen peak and Sb3d 5/2 peaks highlighted red and green respectively. (b) and (c) spectra are normalised to the Sn3d 5/2 peak from the XPS survey scan.*

As compared to the SnO_2 reference samples, the O1s narrow scan (figure 3.5 (a)) shows the presence of three peaks at 535.5 eV, 533.2 eV and 532.7 eV assigned to nitro π-π*, Sn-O-C

bonding and the nitro O in addition to the surface and bulk oxygen (table 3.2(a)).[72, 73, 74] The presence of the nitro π-π* and nitro O peaks provide evidence for NP at the surface while the Sn-O-C peak suggests that the NP is covalently bound through a surface O.

The number of individual peaks contributing to the O1s signal of the unmodified samples gives considerable uncertainty to individual peak areas. Here the following comments based on the listed areas, in table 3.2, are tentative only. The ratio of the N<u>O</u>$_2$ peak area to the Sn-<u>O</u>-C peak area gives a value of 2.4 and 2.7 for moderately and highly doped SnO_2 surfaces respectively which is close of the value of 2.0 expected if all NP groups are bound to the surface through a surface O. However, film thickness measurements were consistent with a multilayer film and in such a structure, not all NP groups would be bound to the surface suggesting that the listed peak areas have significant uncertainty. The data in table 3.2 also show that only for the unmodified highly doped sample is the expected change in a ratio of bulk O: surface O observed.

Table 3.2. *Assigned peaks seen in XPS narrow scans for SnO_2 surfaces spontaneously modified with NBD. (a) O1s, Sb3d; (b) N1s; (c) C1s. Note, for each element the listed percentages are for each component of that element. Abbreviations MD ref, MD NP, HD ref and HD NP refer to moderately doped reference, moderately doped NP modified, highly doped reference and highly doped NP modified respectively. Due to time constraints at the Australian Synchrotron N and C spectra for reference samples were not measured for moderately and highly doped reference samples.*

(a)

Element O1s, Sb3d	Binding Energy (± 0.2 eV)	Assignment	MD ref (%)	MD NP (%)	HD ref (%)	HD NP (%)
	540.3	Sb 3/2 [75]	-	-	✓	✓
	535.5	π-π* (nitro) [73]	-	0.8	-	3.2
	533.2	Sn-O-C [72]	-	8.7	-	18.2
	532.7	NO_2 [74]	-	23.2	-	43.6
	532.0	Surface O [76]	58.1	31.6	38.9	16.9
	531.0	Bulk O [77]	41.9	35.7	61.1	18.1
	530.9	Sb 5/2	-	-	✓	✓

(b)

Element N1s	Binding Energy (± 0.2 eV)	Assignment	MD ref (%)	MD NP (%)	HD ref (%)	HD NP (%)
	406.0	Nitro N [74]		28.8		44.2
	402.6	N^+,NHOH[78]		9.2		4.8
	400.0	-N=N-, NH_2 [79]		62.0		51.0

(c)

Element C1s	Binding Energy (± 0.2 eV)	Assignment	MD ref (%)	MD NP (%)	HD ref (%)	HD NP (%)
	289.0	π-π* Aromatic C		3.3		3.6

285.9	C-O, C-N, Adventitious [80]	25.6	27.9
284.8	C-C, C-H, Adventitious [81]	71.1	68.5

The N1s narrow scan of the modified samples show three peaks at 406, 402.6 and 400 eV assigned to nitro N, N+ or partially reduced N and fully reduced N species.[74, 78, 79] The NO_2 signal gives the clearest evidence that a NP film is present on the surface. It is well known that synchrotron radiation can reduce NO_2 groups to NH_2 - like species, or partially to NH-OH – like species although the mechanism is not completely understood.[74] The signal at 400 eV, may be due to both azo N, typically present in multilayer NP films (as detailed in chapter 1) and to NH_2 – like groups, the BE of these two species are both very close to 400 eV. The small peak at 402.6 eV can reasonably be assigned to $NHOH^+$ - like groups and or NH_3^+.

Because NO_2 groups are likely to have been reduced during collection of the spectra in figure 3.5, no significance can be attributed to the relative amount of NO_2 N and reduced N in the two modified samples however, the total N:Sn3d 5/2 peak area (table 3.3) for the two samples are similar consistent with the presence of NP films of similar thickness.

Assuming the presence of a minimal amount of adventitious C, table 3.3 shows a similar amount of film on each surface.

Table 3.3. *Ratios of peak areas obtained from XPS survey and narrow scans. Peak areas are normalised to the Sn3d 5/2 peak from the XPS survey scan of that surface for moderately and highly doped surfaces spontaneously modified with NBD.*

Sample	Sn-O-C:Sn3d	Surface O:Sn3d	Bulk O:Sn3d	Total N:Sn3d	C total:Sn3d
Moderately doped SnO_2 reference	-	0.5	0.38	-	-
Moderately doped SnO_2 spontaneously modified with NBD	0.1	0.3	0.37	0.2	2.1
Highly doped SnO_2 reference	-	0.4	0.57	-	-
Highly doped SnO_2 spontaneously modified with NBD	0.1	0.1	0.14	0.3	2.0

Figure 3.6 shows XPS valence band spectra for the unmodified and modified SnO_2 samples. The actual band bending at the SnO_2 surface is difficult to determine from valence band XPS due to uncertainties in the fundamental electronic band gap which in turn arise from the complicated nature of the band structure. However, it is possible to make comparisons between the energies of the leading valence band edges between reference and NBD modified samples and make statements about the changes in the band bending. The intercept of a linear fit of the low energy band edge with the instrument background is used to quantify the change to the band edge (Figure 3.6 (b)). The smaller the BE of the intercept the smaller the amount of downwards band bending or the greater amount of upwards band bending at the surface.

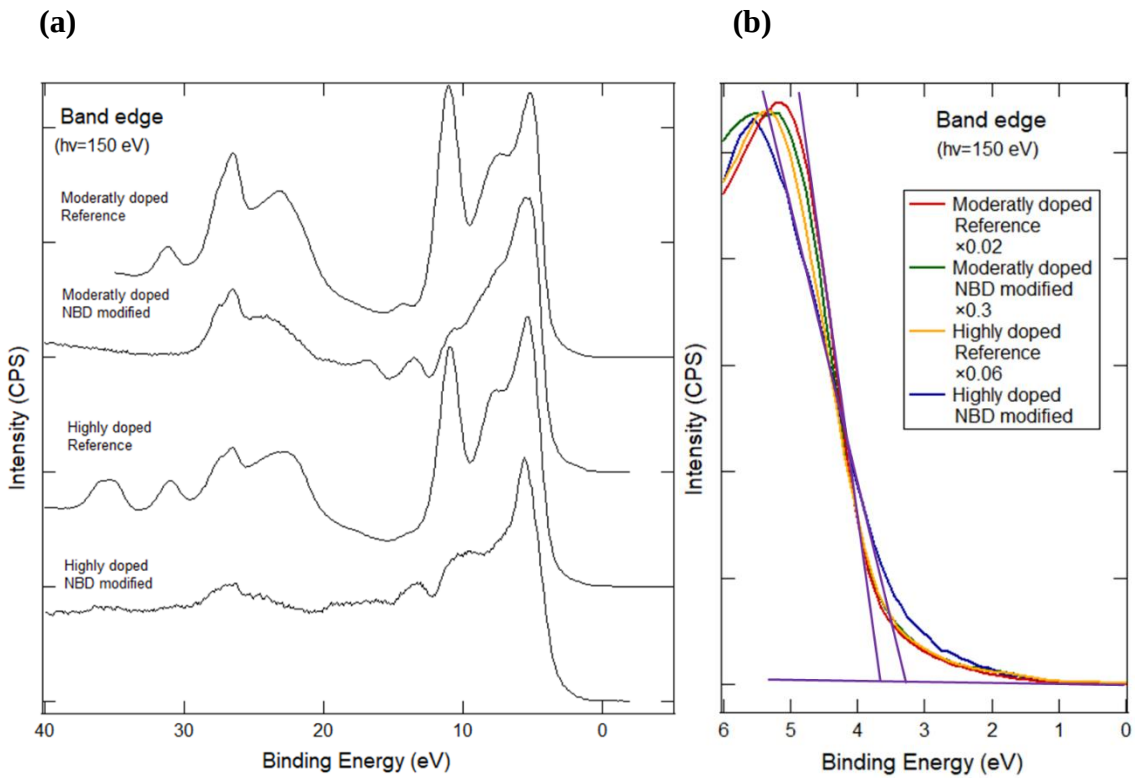

Figure 3.6. *XPS narrow scan of the of the valence band for SnO_2 surfaces Spontaneously modified with NBD and their reference samples. (a) Full scan of the valence band. (b) Overlays of the low energy band edge of both surfaces with a linear fit of the low energy band edge to the background.*

Table 3.4 shows the binding energy of the low energy band edge for moderately and highly doped, reference and modified samples obtained from the spectra in figure 3.6. An upwards change of 0.3 eV to the low energy band edge can be seen for the highly doped modified sample. As discussed above it is apparent that both surfaces have been successfully modified and it is not clear why the effect on the band bending differs for the two samples.

Table 3.4. *Summary of changes to the low energy band edge of SnO_2 surfaces spontaneously modified with NBD and compared to an unmodified reference samples obtained from XPS valence band narrow scans.*

Sample	Low energy band edge (eV)	Change to band edge (eV)	Directional change in band bending
Moderately doped SnO_2 reference	3.7	-	-
Moderately doped SnO_2 spontaneously modified with NBD	3.7	0.0	None
Highly doped SnO_2 reference	3.6	-	-
Highly doped SnO_2 spontaneously modified with NBD	3.3	-0.3	Upwards

The narrow scan of the valence band region of the unmodified samples in figure 3.6a show the expected features due to SnO_2 at ≈ 27, 21.5, 10.5 and 5 eV. There have been attributed to Sn4d spin-orbit coupling states (27 and 21.5 eV),[82, 83] Sn5s electrons (10.5 eV),[84] and O2p electrons (5 eV).[84] The major change in the spectra after modification is the decrease in signal at ≈ 10 eV and there is some decrease in intensity of the peaks at 27 and 21.5 eV. However, a strong peak remains at ≈ 5 eV. A study by Hunger et al.[67] studied the valence band structure of NP films on Si as compared to gas phase spectra of NBD and assigned peaks at 5.3, 6.8 and 9.6 eV to lone pairs on NO_2, π orbitals on the phenyl ring and σ bonds respectively. Hence for all NBD modified samples here, all signals due to the SnO_2 are attenuated by the film and the peak at ≈ 5 eV is due to the NO_2 group not O2p.

To summarise: spontaneous reaction with NBD gives NP films on both moderately and highly doped SnO_2. It appears that there is a similar amount of film on both samples possibly with a slightly thicker film on the highly doped sample. The amount of downwards band bending in the highly doped sample is decreased by modification.

3.3.2. Spontaneous Grafting of CF3BD on Moderately and Highly Doped MBE SnO_2 Surface

SnO_2 surfaces grown by MBE and doped with ≈ 0.02 and 0.2 % Sb for moderately doped and highly doped surfaces respectively (as detailed in section 2.2.2.2.) were spontaneously modified with CF3BD following the procedure in section 2.3.2. The samples were characterised by both CA, AFM and XPS measurements as described in the previous sections for NP-modified samples.

3.3.2.1. CA and AFM Measurements on Spontaneously CF3BD Modified MBE SnO_2 Surfaces

Surface wettability was expected to decrease upon successful surface modification due to the presence of attached CF_3 groups rendering a more hydrophobic surface. Given the smoothness of the MBE sample, surface modification is also expected to increase the surface roughness.

Table 3.5. *Summary of results for CA and AFM surface roughness and modification layer thickness for moderately and highly doped unmodified and CFMP modified SnO_2 samples.*

Sample	CA (°)	Literature CA (°)	Roughness (nm)	Thickness (nm)
Moderately doped SnO_2 reference	99 ± 2	≈96[a]	0.3 ± 0.1	-
Moderately doped SnO_2 spontaneously modified with CF3BD	79 ± 4	-	0.4 ± 0.1	1.3 ± 0.4
Highly doped SnO_2 reference	90 ± 3	≈96[a]	0.2 ± 0.1	-
Highly doped SnO_2 spontaneously modified with CF3BD	93 ± 3	-	1.0 ± 0.2	1.1 ± 0.5

[a] *reference 70.*[70]

Literature value for CAs of films grafted from CF3BD could not be found. However, films grafted from ortho-substituted CF3BD and a benzene diazonium ion with an extended fluorocarbon para substituted gave CAs between 108 – 160°.[85, 86] Given the hydrophobic nature of the CF_3 group in trifluoromethyl phenyl (TFMP) films, expected CA values are in the same range. CA angle results, shown in table 3.5, suggest that after modification a change has occurred at the moderately doped SnO_2 surface however the decrease in CA show a less hydrophobic surface. Nevertheless, AFM topographical imaging and film thickness measurements (figure 3.7(a)) provide convincing evidence that a film approximately 1.3 nm thick has been grafted to the surface.

(a)

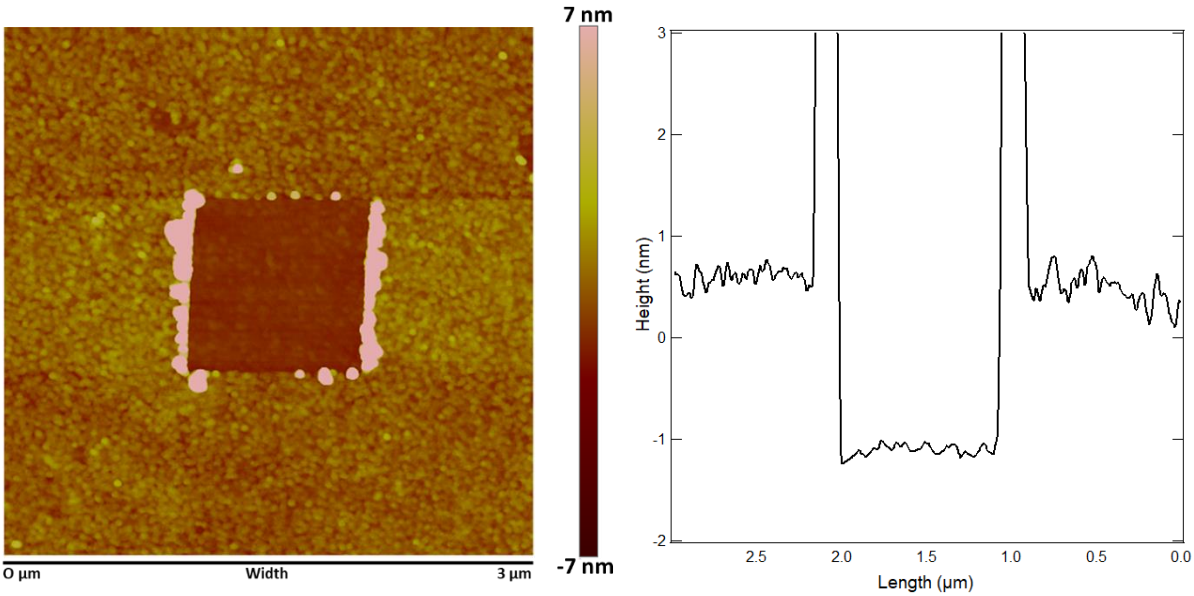

(b)

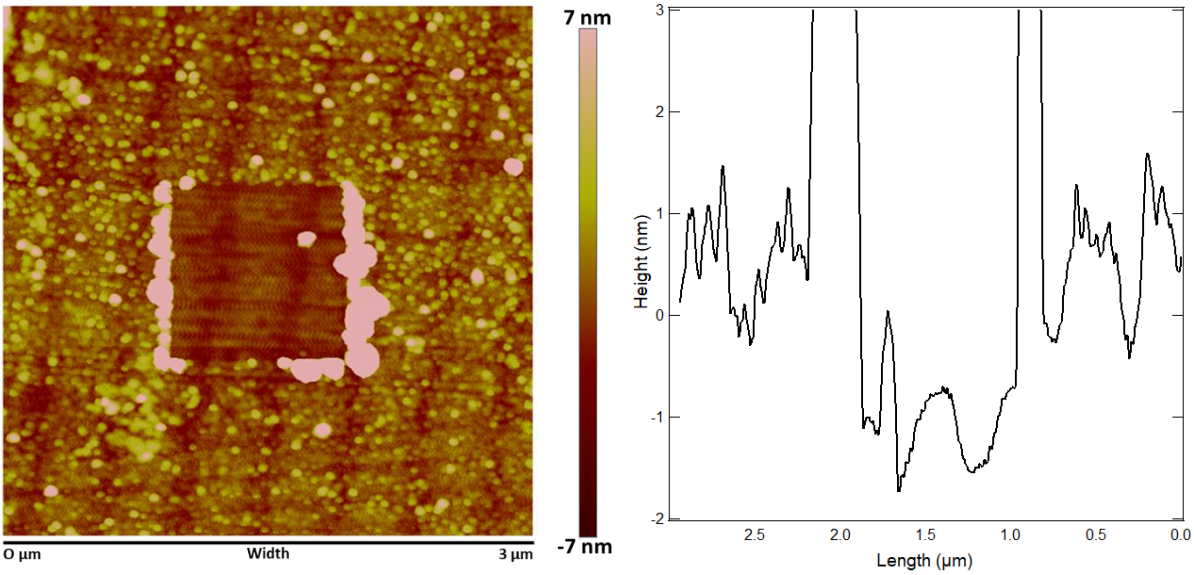

Figure 3.7. *Surface topography measurements taken by AFM showing the modified surfaces after the CFMP layer has been removed in a central area. The corresponding depth profiles of the surfaces are also shown. (a) Moderately doped SnO_2 and (b) highly doped SnO_2.*

Despite discrepancies between water contact angles for the moderately doped CF3BD surface, figure 3.7(a) clearly shows the presence of a film that is distinct from the SnO_2 surface and is very consistently textured. The highly doped SnO_2 surface on the other hand, although showing no change to CA, shows a clear change in surface roughness with a film thickness of approximately 1.1 nm indicative of a multilayer film for a CF3BD moiety length

of ≈ 0.5 nm. The presence of a thin film at the highly doped SnO_2 surface is also apparent in the topographical image in figure 3.7b whereby the underlying step features of the SnO_2 surface from the MBE growth process are clearly visible, seen both on the bare surface and through the TFMP film.

The AFM analysis discussed above suggest that both surfaces have been successfully modified, most notably seen by the film thickness measurements. Further analysis by XPS gave more detailed information about the surface modification.

3.3.2.2. XPS Measurements on Spontaneously CF3BD Modified MBE SnO_2 Surfaces

XPS narrow scans of the F1s, O1s, N1s and C1s regions were expected to confirm the presence of the TFMP modifier. Figure 3.8 displays the spectra table 3.6 gives the assignment of the main peaks found within each spectra, and table 3.7 compares relevant peak areas of modified and unmodified samples.

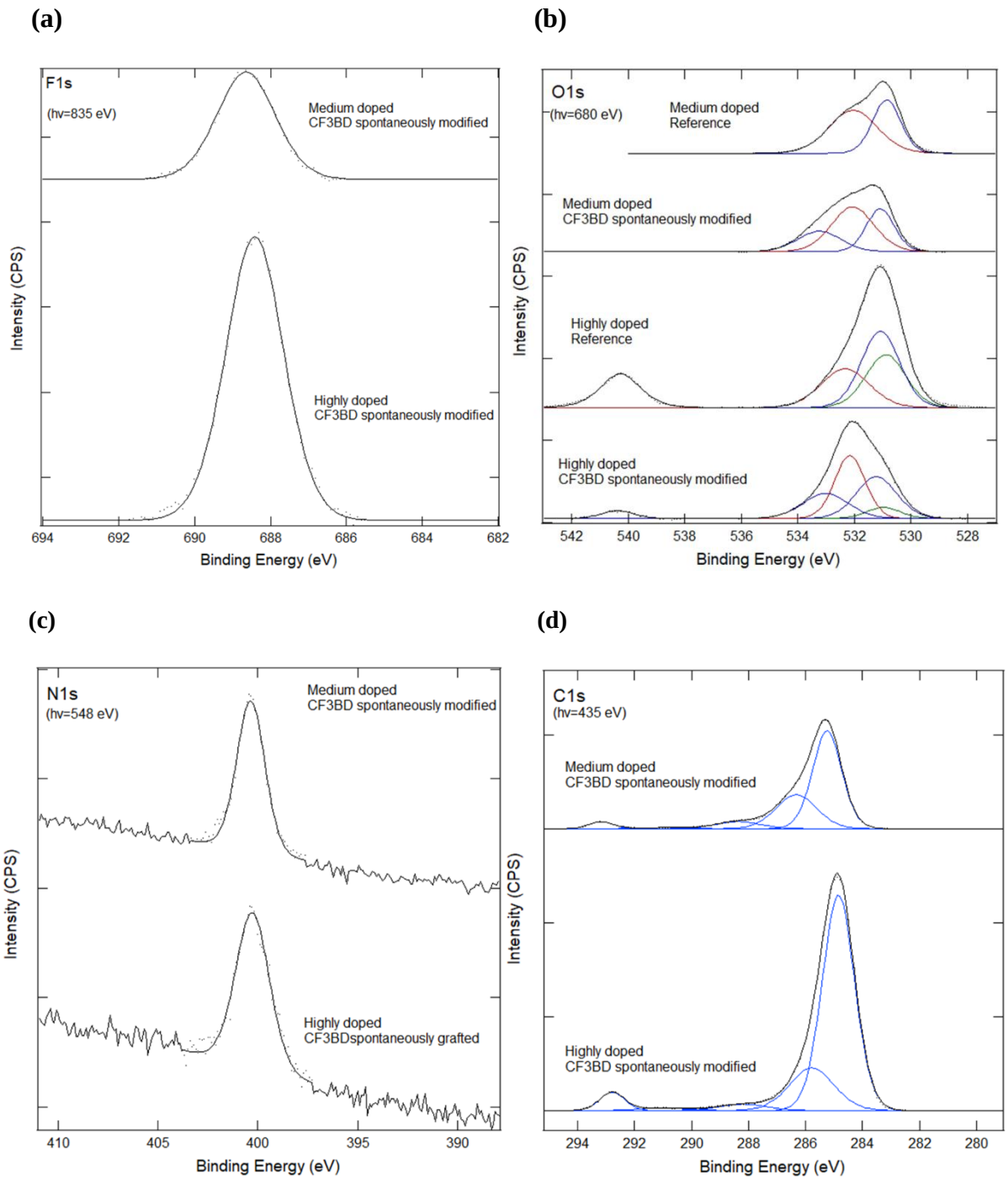

Figure 3.8. *XPS F1s, O1s, N1s and C1s narrow scans, (a), (b), (c) and (d) respectively, of SnO_2 surfaces spontaneously modified with CF3BD and their reference sample. (a), (c) and (d) spectra are normalised to the Sn3d 5/2 peak from the XPS survey scan. (b) spectrum normalised to the O1s surface oxygen peak with surface oxygen peak and Sb3d 5/2 peak highlighted red and green respectively.*

Figure 3.8 (a) clearly shows the presence of F on both modified surfaces at a BE consistent with a CF_3 group.[87] The C1s spectra of the modified surfaces provide further confirmation.

The signal at 293 eV correspond to $\underline{C}F_3$ groups and there is also a trace amount of $\underline{C}F_2$ present at 291 eV.[88] The latter suggests a minor amount of decomposition of the CF_3 substituent. The atomic ratio of F for the highly doped SnO_2 surface to the F of the moderately doped SnO_2 surface is 2.7 which is in excellent agreement with the ratio of the total C bound to F from the C1s spectra of each modified sample. Hence the XPS data suggests that the highly doped SnO_2 surface has a thicker film. However, a ratio of total non-fluorinated carbon to total fluorinated carbon on the same surface would be expected to yield a value of 6 for a contaminant free surface however, values of 19 and 15 for moderately doped and highly doped SnO_2 surfaces respectively, are obtained from the spectra in figure 3.8d. These values show the presence of additional contaminant carbon or the possible degradation of the CF_3 group on the TFMP film.

Table 3.6. *Assigned peaks seen in XPS narrow scans for SnO_2 surfaces spontaneously modified with CF3BD. (a) F1s; (b) O1s, Sb3d; (c) N1s; (d) C1s. Note, for each element the listed percentages are for each component of that element. Abbreviations MD ref, MD TFMP, HD ref and HD TFMP refer to moderately doped reference, moderately doped CF3BD modified, highly doped reference and highly doped CF3BD modified respectively. Due to time constraints N and C spectra for reference samples were not measured for moderately and highly doped reference samples.*

(a)

Element F1s	Binding Energy (± 0.2 eV)	Assignment	MD ref (%)	MD TFMP (%)	HD ref (%)	HD TFMP (%)
	688.8	F-C [87]	-	100	-	100

(b)

Element O1s, Sb3d	Binding Energy (± 0.2 eV)	Assignment	MD ref (%)	MD TFMP (%)	HD ref (%)	HD TFMP (%)
	540.3	Sb 3/2	-	-	✓	✓
	533.4	Sn-O-C	-	22.2	-	24.0
	532.0	Surface O	58.1	47.8	38.7	40.5
	531.0	Bulk O	41.9	30.0	61.3	35.5
	530.9	Sb 5/2	-	-	✓	✓

(c)

Element N1s	Binding Energy (± 0.2 eV)	Assignment	MD ref (%)	MD TFMP (%)	HD ref (%)	HD TFMP (%)
	400.0	-N=N-, NH_2		100		100

(d)

Element C1s	Binding Energy (± 0.2 eV)	Assignment	MD ref (%)	MD TFMP (%)	HD ref (%)	HD TFMP (%)
	293.0	C-F_3 [88]		3.4		4.5
	291.2	C-F_2 [88]		1.1		1.4
	289.0	π-π* Aromatic C		6.6		3.2
	285.9	C-O, C-N, Adventitious		29.0		19.5
	284.8	C-C, C-H, Adventitious		59.9		71.4

The O1s narrow scans of the modified surfaces (figure 3.8(b)) show presence of Sn-O-C peaks at 533.4 eV consistent with covalently bound films on the surface.[72] However, both figure 3.8(b) and table 3.7 show no significant attenuation of the bulk O signal for the modified samples compared to the reference samples and, more surprisingly, an increase in the surface O:Sn3d 5/2 signal for the modified highly doped SnO_2 surface. The origin of this increase is not known but a possible explanation is that etching of the sample occurs during the modification process, increasing the surface area of the sample. Comparison of the O1s Sn-O-C peaks for both surfaces show that the highly doped SnO_2 surface has twice the related intensity of the moderately doped SnO_2 surface (table 3.7). Taken together these XPS and AFM results can be explained by the highly doped modified sample having a high surface area caused by etching by comparison with a non-etched moderately doped modified sample. This would be expected to lead to a greater concentration of Sn-O-C bonds and a high surface concentration of TFMP groups (i.e. a high-density film) for the same film thickness (figure 3.9).

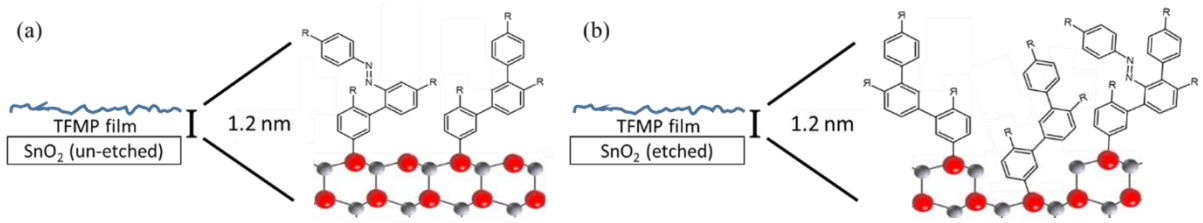

Figure 3.9. *Proposed explanation for increased TFMP film for the same film thickness due to etching at SnO_2 surface. (a) Un-etched SnO_2 surface, (b) etched SnO_2 surface showing increased TFMP film due to increased surface area.*

N1s narrow scans show the presence of azo linkages on the modified surfaces consistent with the expected multilayer structure (figure 3.1). It is noted however, that although there are different amounts of modifier at the two surfaces the N:Sn3d ratios are approximately the same, accounting for rounding (table 3.7). This may be accounted for by the film grafting pathway were C-C links between phenyl groups result from radical attack at already-grafted groups whereas azo links result from electrophilic substitution of the diazonium ions on already grafted groups. It is reasonable to propose that for the highly doped, more conductive surface, a greater proponent of film grafting occurs via reduction of the CF3BD to give the corresponding radical, than at the moderately doped surface. At the SnO_2 surface, the azo coupling pathway may compete more effectively the radical pathway. As such additional ratios shown in table 3.7 confirm that for similar film thicknesses, the highly doped surface has more modifier grafted to it.

Table 3.7. *Ratios of peak areas obtained from XPS survey and narrow scans. Peak areas are normalised to the Sn3d 5/2 peak from the XPS survey scan of that surface for moderately and highly doped surfaces spontaneously modified with CF3BD.*

Sample	F:Sn3d	CF_3:Sn3d	N:Sn3d	Sn-O-C:Sn3d	Surface O:Sn3d	Bulk O:Sn3d	C total:Sn3d 5/2
Moderately doped SnO_2 reference	-	-	-	-	0.5	0.4	-
Moderately doped SnO_2 spontaneously modified with CF3BD	0.3	0.1	0.1	0.2	0.5	0.3	2.3
Highly doped SnO_2 reference	-	-	-	-	0.4	0.6	-
Highly doped SnO_2 spontaneously modified with CF3BD	0.7	0.2	0.2	0.4	0.7	0.6	5.1

Figure 3.9 shows valence band spectra for all samples. the expanded spectrum in figure 3.9(b) reveals that there is a shift to higher BE after modification of the samples indicating decrease in the downwards band bending. Surprisingly the shift is largest for the moderately doped samples (table 3.8 and the reason for this is unknown.

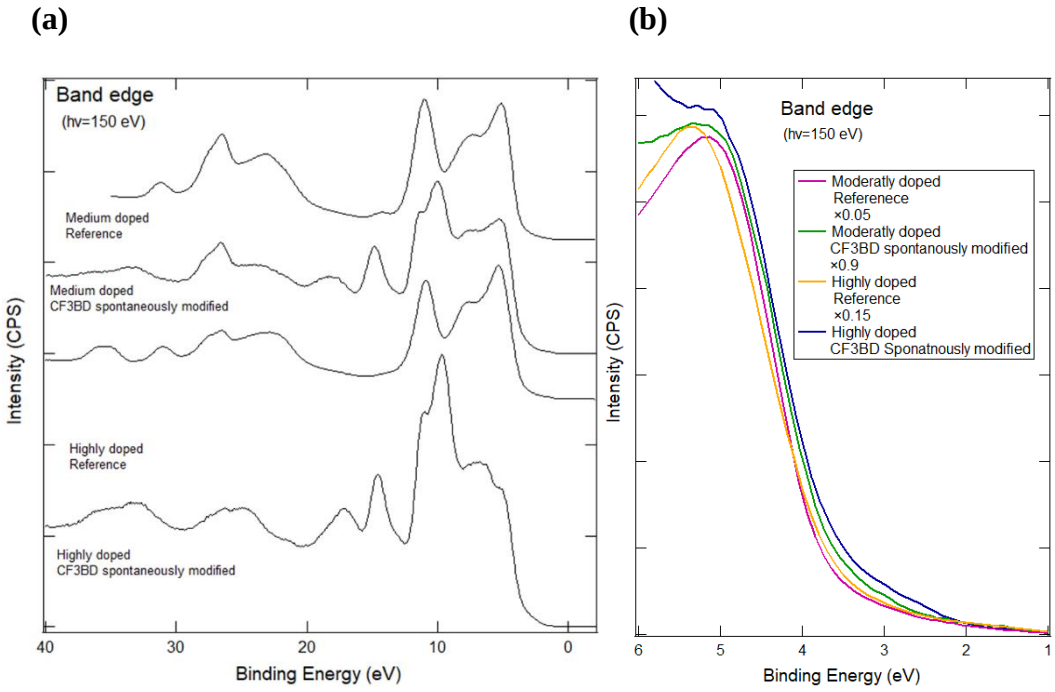

Figure 3.10. *XPS narrow scan of the of the valence band for SnO_2 surfaces spontaneously modified with CF3BD and their reference sample. (a), full valence band scan. (b) overlay of the leading bands from the valence band scan.*

The XPS narrow scan of the valence band region for the two modified samples (figure 3.9(a)) show the appearance of three new peaks at ≈ 9, 14 and 16 eV. These are assumed to be due to the grafted TFMP film. Notably the peak at 5 eV attributed to O2p of the SnO_2, prominent in the spectra of the unmodified sample appear to lose definition at its highest point. This is assumed to be due to a loose of its relative intensity with respect to the appearance of the new feature at 9 eV of the TFMP film. These spectra support the interpretation provided in section 3.3.1.2 regarding the same peak in the NBD modified samples. For those samples the peak was almost diminished after modification and it was suggested that this because of the presence of a peak originating from NP groups (the lone pairs of the NO_2 group).

Table 3.8. *Summary of changes to the low energy band edge of SnO_2 surfaces spontaneously modified with CF3BD and compared to an unmodified reference samples obtained from XPS valence band narrow scans.*

Sample	Low energy band edge (eV)	Change to band edge (eV)	Directional change in band bending
Moderately doped SnO_2 reference	3.7	-	-
Moderately doped SnO_2 spontaneously modified with CF3BD	3.5	-0.2	Upwards
Highly doped SnO_2 reference	3.6	-	-
Highly doped SnO_2 spontaneously modified with CF3BD	3.5	-0.1	Upwards

Figure 3.10(a) and table 3.8 Show changes to the SnO_2 low energy band edge. For both moderately and highly doped SnO_2 surfaces the addition of a TFMP film has caused a decrease in the downward band bending. This result is consistent with expectation where the TFMP film was expected to withdraw electron density away from the SnO_2 surface and cause a decrease in the downwards band bending.

To summarise, moderately and highly doped SnO_2 surfaces have been spontaneously modified with CF3BD. While both surfaces show similar film thickness, the highly doped surface appears to have approximately double the amount of TFMP film grafted on it. This difference is account for by possible etching at the highly doped surface during modification producing a higher surface area. Additionally, both surfaces show a decrease in downwards band bending.

3.4. Highly Doped MBE SnO_2 Surfaces Electrochemically Modified with CF3BD

SnO_2 surfaces were also modified with CF3BD using an electrochemical method. Electrochemical grafting is known to give relatively thick films offer a wider degree of control and quantitative analysis.[89] Electrochemical modification of diazonium salts requires a surface that is highly conductive and for this work only the SnO_2 highly doped surface was sufficiently conducting. The use of CF3BD would offer the same advantages for analysis by XPS as demonstrated in previous sections in this chapter while also enabling comparison with surfaces spontaneously modified with CF3BD.

A highly doped SnO_2 surface was prepared and electrochemically grafted following the procedures in section 2.3 and 2.3.2, after the method developed in section 3.2. Figure 3.10 shows repeat CVs of CF3BD at highly doped SnO_2. For the first scan (blue) there is a large reduction peak between 0.1 - -0.3 V attributed to reduction of CF3BD producing the radical intermediate which forms a layer on the SnO_2 surface. In the second scan, run immediately after the first, the diminished reduction peak confirms the formation of a film at the SnO_2 surface which blocks much of the electrode surface.

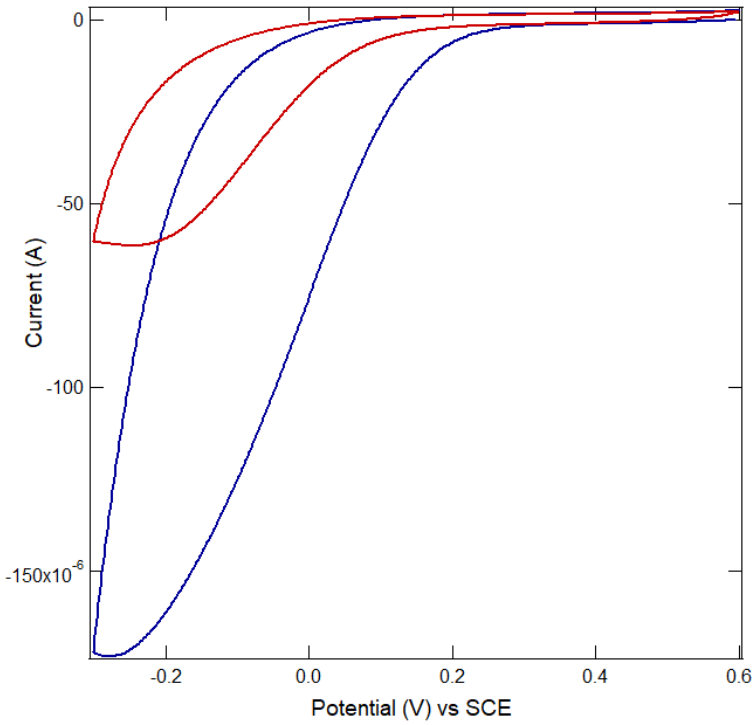

Figure 3.11. *Two repeat CVs of 10 mM CF3BD in 0.1 M [Bu_4N]BF_4 in ACN obtained at a GC disk electrode at 0.2 V/s. First scan: blue, second scan: red.*

The highly doped electrochemically modified SnO_2 surface was then characterised by CA, AFM and XPS measurements. The following sections will first present and discuss CA and AFM results together, followed by XPS and lastly SnO_2 surfaces modified with CF3BD spontaneously and electrochemically will be compared. It is important to note that the reference sample used for comparison with the electrochemically modified surface was from a different but similar growth to that used for the surface modification as no reference material from the same growth was available.

3.4.1. CA and AFM Measurements on Electrochemically CF3BD Modified MBE SnO_2 Surfaces

As discussed in section 3.3.2.1, for the CA and AFM measurements of SnO_2 surfaces spontaneously modified with CF3BD, a large increase in CA would be expected for a thin film consisting of the hydrophobic TFMP moiety. Table 3.9 CA results, although showing a change in surface wettability as compared to a reference sample, show a change to a more hydrophilic surface. The same behaviour was observed after spontaneous grafting TFMP groups to moderately doped SnO_2 (table 3.5). For the present film, AFM measurements (table

3.9) reveal that it has a high surface roughness with an average thickness corresponding to approximately three layers of TFMP groups. The high roughness and disorder of the multilayer film may lead to unexpectedly low water contact angles.

Table 3.9. *Summary of results for CA and AFM surface roughness and modification layer thickness for highly doped unmodified and electrochemically modified TFMP SnO_2 sample.*

Sample	CA (°)	Roughness (nm)	Thickness (nm)
Highly doped SnO_2 reference sample (different batch)	90 ± 3	0.2	-
Highly doped SnO_2 electrochemically modified with CF3BD	82 ± 5	1.2 ± 0.3	2.2 ± 1.1

The AFM images provide clear evidence that the highly doped electrochemically modified SnO_2 surface has been modified forming a TFMP film. The topographical AFM image of figure 3.12 SnO_2 surface step edges can be seen through the modification consistent with a thin layer of TFMP. The relatively thin (< 3 nm) grafted film is consistent with the CVs in figure 3.11 where the observation of a reducing peak on the second scan in figure 3.11 indicates that a relatively thin film has grafted. In fact, it is possible that the grafted film is patchy in nature which would account for the large error associated with the film thickness (table 3.9)

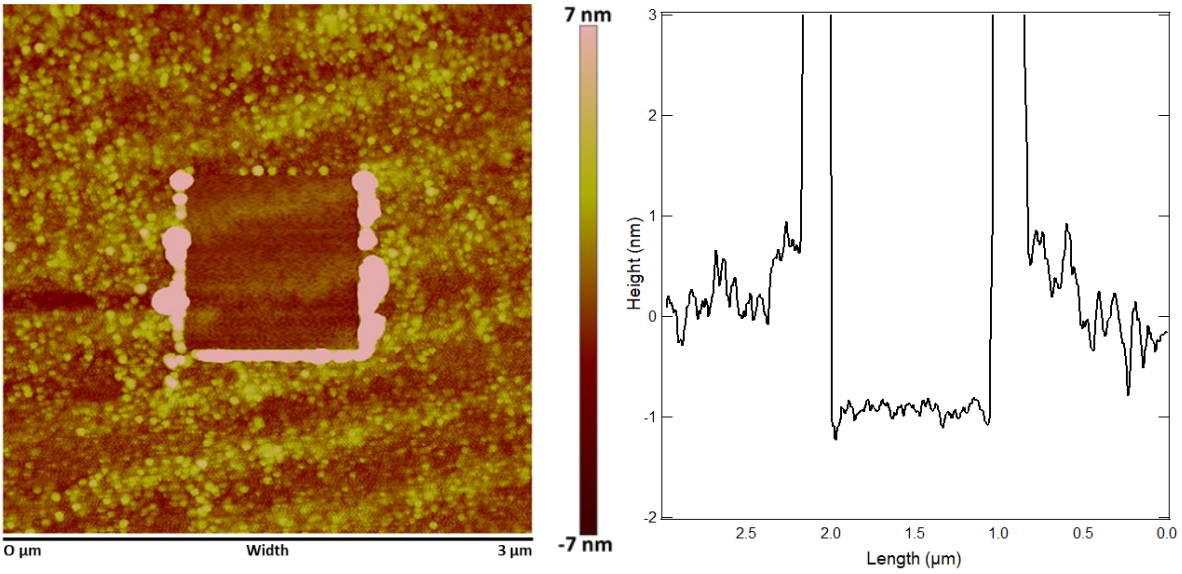

Figure 3.12. *Surface topography measurements taken by AFM showing the modified surfaces after the CFMP layer has been removed in a central area. The corresponding depth profiles of the surfaces are also shown.*

3.4.2. XPS Spectroscopy Measurements on Electrochemically CF3BD Modified MBE SnO_2 Surfaces

As in section 3.3.2.2 XPS narrow scans were taken of the F1s, O1s, N1s, C1s and the valence band regions to identify elements of interest with the presence of F acting as a marker for TFMP at the SnO_2 surface and the O1s indicating changes to the SnO_2 surface environment with peak assignment seen in table 3.10(a-d). Figure 3.13 shows the XPS spectra.

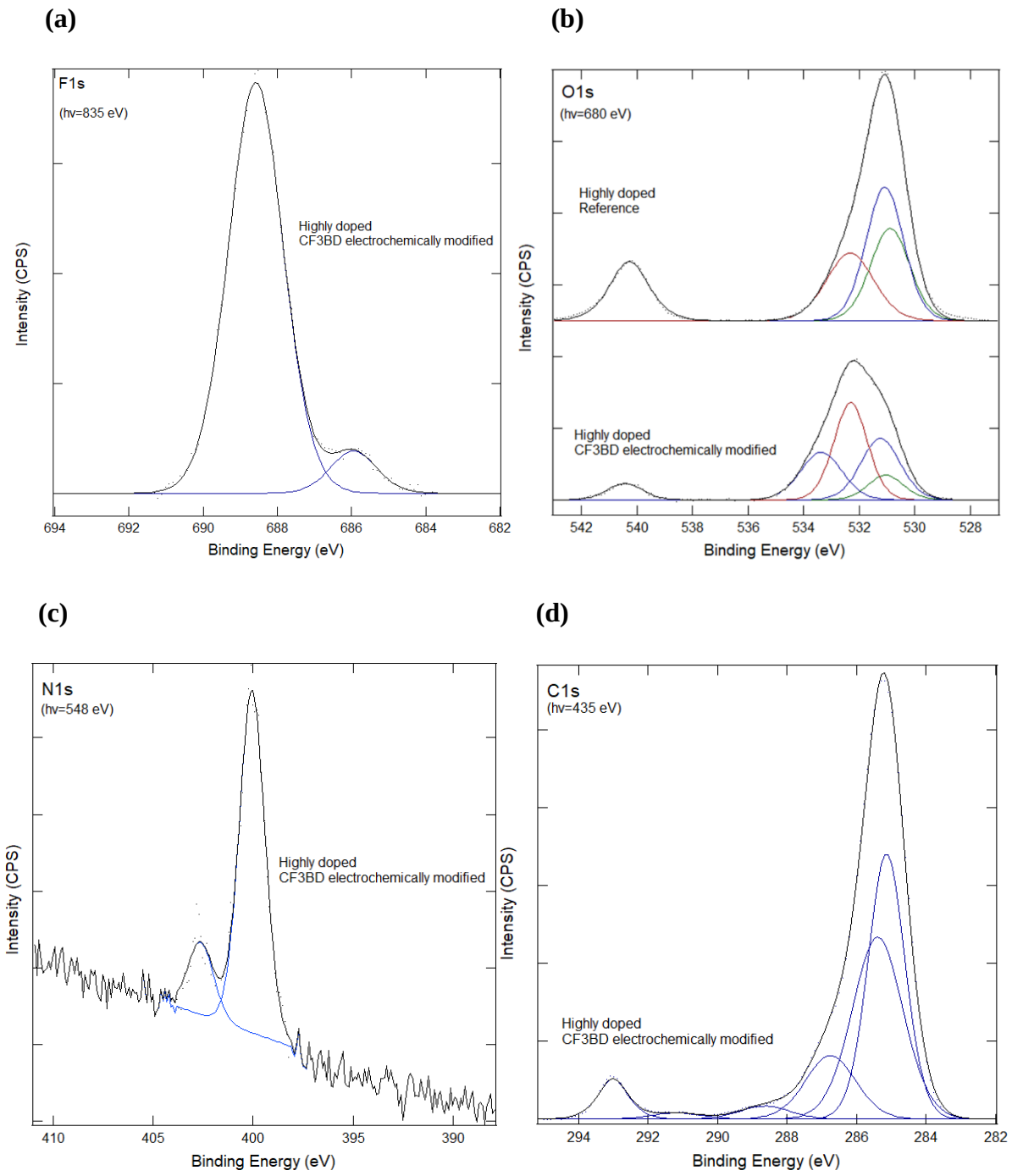

Figure 3.13. *XPS F1s, O1s, N1s and C1s narrow scans, (a), (b), (c) and (d) respectively, of SnO_2 surfaces electrochemically modified with CF3BD and their reference sample. (a), (c) and (d) spectra are normalised to the Sn3d 5/2 peak from the XPS survey scan. (b) spectrum normalised to the O1s surface oxygen peak with surface oxygen peak and Sb 5/2 peak highlighted red and green respectively.*

The F1s narrow scan spectrum (figure 3.12(a)) shows two F signals at 688.8 and 686.2 eV. These are assigned to F-C and F-B respectively.[88, 90] The F-C signal arise from the CF_3 group

of the TFMP modification and the presence of F-B is attributed to the supporting electrolyte, $[Bu_4N]BF_4$, present during the electro grafting process and also in the solution used to clean the TFMP modified surface. This assignment is also supported by the presence of a signal consistent with N^+ at 402.6 eV in the N1 narrow scan.[78]

With a TFMP film at the surface, the O1s narrow scan confirms covalent modification to the SnO_2 surface were, as compared to a reference sample, an additional Sn-O-C peak is present at 533.4 eV assigned to TFMP bound to the surface through surface O.[72] A sharp decrease in bulk O:surface O ratio is also seen for the modified surface, (0.6), as compared to the reference surface, (1.4), showing attenuation of the XPS signal from the SnO_2 bulk material due to the presence of the overlying TFMP film.

Table 3.10. *Assigned peaks seen in XPS narrow scans for SnO_2 surface electrochemically modified with CF3BD. (a) F1s; (b) O1s, Sb3d; (c) N1s; (d) C1s. Note, for each element the listed percentages are for each component of that element. HD ref and HD CFMP refer to highly doped reference and highly doped CF3BD modified respectively.*

(a)

Element F1s	Binding Energy (± 0.2 eV)	Assignment	HD ref (%)	HD TFMP (%)
	688.8	F-C		94.4
	686.2	F-B [90]		5.6

(b)

Element O1s, Sb3d	Binding Energy (± 0.2 eV)	Assignment	HD ref (%)	HD TFMP (%)
	540.3	Sb 3/2	✓	✓
	533.4	Sn-O-C	-	25.7
	532	Surface O	38.9	42.8
	531	Bulk O	61.1	31.6
	530.9	Sb 5/2	✓	✓

(c)

Element N1s	Binding Energy (± 0.2 eV)	Assignment	HD ref (%)	HD TFMP (%)
	402.6	N^+		17.4
	400	-N=N-		82.6

(d)

Element C1s	Binding Energy (± 0.2 eV)	Assignment	HD ref (%)	HD TFMP (%)
	293.0	C-F_3		5.1
	291.2	C-F_2		1.3

	289.0	π-π* Aromatic C	2.7
	285.9	C-N, Adventitious	13.1
	285.4	C-(COO)-C, Adventitious C [91]	37.8
	284.8	C-C, C-H, Adventitious	40.0

The C1s spectra show C signals attributed to CF_3 and CF_2 at 293.0 and 291.2 eV respectively confirming that F at the surface is from the TFMP modifier but also showing that the CF_3 group has partially degraded.[88] Again, a ratio of total non-fluorinated C environments to fluorinated C environments would be expected to give a value of ≈ 6 (for 6 C of the aryl group to one CF_3 group). A ratio of 8.14 is obtained however which is in reasonable agreement. This ratio has excluded the C-(COO)-C/adventitious C peak at 285.4 eV.[91] This peak has not been present for any other surface and its origins are unknown. One possible origin could be the electrochemical grafting process itself.

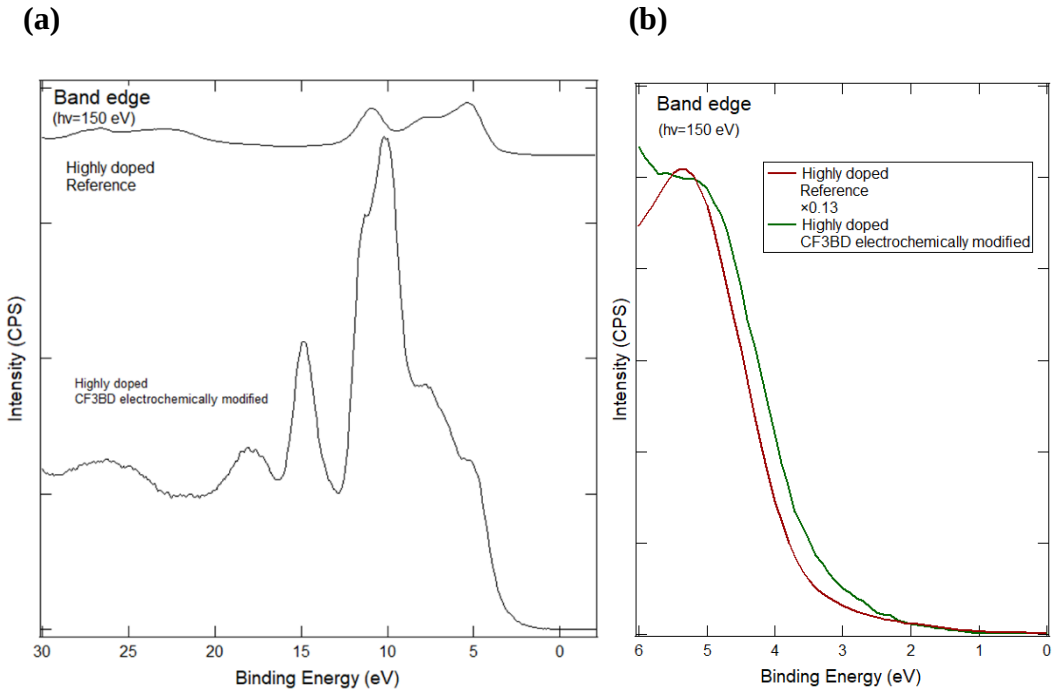

Figure 3.14. *XPS narrow scan of the of the valence band for SnO_2 surfaces spontaneously modified with CF3BD and the reference sample. (a), is the full valence band scan. (b) is an overlay of the leading band from the valence band scans.*

From the valence band spectra (figure 3.14), changes to the band edge show a decrease in downwards band bending of 0.3 eV (table 3.11) consistent with the electron withdrawing nature of the TFMP film and also in good agreement with other TFMP modified surfaces, described in previous sections.

The extended SnO_2 valence band spectrum of the electrochemically modified surface (Figure 3.14(a)) is similar to that of SnO_2 surfaces spontaneously modified with CF3BD (figure 3.10) and similar comments apply to this spectrum.

Table 3.11. *Summary of changes to the low energy band edge of SnO_2 surfaces electrochemically modified with CF3BD and compared to a reference an unmodified reference sample obtained from XPS valence band narrow scan.*

Sample	Low energy band edge (eV)	Change to band edge (eV)	Directional change in band bending
Highly doped SnO_2 reference (different batch)	3.6	-	-
Highly doped SnO_2 electrochemically modified with CF3BD	3.3	-0.3	Upwards

As discussed in section 3.3.2.2, regarding potential degradation of fluorinated C, and in consideration of the stability of any surface modification for use in future devices, an additional analysis was performed to evaluate the stability of the CF_3 group under the X-ray beam. The stability of the CF_3 group modified surface was assessed by carrying out multiple F1s narrow scans at the same location with an increased (approximately double) intensity of the X-ray beam.

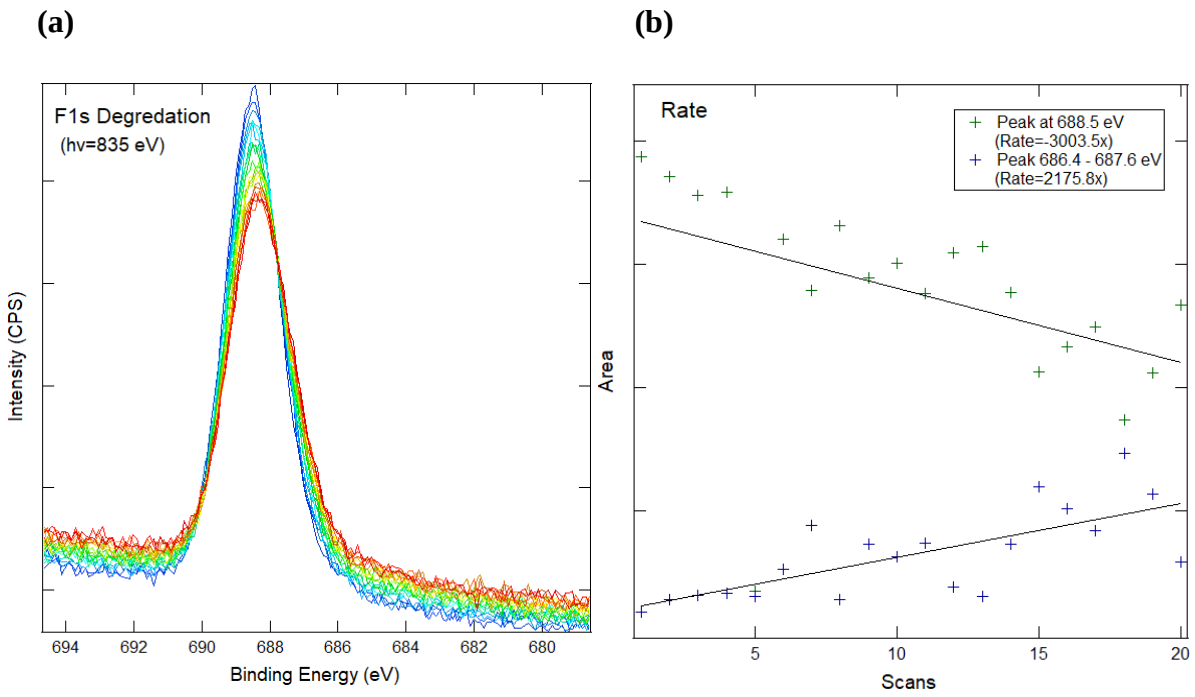

Figure 3.15. *XPS F1s narrow scan series at a higher photon intensity showing the degradation of the electrochemically grafted TFMP film on the highly doped SnO_2 surface. (a), F1s narrow scan series with blue being the first scan and red being the final scan, (b), rate of disappearance and appearance of peaks fitted at 688.5 and 687 eV respectively.*

Figure 3.15(a) shows an overlap of 20 F1s scans at the same spot on the electrochemically grafted SnO_2 surface at a higher X-ray flux. As the number of scans increase (blue through to red), a decrease in peak area can be seen. This peak is also seen to shift slightly to lower BE. The F1s peak in each scan consists of a component at 688.5 eV and another that ranges from 686.4 – 687.6 eV. The peak at 688.5 eV is assigned to F-C of the CF_3 group on the TFMP film.[87] The second peak although could be that of F-B from contaminant $[Bu_4N]BF_4$, is not entirely accurate as this peak is far less prominent than that seen in figure 3.13(a) for F-B. Also while literature reports F-B at a range of BE (685.6 - 687.0 eV) .[90, 92, 93] this is still not consistent with such a larger variation (≈ 1 eV). Furthermore, the rate of appearance of F-B is seen to increase while F-C decreases (figure 3.15(b), however no B has been added to the surface to allow for this increase. As such, assignment of the peak at 686.4 – 687.6 eV in the degradation scan remains unknown were assignment of this peak to $[Bu_4N]BF_4$ does not explain such extreme shifts in BE and assignment of this peak to anything else does not explain a lack of expected $[Bu_4N]BF_4$. As such, results do show that TFMP films are susceptible to degradation from X-rays.

The results presented above show that highly doped SnO_2 surfaces can be electrochemically modified with CF3BD with the formation of a TFMP thin film covalently bound to the SnO_2 surface. Additionally, modified surfaces show a decrease in the downwards band bending while also showing a susceptibility of the CF_3 group to degradation via X-rays.

3.5. Comparison Between Spontaneously and Electrochemically CF3BD Modified MBE SnO_2 Surfaces

After comparisons of the use of different modifiers with the same method on SnO_2 surface (section 3.3), this section compares the effectiveness of the same modifiers applied by different methods so an overall effectiveness for the use of diazonium salts as a surface modifier for SnO_2 surface can be deduced.

3.5.1. Comparison of CA and AFM Measurements on Spontaneously and Electrochemically CF3BD Modified MBE SnO_2 Surfaces

CA of all CF3BD modified surfaces (table 3.12) show minor changes in surface wettability. Given that a TFMP surface is expected to increase the hydrophobicity of the surface, this result is unexpected. As discussed in earlier sections, may be explained by the formation of rough and disordered multilayer films with the CF_3 group only partially influencing wettability at the surface.

Table 3.12. *Summary of results for CA and AFM surface roughness and modification layer thickness for moderately and highly doped unmodified and CF3BD spontaneously and electrochemically modified SnO_2 samples.*

Sample	CA (°)	Roughness (nm)	Thickness (nm)
Moderately doped SnO_2 spontaneously modified with CF3BD	79 ± 4	0.4 ± 0.1	1.3 ± 0.4
Highly doped SnO_2 spontaneously modified with CF3BD	93 ± 3	1.0 ± 0.2	1.1 ± 0.5
Highly doped SnO_2 electrochemically modified with CF3BD	82 ± 5	1.2 ± 0.3	2.2 ± 1.1

Film thickness measurements show comparable film thickness for both spontaneously modified surfaces while the electrochemically modified surface has almost twice the average thickness as well as having the most variability and the highest surface roughness. These results indicate that thicker films can be grown by electrochemical modification while spontaneous modification produces films of similar thickness regardless of doping level.

3.5.2. Comparison of XPS Measurements on Spontaneously and Electrochemically CF3BD Modified MBE SnO_2 Surfaces

A comparison of peak ratios from all SnO_2 surfaces both spontaneously and electrochemically modified with CF3BD (table 3.15) show a trend for increased SnO_2 surface modification as follows: highly doped electrochemically modified > highly doped spontaneously modified > moderately doped spontaneously modified. This suggests that Sb-doping does have an effect on the spontaneous modification of SnO_2 surfaces.

The $\underline{C}F_3$:Sn-$\underline{O}$-C peak ratio are 1.2, 1.8 and 3.0 for moderately doped spontaneously modified, highly doped, spontaneously modified, and highly doped electrochemically

modified surfaces respectively. The values for the spontaneously modified films are consistent with an increased presence of TFMP moieties for a similar film thickness, while the larger value for the electrochemically modified film (almost twice that of spontaneously modified surfaces) indicates a greater average film thickness which must include a greater number of TFMP groups which are not directly bound to the surface.

Table 3.13. *Ratios of peak areas obtained from XPS survey and narrow scans. Peak areas are normalised to the Sn3d 5/2 peak from the XPS survey scan of that surface for moderately and highly doped surfaces spontaneously and electrochemically modified with CF3BD.*

Sample	F-C:Sn3d	CF_3:Sn-O-C	Surface O:Bulk O	Azo:F-C	C total:Sn3d	Shift to band edge (eV)
Moderately doped SnO_2 spontaneously modified with CF3BD	0.3	1.2	1.6	0.2	2.3	-0.2
Highly doped SnO_2 spontaneously modified with CF3BD	0.7	1.8	1.2	0.5	5.1	-0.1
Highly doped SnO_2 electrochemically modified with CF3BD	2.1	3	1.4	0.2	7.6	-0.3

The azo:F-C ratios are consistent the formation of azo links being influenced by Sb-doping as previously explained. Values of 0.5, 0.2 and 0.2 are shown for moderately doped spontaneously modified, highly doped, spontaneously modified, and highly doped electrochemically modified surfaces respectively. This suggests that increased Sb-doping appears to cause a shift in competing grafting mechanism causing more azo links to form at the surface by electrophilic substitution.

Ratios of surface to bulk O for all surfaces yield 1.6, 1.2 and 1.4 for moderately doped spontaneously modified SnO_2, highly doped spontaneously modified SnO_2 and highly doped electrochemically modified SnO_2 surface respectively. These values are similar within the uncertainty accompanied with the O1s peak fitting.

Lastly all SnO_2 surface show a positive shift in the low energy band edge of the valence band spectra with the electrochemically modified SnO_2 surface showing the largest change of -0.3 eV and the spontaneously modified highly doped surface showing the smallest changes of -0.1 eV. These shifts correspond to a decrease in downwards band bending. While these changes to the band edge are consistent with the electron withdrawing nature of the CF_3 moiety, the magnitude of each change is not entirely understood. An explanation may be related to TFMP film thickness. It might be assumed that a particular molecule would have a set ability to withdraw electron density away from the surface. However, studies have shown that band bending will initially change with the thickness of a surface film but then become constant after a certain depth is achieved.[94, 95]

Results shown in this section highlight the use of the CF3BD as an effective SnO_2 surface treatment via a spontaneous pathway for both moderately and highly doped SnO_2 surface and an electrochemical pathway for highly doped SnO_2 surface.

3.6. Conclusions

Results for moderately and highly doped SnO_2 surface modified with NBD and CF3BD via spontaneous and electrochemical pathways have been presented in this chapter. Surfaces have then been characterised via CA, and AFM measurements showing the SnO_2 surface can be modified with diazonium salts. The presence of a thin film has been observed along with some changes to surface wettability and roughness. Notable upwards shift to the SnO_2

valence band edge have also been shown except for the moderately doped spontaneously NBD modified SnO_2 surface that shows no change in band bending.

While some results obtained from different techniques have appeared somewhat inconsistent, there is no doubt that use of diazonium salt grafting produces a covalently bound thin film on SnO_2 surfaces. It is important to note however that minimal previous research has been conducted on the use of diazoniums salts for the surface modification of SnO_2 and as such these are preliminary results requiring repeat experimentation and further investigation before a firm understanding can be achieved.

XPS narrow scans of surfaces have identified the covalent attachment of the diazonium modifiers to the surface via Sn-O-C bond and have shown in an increase in azo formation with increased Sb-doping of the SnO_2 film.

Due to a limited supply of high quality SnO_2 surfaces and strictly limited opportunities to obtain XPS measurements at the Australian Synchrotron, all results discussed here are from single samples. This raises the possibility that first, results might not be truly representative, and second that sample damage and contamination could have occurred during the series of measurements.

Chapter 4. Phosphonic Acids Surface Modification

4.1. Introduction

As mentioned in chapter 1, phosphonic acids have been used for the surface modification of a variety of materials including metal oxides. In particular is their use on ITO surfaces where phosphonic acid modification can have an influence on both the material properties of the underlying substrate and physical properties of the modified surface. While studies have looked into the modification of SnO_2 with silanes and thiols,[49, 96] little research has been conducted on the use of phosphonic acids as a surface modification treatment. As such, the precise nature of interactions between SnO_2 surfaces and phosphonic acid moieties is not well known. It is reasonable to assume similar binding modes to those for ITO, giving surface structures seen in figure 4.2. Bonding to the surface proceeds via condensation reactions with the resulting multiple possible binding modes. The surface structures in figure 4.1 do not include dipole interactions or dopant bonding interactions at the surface both of which have been proposed to play a part in SAM formation.[25]

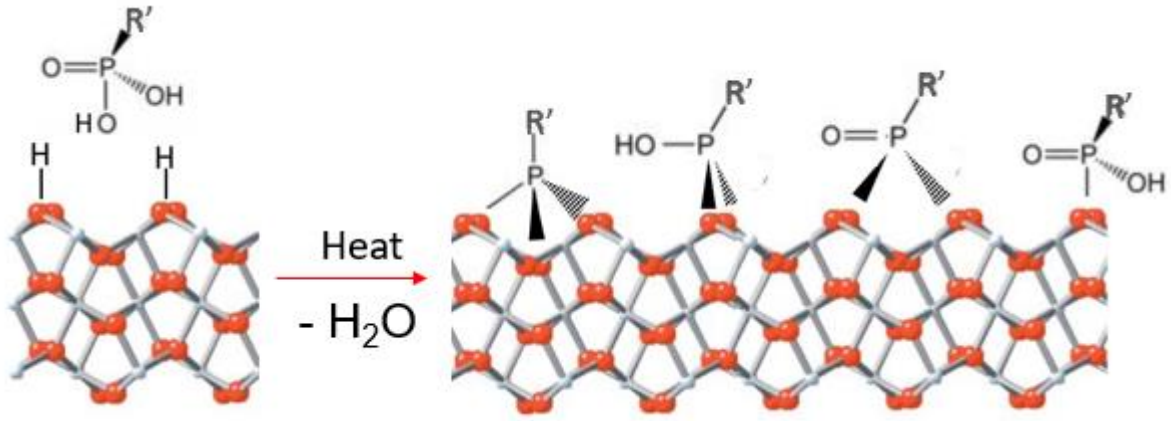

Figure 4.1. *Addition of phosphonic acids to SnO_2 surface via condensation reaction showing various possible binding modes.*

It has been found that changes to a material's band structure via surface treatment is influenced by the dipole of the surface moiety (also shown by the work in chapter 3), the type of binding of that moiety to the surface and coverage on the surface.[96, 97] With respect to changing the band bending at the SnO_2 surface through modification with phosphonic acids it might be expected that the mode of binding would have an influence.

This research aimed to modify SnO_2 surfaces with octadecyl phosphonic acid (ODPA), tridecafluoro octadecyl phosphonic acid (F13OPA), and benzene pentafluoro phosphonic acid (PFBPA) seen in figure 4.2. Opposing dipoles of -2.7 D and 1.7 D for ODPA and F13OPA respectively,[98] were expected to oppositely influence the SnO_2 valence band however during the course of this work, results reported for a similar study using ZnO suggested this might not be the case.[50] The use of PFBPA allows for investigation of conjugated systems on SnO_2 surfaces where a study by Frantz et al.[99] found changes in redox potential of ferrocene after being bound to SnO_2 particles via a conjugated phenyl phosphonic acid.

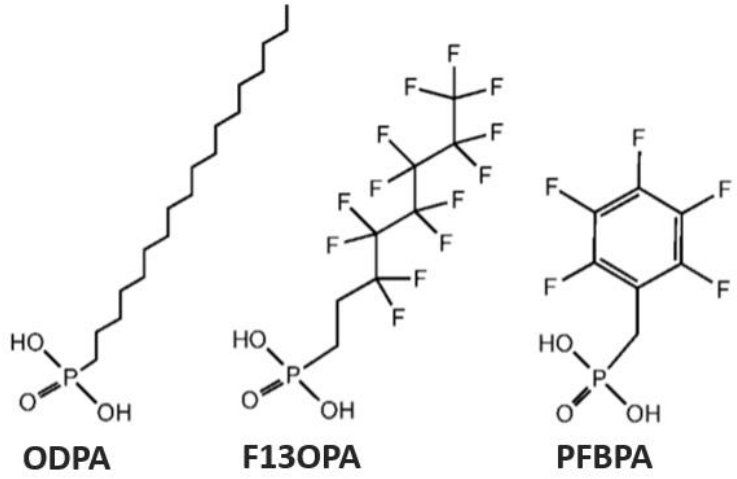

Figure 4.2. *Chemical structure of ODPA, F13OPA and PFBPA. Figure adapted from reference 48.*[48]

SnO_2 grown by both CVD and MBE were used in this work. The CVD-grown material is readily available and was used to establish whether modification could be achieved using phosphonic acids. Having successfully modified that material, experiments were repeated using the MBE-grown films. This material has a well-defined (101) surface with low roughness. It was anticipated that this would enable a more detailed investigation of SAM formation and the effect of surface modification on SnO_2 electrical properties. Modification was also carried out on un-doped and doped materials, again to investigate the impact of modification on the electrical properties.

4.2. Indium Tin Oxide Method Development

Method development for the surface modification of SnO_2 surfaces with phosphonic acids, detailed in section 2.3, was done using F13OPA on ITO. The starting point was the procedure used by Gooding et al.[4] for the surface modification of ITO with phosphonic acids with changes to cleaning and annealing steps based on the work by McNeill et al.[50] for the surface modification of ZnO with phosphonic acids. Experimental variable such as solvents, sonicating and annealing times and post modification cleaning procedures were altered to optimise CA and CV results guided by the expected literature values. Modified ITO surfaces were characterise by CAs, CVs and infra-red spectroscopy (IR).

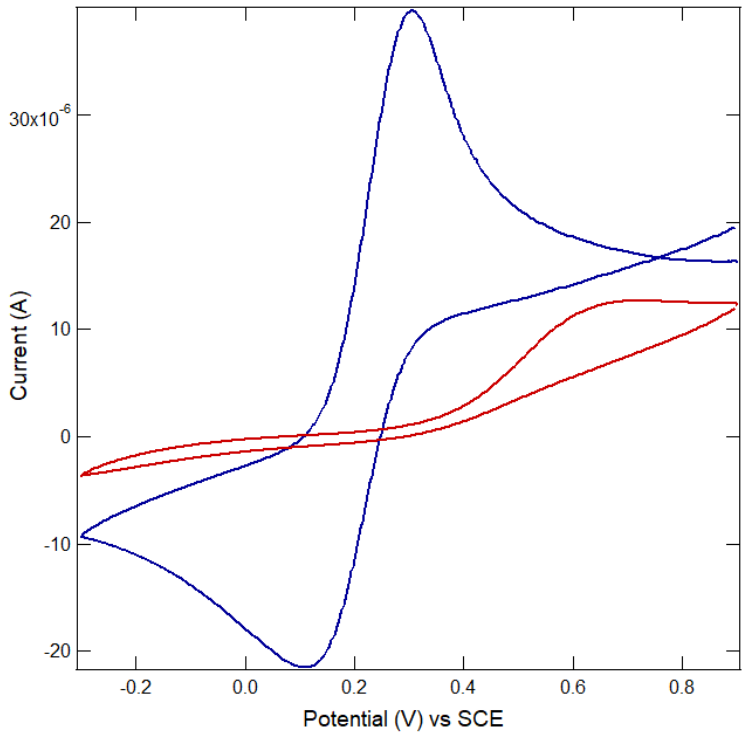

Figure 4.3. *CVs obtained at bare (blue) and F13OPA modified (red) ITO surface of 1 mM $K_3[Fe(CN)_6]$ in 0.1 M KCl with a scan rate of 0.1 V/s.*

The use of IR yielded inconclusive evidence of surface modification which was attribute to the rough surface of the ITO material leading to poor contact between the surface and the ATR crystal. As such, IR was not used further. CA results showed marked changes to surface wettability in accordance with literature values for modified ITO surfaces. CVs (figure 4.3) showed the presence of a blocking layer at ITO surfaces after modification with results like that seen in section 3.2. for electrochemical grafting of NBD on GC.

The optimised method involved, cleaning the substrate by sonicating the sample for 10 mins in DCM, followed by methanol and then IPA, soaking the sample in a 5 mM solution of THF and the phosphonic acid to modify the sample, rinsing the sample in fresh THF followed by annealing at 150 °C for 24 hours to drive SAM formation, and finally, sonicate the sample for 4 min in fresh THF, to remove any remaining debris, followed by drying with N_2.

4.3. Doped and Un-doped Chemical Vapour Deposition and Molecular Beam Epitaxy SnO_2 Surfaces Modified with 3,3,4,4,5,5,6,6,7,7,8,8,9,9,9-tridecafluorooctadecylphosphonic Acid, Octadecyl Phosphonic Acid and Benzene Pentafluoro Phosphonic Acid

Using the optimised modification method developed for ITO, a series of Sb doped and un-doped SnO_2 surface grown by both CVD and MBE were modified with F13OPA and ODPA. Modified and reference samples were characterised by laboratory based XPS with the aim of investigating the effectiveness of phosphonic acid surface modification on the different SnO_2 sample types.

4.3.1. Laboratory Based XPS Analysis of Doped and Un-Doped CVD and MBE Surfaces Modified with F13OPA and ODPA

XPS survey scans, F1s, O1s, C1s, P2p narrow scans and valence band spectra SnO_2 samples were recorded by Dr Colin Doyle, Department of Chemical and Materials Engineering, The University of Auckland and Alex McNeill, Department of Chemistry, The University of Canterbury.

Elemental compositions of surfaces were obtained from survey scans, specific elemental environments and peak ratios were obtained from F1s, O1s C1s and P2p narrow scans and changes to the SnO_2 low energy band edge were obtained from the narrow scan of the valence band of reference and modified SnO_2 surfaces. Results are discussed below in that order.

4.3.1.1. Laboratory Based XPS Analysis of CVD SnO_2 Surfaces Modified with F13OPA

XPS analysis of doped and un-doped, CVD grown SnO_2 surface modified with F13OPA, when compared to an unmodified reference sample, was expected to show the presence of both F and P. Furthermore, $\underline{C}F_3$, $\underline{C}F_2$ and P-$\underline{O}$ environments were expected to be present in C1s and O1s narrow scans respectively.

Table 4.1. *Elemental composition of CVD doped and un-doped SnO_2 surfaces modified with F13OPA obtained from XPS survey scans.*

Sample	F (%)	Sb (%)	O (%)	Sn (%)	C (%)	P+Sn[a] (%)
Un-doped CVD grown SnO_2 Reference	-	-	62.1	14.7	23.2	-
Un-doped CVD grown SnO_2 modified with F13OPA	25.3	-	43.3	10.2	14.4	6.8
Doped CVD grown SnO_2 Reference	-	5.3	60.0	10.8	24.9	-
Doped CVD grown SnO_2 modified with F13OPA	27.4	3.6	39.4	7.4	16.7	5.5

[a] *P2p and Sn4s cannot be resolved and fitted. The Sn4s peak is much larger the P2p.*

Elemental composistions (table 4.1) of the reference sample clearly shows the presence of Sb on doped samples. Additionaly, % Sn and O are equivilent between doped and un-doped samples. The amount of O on the surface is slightly greater than would be expected for stoicheometric Sn^{4+} however this is attributed to O being added to the surface via contamination (evidanced by the relatively high % of C at the surfaces). Although the total peak area of C on both modified and unmodified surfaces are similar, reference surfaces were measured as received and did not undergo the cleaning steps applied to modified samples. As expected, both F13OPA modified samples show the appearance of F and P at the surface gives direct evidence for the presence of F13OPA at the SnO_2 surfaces. It is noted (for this chapter) the % P also incorporates a portion of Sn due to overlap of the P2p and the Sn4s peaks. Therefore % P is only a qualitative measure and not entirely true of the total amount of P present at the surface.

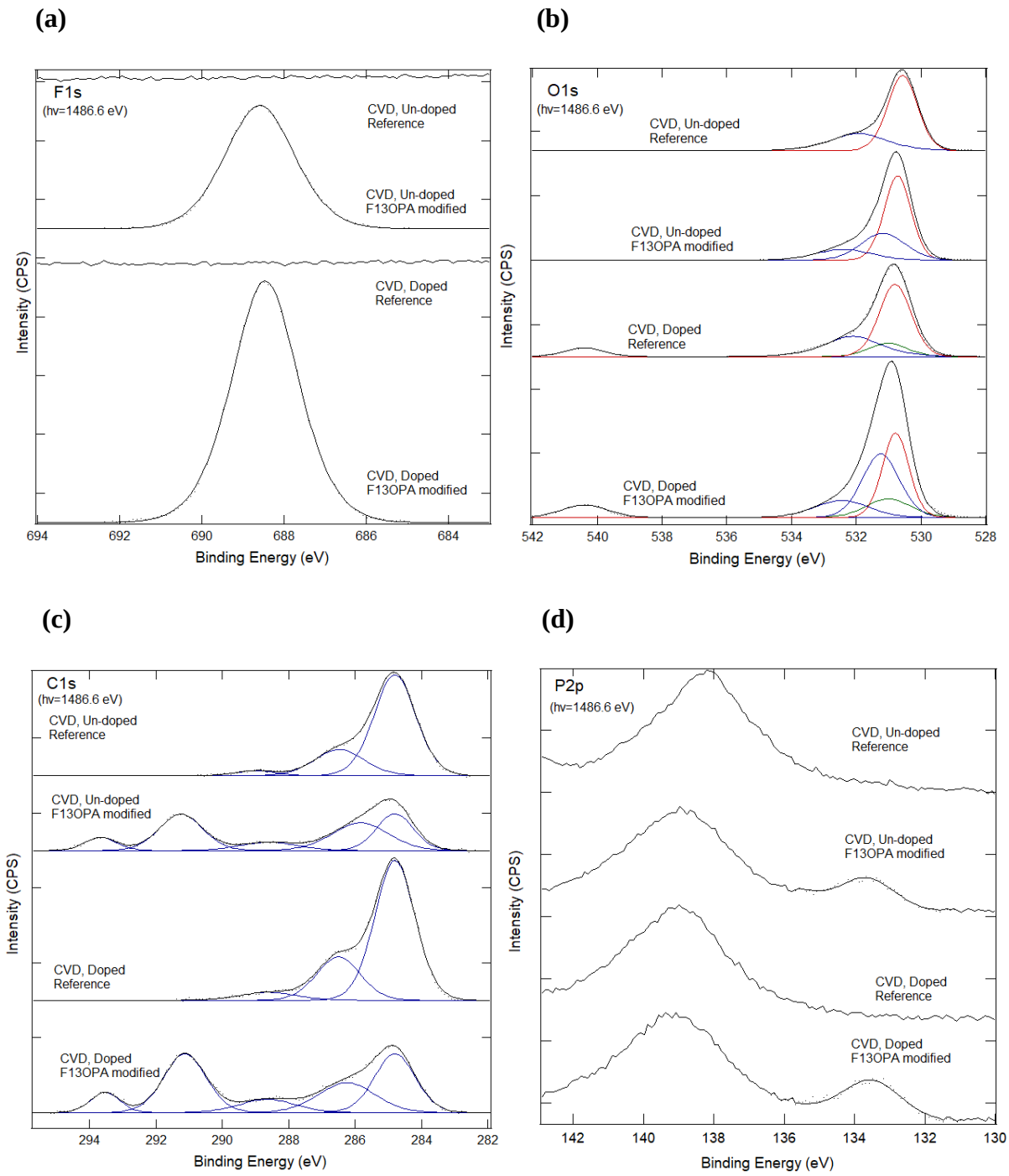

Figure 4.4. *XPS F1s, O1s, C1s and P2p narrow scans, (a), (b), (c) and (d) respectively, of CVD SnO_2 surfaces modified with F13OPA and their reference samples. (b) Spectrum normalised to the O1s bulk oxygen peak with bulk O peak and Sb3d 5/2 peaks highlighted red and green respectively. (a), (c) and (d) spectra are normalised to the Sn3d 5/2 peak from the XPS Sn3d narrow scan.*

Figure 4.4 shows narrow scans of the F1s, O1s, C1s and P2p regions. For these spectra and all other narrow scan spectra in this chapter the O1s spectra are normalised to the bulk O of

that sample and the F1s, C1s and P2p are normalised to the Sn3d 5/2 peak obtained from the narrow scan of the Sn3d region of that sample. All peak ratios obtained by laboratory based XPS have, have been divided by the RSF value for their respective elemental allowing a direct comparison of different elements.

The F1s narrow scans (figure 4.4(a)) confirm that there is a single F signal of modifier at each surface. This peak at 688.8 eV (table 4.2(a)) has been assigned to F of the F13OPA modifier.[87] It is noted that after normalisation of spectra to the Sn3d 5/2 peak of each sample, that the doped F13OPA modified sample shows an increased presence of F over the un-doped sample. No F could be detected in the narrow scan of the unmodified samples.

As shown in chapter 3, O1s narrow scan of reference samples show two peaks for surface and bulk O at 532.0 eV and 530.7 eV respectively.[76, 77] Bulk O signal shows a shift to slightly lower BE as seen in chapter 3 but is attributed to the much greater probing depth of the laboratory based XPS compared with synchrotron, and is consistently seen within all laboratory based XPS O1s spectra. While the modified samples retain bulk O signals, surface O signals are lost and two additional peaks are seen at 531.5 eV and 532.6 assigned to P-O and P-O-M respectively.[100] While no surface O peak is assigned for modified samples it is believed to hidden in the P-O peak.

Table 4.2. *Assigned peaks seen in XPS narrow scans for CVD doped and un-doped, SnO_2 surfaces modified with F13OPA. (a) F1s; (b) O1s, Sb3d; (c) C1s; (d) P2p. Note, for each element the listed percentages are for each component of that element. UD REF, UD MOD, D REF and D MOD refer to un-doped reference SnO_2, un-doped SnO_2 modified with F13OPA, doped reference SnO_2 and doped SnO_2 modified with F13OPA respectively.*

(a)

Element F1s	Binding Energy (± 0.2 eV)	Assignment	UD REF (%)	UD MOD (%)	D REF (%)	D MOD (%)
	688.8	F-C	-	100	-	100

(b)

Element O1s, Sb3d	Binding Energy (± 0.2 eV)	Assignment	UD REF (%)	UD MOD (%)	D REF (%)	D MOD (%)
	540.3	Sb 3/2	-	-	✓	✓
	532.6	Sn-O-P [100]	-	14.8	-	16.9
	532.0	Surface O	31.4	-	36.1	-
	531.5	P-O [100]	-	29.3	-	42.6
	530.9	Sb 5/2	-	-	✓	✓
	530.7	Bulk O	68.6	55.9	63.9	40.5

(c)

Element C1s	Binding Energy (± 0.2 eV)	Assignment	UD REF (%)	UD MOD (%)	D REF (%)	D MOD (%)
	293.0	C-F_3	-	7.6	-	7.5
	291.2	C-F_2	-	29.3	-	31.4
	288.8	π-π^*, Aromatic C	3.4	8.8	5.7	9.4

	286.5	C=O,[101] Adventitious C	22.7	-	23.8	-
	285.9	C-P,[101, 102] Adventitious C	-	29.1	-	21.4
	284.8	C-C, C-H, Adventitious C	73.9	25.2	70.5	30.3

(d)

Element P2p, Sn4s	**Binding Energy (± 0.2 eV)**	**Assignment**	**UD REF (%)**	**UD MOD (%)**	**D REF (%)**	**D MOD (%)**
	138.5	Sn [103]	100	85.6	100	83.8
	133.1	P-O [104]	-	14.4	-	16.2

C1s narrow scans (figure 4.4(c)) confirm the presence of F bound to C for the modified samples. The peaks at 293.0 and 291.2 eV assigned to CF_3 and CF_2 respectively.[88] These peaks directly connect the presence of F to the F13OPA modifier.

Figure 4.2(b) shows the P2p narrow scans. The small peak at 133.1 eV is assigned to P of the phosphonic acid.[104] An additional feature is seen at 139.0 eV assigned to Sn 4s electrons.[103] It is important to note that the P2p peak is made up of P2 $_{1/2}$ and P2 $_{3/2}$ peaks as a result of spin orbit coupling, however the sensitivity of the laboratory based XPS does not allow for accurate discrimination between them as such are counted as one for all calculations.

Table 4.3. *Ratios of peak areas obtained from XPS survey and narrow scans. Peak areas are normalised to the Sn3d 5/2 peak from the XPS narrow scan of that surface for CVD doped and un-doped SnO_2 surfaces modified with F13OPA.*

Sample	$\underline{C}F_2$:$\underline{C}F_3$	$\underline{C}F_3$:P	F:P	P:Sn3d	Surface $O_{(total)}$:Bulk O
Un-doped CVD grown SnO_2 Reference	-	-	-	-	0.5
Un-doped CVD grown SnO_2 modified with F13OPA	3.8	1.0	15.7	0.1	0.8
Doped CVD grown SnO_2 Reference	-	-	-	-	0.6
Doped CVD grown SnO_2 modified with F13OPA	4.2	1.1	18	0.1	1.4

Table 4.3 shows the ratios of relevant peak areas which highlight changes to the SnO_2 surface after modification. Ratios involving F, P and $\underline{C}$-F originate solely from the F13OPA modifier. And therefore, should give values equivalent to those elements within the F13OPA modifier. A ratio $\underline{C}F_2$:$\underline{C}F_3$ gives a value of approximately four for both modified surfaces. Although a value of five is expected for the five $\underline{C}F_2$ to one $\underline{C}F_3$, this result is within reasonable expectation considering equipment sensitivity. A ratio $\underline{C}F_3$:P for modified surfaces, where a value of one is expected, gives 1 and 1.1 for un-doped and doped modified surfaces respectively. And a ratio of F:P which would be expected to give a value of 13, is in reasonable agreement with the calculated 15.7 and 18 for un-doped and doped SnO_2 modified surfaces respectively. Furthermore, ratios of elements to Sn give a comparative measure of surface modification when compared to unmodified reference samples. Both modified surface shows an increase in surface O in relation to bulk O after modification. This attenuation of the bulk O signal shows the presence of a thin film at the surface reducing the probing depth of the X-rays. A possible explanation for the increased attenuation of the doped sample could be due to a more organised SAM allowing the phosphonic acid tail groups to organise in a more vertical increasing the film thickness in relation to the un-doped sample and thus increase the attenuation of the bulk O signal.

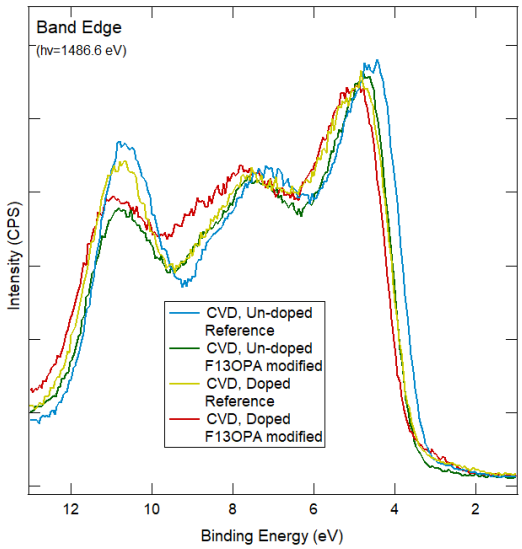

Figure 4.5. *XPS narrow scan of the of the valence band for CVD doped and un-doped SnO_2 surfaces modified with F13OPA and their reference samples.*

Figure 4.5 shows the overlay of XPS narrow scans of the valence band of modified and reference SnO_2 samples. The spectra show a shift to higher BE for the low energy band edge of modified SnO_2 surfaces, as well as attenuation of the Sn4d peak (10.5 eV) after modification. These results indicate an increase in downwards band bending of 0.2 and 0.1 eV for un-doped and doped F13OPA modified SnO_2 surfaces (table 4.5). While this change in band bending might seem surprising given a fluorinated modifier has been bonded to the SnO_2 surface, a similar result has been reported for ZnO surfaces.[50] This was attributed to the absence of conjugation in the phosphonic acid reducing its inductive effect on the SnO_2 surface. The phosphonic acid head group which acts as a separator between the surface and fluorocarbon tail makes changes to the band edge the result of the phosphonic acid group at the surface, not the entire modifier itself.

Table 4.4. *Summary of changes to the low energy band edge obtained from XPS valence band narrow scans of CVD doped and un-doped SnO_2 surfaces modified with F13OPA and compared to an unmodified reference samples.*

Sample	Low energy band edge (eV)	Change to band edge (eV)	Directional change in band bending
Un-doped CVD grown SnO_2 Reference	3.3	-	-
Un-doped CVD grown SnO_2 modified with F13OPA	3.5	0.2	Downwards
Doped CVD grown SnO_2 Reference	3.5	-	-
Doped CVD grown SnO_2 modified with F13OPA	3.7	0.1	Downwards

In summary, XPS results show that doped and un-doped SnO_2 surfaces grown by CVD can be modified with F13OPA. While both surfaces appear to have the same amount of modifier at the surface within experimental uncertainty, the greater attenuation of the bulk O signal seen for the doped F13OPA modified surface could be the result of a either more ordered SAM or increased presence of mono-dentate binding, however further experimentation would be required. The addition of the F13OPA to SnO_2 surfaces gives a small increase in the downwards band bending at the SnO_2 surface.

4.3.1.2. Laboratory Based XPS Analysis of MBE SnO_2 Surfaces Modified with F13OPA

XPS analysis of doped and un-doped, MBE grown SnO_2 surfaces modified with F13OPA were expected to show the presence of both F and P at the modified surface resultant from the F13OPA. Furthermore, $\underline{C}F_3$, $\underline{C}F_2$ and P-O environments were expected to be present in C1s and O1s narrow scans respectively.

Table 4.5. *Elemental composition of MBE, doped and un-doped SnO_2 surfaces modified with F13OPA obtained from XPS survey scans. Note: P/Sn % consists of the peak area of overlapping P2p and Sn4s peak. Due to the sensitivity of the survey scan these peaks could not be distinguished from one another.*

Sample	F (%)	Sb (%)	O (%)	Sn (%)	C (%)	P+Sn[a] (%)
Un-doped MBE grown SnO_2 Reference	-	-	55.9	13.0	31.1	-
Un-doped MBE grown SnO_2 modified with F13OPA	14.3	-	45.3	10.4	23.0	7.0
Doped MBE grown SnO_2 Reference	-	5.4	59.2	12.6	22.8	-
Doped MBE grown SnO_2 modified with F13OPA	28.3	3.1	34.3	6.7	21.5	6.1

[a] *P2p and Sn4s cannot be resolved and fitted. The Sn4s peak is much larger the P2p.*

Table 4.5 lists the atomic % of elements for all samples obtained from XPS survey scaans. As in section 4.3.1.1 both F13OPA modified surface show a strong presence of F and P. While the % of P is comparable at both surfaces it is noted that the un-doped F13OPA modified surface has half the amount of F detected at the modified doped surface. Elemental O and Sn are also shown to decrease after modification for doped SnO_2 indicating a thin film at the surface.

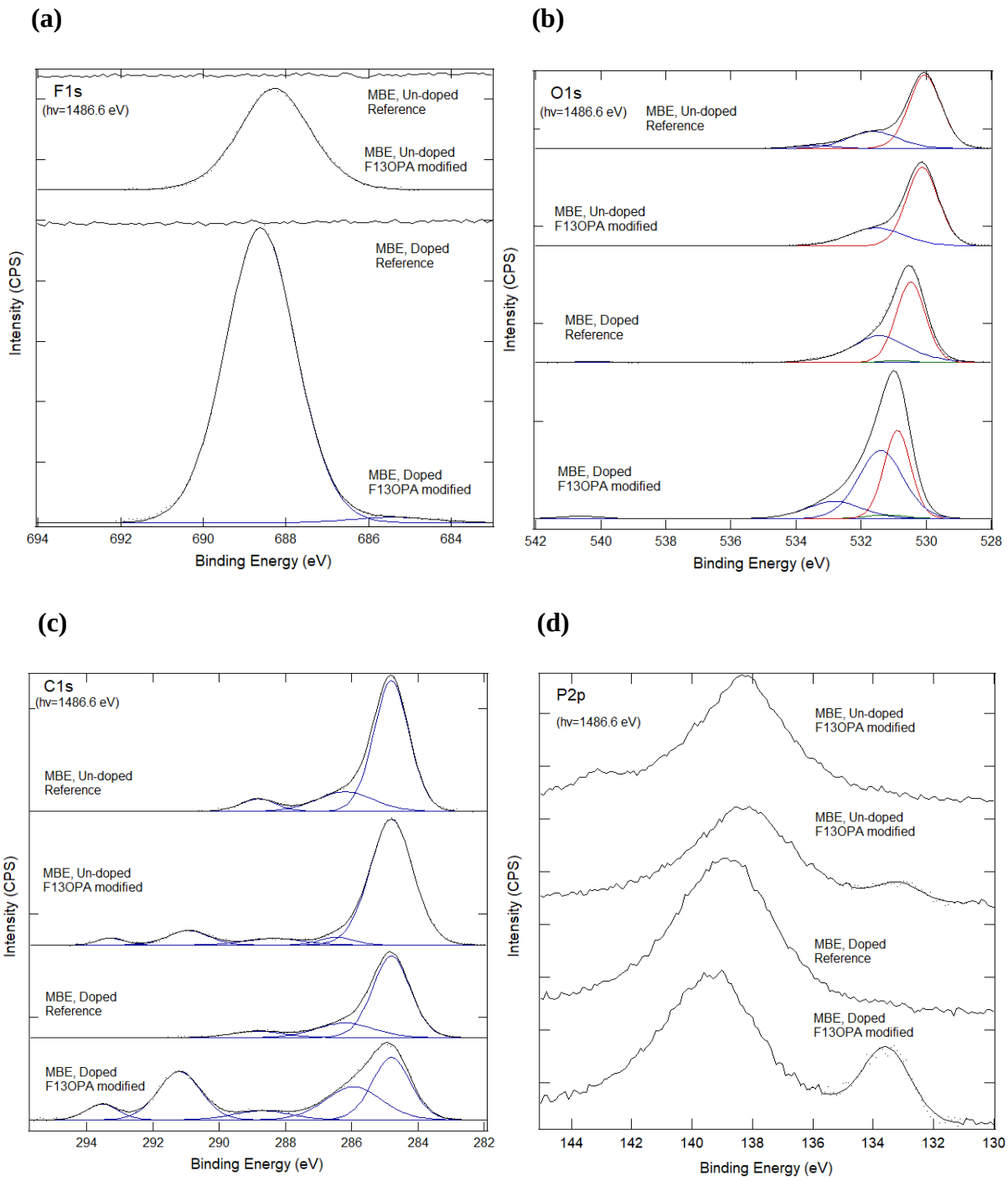

Figure 4.6. *XPS F1s, O1s, C1s and P2p narrow scans, (a), (b), (c) and (d) respectively, of MBE SnO_2 surfaces modified with F13OPA and their reference samples. (b) Spectrum normalised to the O1s bulk oxygen peak with bulk O peak and Sb3d 5/2 peaks highlighted red and green respectively. (a), (c) and (d) spectra are normalised to the Sn3d 5/2 peak from the XPS Sn3d narrow scan.*

Figure 4.6 and table 4.6 present data from XPS narrow scans. F1s (figure 4.6(a)) narrow scans again show the presence of F-C at both modified surfaces with a notable increase in F

at the doped surface. This is consistent with the results from the survey scan. The doped F13OPA modified surface shows an additional peak at lower BE (≈ 685eV) which is assigned to F bound to Sn (table 4.6).[105] The presence of F bound to Sn suggests a small amount of degradation of the F13OPA moiety.

In the O1s spectra (figure 4.6(b) and table 4.6), doped reference and modified surface, seen in the O1s spectra, show similar peaks to those for CVD surfaces modified with F13OPA (figure 4.4(a)). The doped reference surface shows bulk and surface O enviroments at ≈ 530.7 and 532.0 eV. After modification the BE for the bulk O is shifted and the surface O enviroment is split into two peaks relating to the P-O-Sn and the P-O. Un-doped surfaces however show a strong shift to lower BE in all peaks by ≈ 0.5 eV. The un-doped reference surface also shows an additional peak at 533.4 eV which is assigned to H_2O absorbed onto the surface. The un-doped modified surface however shows two peaks relating to the shifted bulk and surface O as well as P-O at 531.5 eV but no peak relating to Sn-O-P. A lack of P-O-Sn enviroments would suggest that F13OPA is only physisorbed onto the SnO_2 surface.

Table 4.6. *Assigned peaks seen in XPS narrow scans for MBE doped and un-doped, SnO_2 surfaces modified with F13OPA. (a) F1s; (b) O1s, Sb3d; (c) C1s; (d) P2p. Note, for each element the listed percentages are for each component of that element of UD REF, UD MOD, D REF and D MOD refer to un-doped references SnO_2, un-doped SnO_2 modified with F13OPA, doped reference SnO_2 and doped SnO_2 modified with F13OPA respectively.*

(a)

Element F1s	Binding Energy (± 0.2 eV)	Assignment	UD REF (%)	UD MOD (%)	D REF (%)	D MOD (%)
	688.8	F-C	-	100	-	97.9
	685.2	F-Sn [105]	-	-	-	2.1

(b)

Element O1s, Sb3d	Binding Energy (± 0.2 eV)	Assignment	UD REF (%)	UD MOD (%)	D REF (%)	D MOD (%)
	540.3	Sb 3/2	-	-	✓	✓
	533.4	H_2O	3.3	-	-	-
	532.6	Sn-O-P	-	-	-	14.8
	532.0 – 531.5	Surface O	25.7	-	40.3	-
	531.5	P-O	-	28.5	-	48.2
	531.0 – 530.1	Bulk O	71.0	71.5	59.7	37.0
	530.9	Sb 5/2	-	-	✓	✓

(c)

Element C1s	Binding Energy (± 0.2 eV)	Assignment	UD REF (%)	UD MOD (%)	D REF (%)	D MOD (%)
	293.0	C-F_3	-	2.8	-	6.9
	291.2	C-F_2	-	8.7	-	28.1

	288.8	π-π^*, Aromatic C	7.2	5.5	7.9	7.0
	286.5	C=O, Adventitious C	18.0	-	19.7	-
	285.9	C-P, Adventitious C	-	3.8	-	25.4
	284.8	C-C, C-H, Adventitious C	74.8	79.2	72.4	32.6

(d)

Element P2p	**Binding Energy (± 0.2 eV)**	**Assignment**	**UD REF (%)**	**UD MOD (%)**	**D REF (%)**	**D MOD (%)**
	138.5	Sn	100	91.8	100	79.4
	133.1	P-O	-	8.2	-	20.6

Figure 4.6(c) of the C1s narrow scan, shows two peaks at 293.0 eV and 291.2 eV for the F13OPA CF_3 and CF_2 groups respectively for modified SnO_2 surfaces. These peaks are seen to be larger for the doped SnO_2 surface which is consistent with the largest amount of F discussed above.

Figure 4.6(d) shows the presence of a P-O signal at 133.1 eV for both modified surfaces. No peak is present at this binding energy on the unmodified reference samples. This normalised spectra reveals a marked increase of P on the doped modified surface over the un-doped modified surface. While this is not supported by the elemental composition (table 4.5), an explanation for this could be due to a decreased presence of F seen on the un-doped sample. This would mean that less F13OPA is on the un-doped sample and as such % O and Sn is increase by comparison increasing the presence of Sn in % P/Sn.

Table 4.7. *Ratios of peak areas obtained from XPS survey and narrow scans. Peak areas are normalised to the Sn3d 5/2 peak from the XPS narrow scan of that surface for MBE doped and un-doped SnO_2 surfaces modified with F13OPA.*

Sample	$\underline{C}F_2$:$\underline{C}F_3$	$\underline{C}F_3$:P	$F_{(total)}$:P	P:Sn3d	Surface $O_{(total)}$:Bulk O
Un-doped MBE grown SnO_2 Reference	-	-	-	-	0.4
Un-doped MBE grown SnO_2 modified with F13OPA	3.1	1.2	17.7	<0.1	0.4
Doped MBE grown SnO_2 Reference	-	-	-	-	0.7
Doped MBE grown SnO_2 modified with F13OPA	4.1	1.1	17.3	0.1	1.6

Ratios of elements (table 4.7) pertaining strictly to the modifier further confirm the presence of F13OPA at the surface. Ratios of $\underline{C}F_2$:$\underline{C}F_3$, $\underline{C}F_3$:P and $F_{(total)}$:P give 3.1, 1.2 and 17.7 for the un-doped F13OPA modified surface, and 4.1, 1.1 and 17.3 for the doped F13OPA modified surface (table 4.7). These values are in reasonable agreement with expected values for a F13OPA moiety with deviations attributed to uncertainty of the P2p peak area based on its overlap with the Sn4s signal. Surface to bulk O ratios surprisingly, show no significant changes between reference and modified samples for the un-doped surface. This could be due to the organisation of the SAM were reduced presence of F13OPA means more horizontally orientated F13OPA tail group reducing the film thickness. A large change in the surface to bulk O ratio is seen for the doped modified sample however consistent with the presence of a thin film.

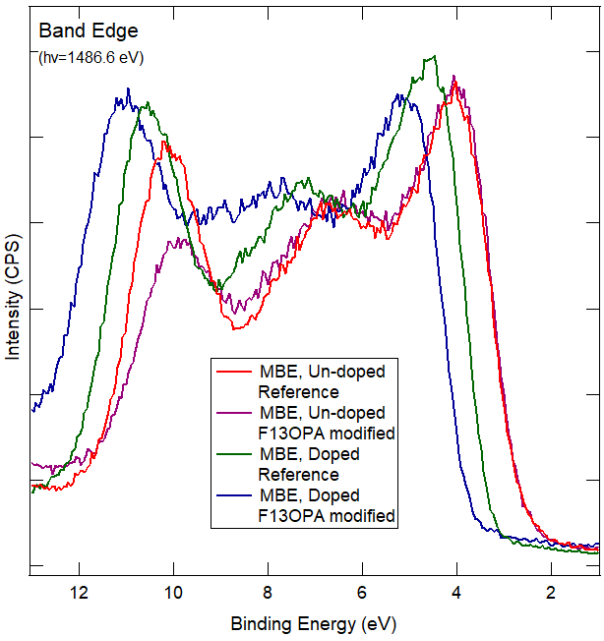

Figure 4.7. *XPS narrow scan of the of the valence band for MBE doped and un-doped SnO_2 surfaces modified with F13OPA and their reference samples.*

Figure 4.7 shows changes to the to the low energy band edge of MBE grown doped and un-doped SnO_2 surface. Apart from the un-doped F13OPA modified surface, SnO_2 surfaces show little attenuation of the Sn4d peak at ≈ 10.5 eV. This is surprising because as the discussed above other results suggest there is not much F13OPA at the un-doped surface. The reason for these apparently contradictory results is not known. Shifts in the low energy band edge are listed in table 4.8 with the doped F13OPA modified surface showing a large increase in downwards band bending. This result is consistent with results discussed earlier for CVD surfaces modified with F13OPA. In contrast, Figure 4.7 shows there is a negligible shift in the low energy band edge after modification of the un-doped material.

Table 4.8. *Summary of changes to the low energy band edge obtained from XPS valence band narrow scans of MBE doped and un-doped SnO_2 surfaces modified with F13OPA and compared to an unmodified reference samples.*

Sample	Low energy band edge (eV)	Change to band edge (eV)	Directional change in band bending
Un-doped MBE grown SnO_2 Reference	2.6	-	-
Un-doped MBE grown SnO_2 modified with F13OPA	2.6	0.0	None
Doped MBE grown SnO_2 Reference	3.3	-	-
Doped MBE grown SnO_2 modified with F13OPA	3.8	0.5	Downwards

Results for MBE grown SnO_2 show that both surfaces have been successfully modified with F13OPA showing a strong presence of F and P at the surface. The un-doped SnO_2 surface appears to be less well modified showing a decreased presence of P and F as compared to the modified doped sample. This result is also evidenced by no attenuation of the bulk O signal in relation to surface O and with no change in band bending. An increase in the downwards band bending of the modified doped SnO_2 surface.

4.3.1.3. Laboratory Based XPS Analysis of CVD SnO_2 Surfaces Modified with ODPA

XPS analysis of doped and un-doped, CVD grown SnO_2 surface modified with ODPA, were expected to show the presence of P at the modified surfaces with a marked increase in the presence of C at the surface after modification.

Table 4.9. *Elemental composition of CVD doped and un-doped SnO_2 surfaces modified with ODPA obtained from XPS survey scans*

Sample	Sb (%)	O (%)	Sn (%)	C (%)	P+Sn[a] (%)
Un-doped CVD grown SnO_2 Reference	-	62.1	14.7	23.2	-
Un-doped CVD grown SnO_2 modified with ODPA	-	52.5	12.6	26.3	8.3
Doped CVD grown SnO_2 Reference	5.3	60.0	10.8	24.9	-
Doped CVD grown SnO_2 modified with ODPA	3.6	39.4	8.5	42.2	6.3

[a] *P2p and Sn4s cannot be resolved and fitted. The Sn4s peak is much larger the P2p.*

Table 4.9 shows the expected presence of Sb, for both doped surfaces and P for both modified surfaces. The % O and Sn are shown to decrease after modification whereas there is an increase in C. The un-doped modified surface shows a higher percentage of P at the surface than does the doped modified surface. However, there is a significantly larger proportion of C at the doped modified surface. this suggest that adventitious C contamination may be important for the doped modified surface.

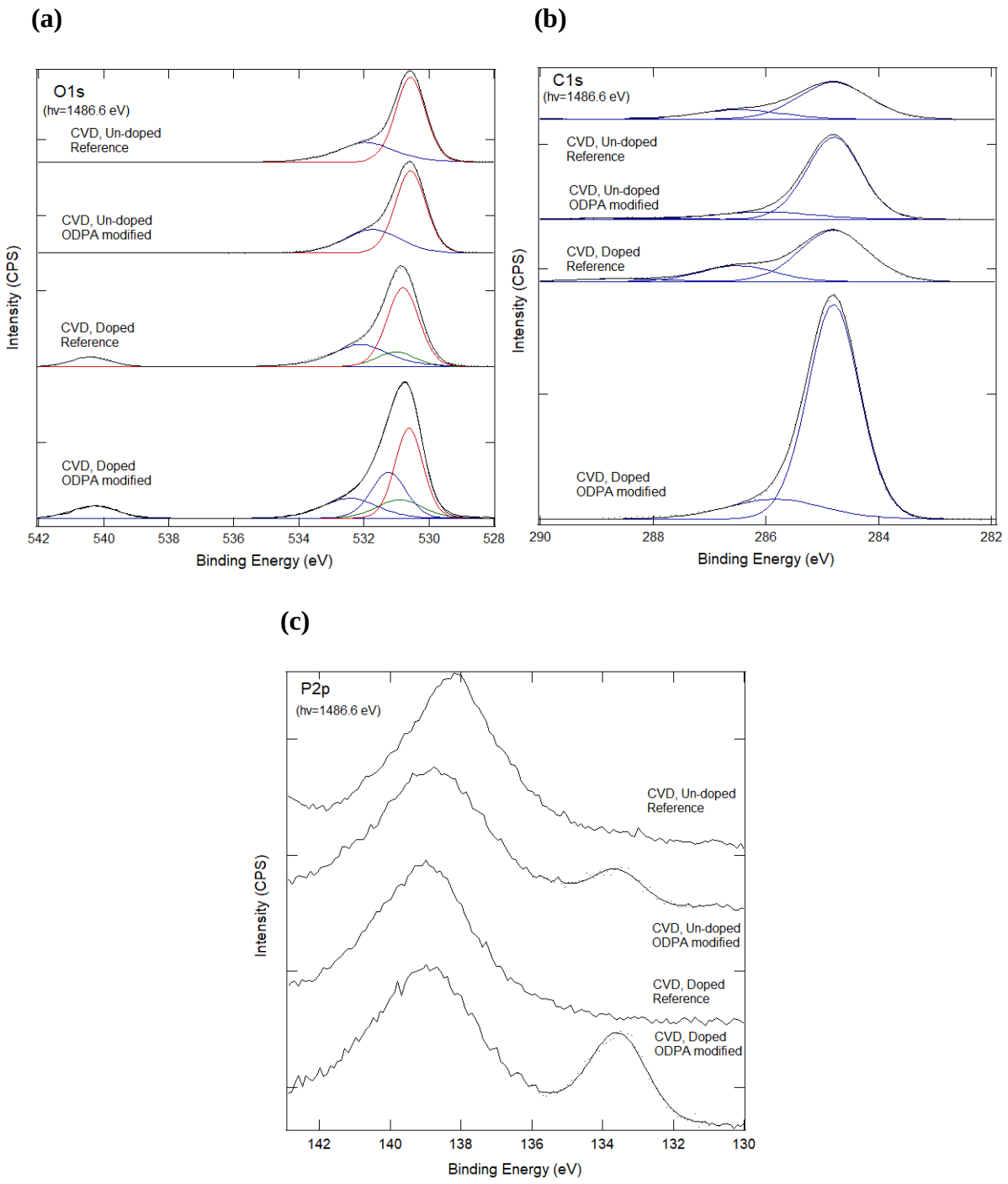

Figure 4.8. *XPS O1s, C1s and P2p narrow scans, (a), (b), and (c) respectively, of CVD SnO_2 surfaces modified with ODPA and their reference samples. (a) Spectrum normalised to the O1s surface oxygen peak with bulk oxygen peak and Sb3d 5/2 peaks highlighted red and green respectively. (c) and (d) spectra are normalised to the Sn3d 5/2 peak from the XPS Sn3d narrow scan.*

XPS narrow scans are shown in figure 4.8 and table 4.10 lists the peak assignments. The O1s narrow scans (figure 4.8(a)) show bulk and surface O signals for both doped and un-doped

reference samples at ≈ 530.7 eV and ≈ 532.0 eV respectively (table 4.10). After modification, both modified surfaces show the disappearance of the surface O signal and addition of the P-O peak of the phosphonic acid at 531.5 eV. The modified doped surface also shows an additional peak at 532.6 eV assigned to Sn-O-P. This evidence suggests that phosphonic acids are only covalently bound on the doped SnO_2 surface.

C1s narrow scans for doped and un-doped reference samples show three peaks at 284.8 eV, 286.5 eV and 288.8 eV assigned to adventitious C. After modification of both un-doped and doped samples, there is an increase in the peak at 284.5 eV, consistent with addition of the ODPA modifier. there is also a much smaller peak at 285.9 eV which is assigned to P bound to C.[101, 102] Both peaks are larger at the modified doped sample suggesting the surface has a higher concentration of ODPA. The P2p signals (figure 4.8(c)) are consistent with this interpretation with a larger peak seen for the modified doped sample than the un-doped.

Table 4.10. *Assigned peaks seen in XPS narrow scans for CVD doped and un-doped, SnO_2 surfaces modified with ODPA. (a) O1s, Sb3d; (b) C1s; (c) P2p. Note, for each element the listed percentages are for each component of that element of UD REF, UD MOD, D REF and D MOD refer to un-doped references SnO_2, un-doped SnO_2 modified with ODPA, doped reference SnO_2 and doped SnO_2 modified with ODPA respectively.*

(a)

Element O1s, Sb3d	Binding Energy (± 0.2 eV)	Assignment	UD REF (%)	UD MOD (%)	D REF (%)	D MOD (%)
	540.3	Sb 3/2	-	-	✓	✓
	532.6	Sn-O-P	-	-	-	21.0
	532.0	Surface O	31.4	-	36.1	-
	531.5	P-O	-	34.1	-	30.6
	531.0 – 530.1	Bulk O	68.6	65.9	63.9	48.4
	530.9	Sb 5/2	-	-	✓	✓

(b)

Element C1s	Binding Energy (± 0.2 eV)	Assignment	UD REF (%)	UD MOD (%)	D REF (%)	D MOD (%)
	288.8	π-π*, Aromatic C	3.4	2.2	5.7	-
	286.5	C=O, Adventitious C	22.7	-	23.8	-
	285.9	C-P	-	13.3	-	14.7
	284.8	C-C, C-H, Adventitious C	73.9	84.5	70.5	85.3

(c)

Element P2p	Binding Energy (± 0.2 eV)	Assignment	UD REF (%)	UD MOD (%)	D REF (%)	D MOD (%)
	138.5	Sn	100	89.0	100	77.6
	133.1	P-O	-	11.0	-	22.4

For an ODPA modified surface free of any adventitious C, a ratio of $C_{(total)}$:P would yield a value of 18 for the 18 C of the ODPA aliphatic chain to the one P of the phosphonic acid head group. Table 4.11 gives vales of 27.9.2 and 26.2 for un-doped and doped ODPA modified surface respectively. While this is in reasonable agreement with the expected presence of C, it does show the presence of adventitious C on both surfaces.

Table 4.11. *Ratios of peak areas obtained from XPS survey and narrow scans. Peak areas are normalised to the Sn3d 5/2 peak from the XPS narrow scan of that surface for CVD doped and un-doped SnO_2 surfaces modified with ODPA.*

Sample	$C_{(total)}$:P	P:Sn3d	$C_{(total)}$:Sn3d	Surface $O_{(total)}$:Bulk O
Un-doped CVD grown SnO_2 Reference	-	-	1.2	0.5
Un-doped CVD grown SnO_2 modified with ODPA	27.9	0.1	1.7	0.5
Doped CVD grown SnO_2 Reference	-	-	1.6	0.6
Doped CVD grown SnO_2 modified with ODPA	26.2	0.2	4.3	1.1

Ratios for the doped modified SnO_2 surface show a more effective surface treatment, where larger P:Sn, C:Sn and an increase in Surface O:Bulk O ratios after modification are all indicative of a greater presence of ODPA at the surface than for the modified un-doped surface.

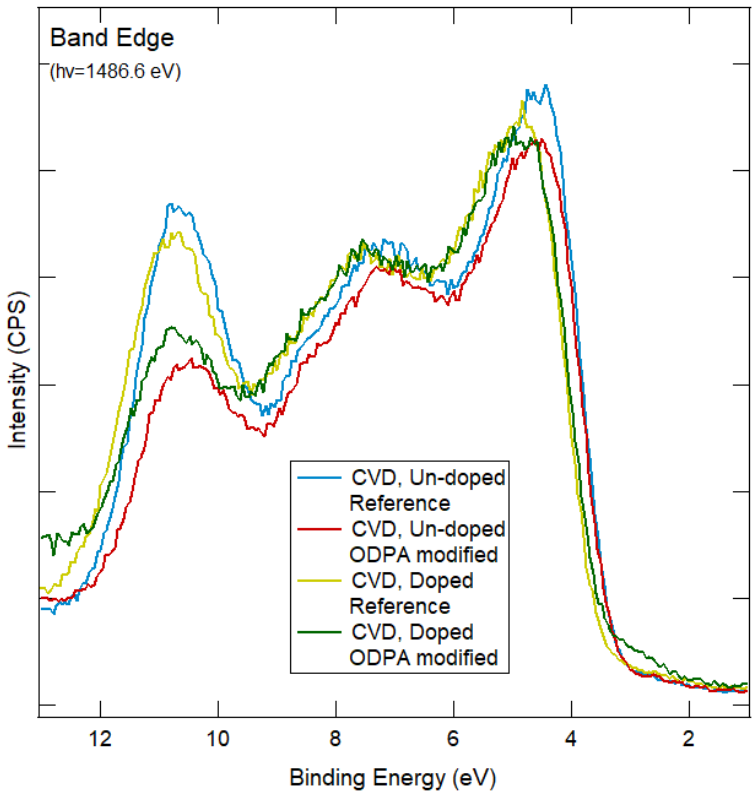

Figure 4.9. *XPS narrow scan of the of the valence band for CVD doped and un-doped SnO_2 surfaces modified with ODPA and their reference samples.*

Valence band narrow scans (figure 4.9) show the expected drop in the Sn4d signal at ≈ 10.5 eV for modified surfaces as a result of the attenuation of electrons by the modifying layer. The presence of Sb is shown to influence the band edge with doped surfaces being at higher binding energies. While ODPA was expected to increase the downwards band bending, table 4.12 shows no change to the valence band for the un-doped modified surface. A decrease in downwards band bending for the doped modified surface is seen however, with a shift of 0.1 eV. This result is unexpected where a similar experiment by McNeill et al.[50] modified the different faces of ZnO with ODPA finding that the ZnO downwards band bending was increase for all ZnO faces modified with ODPA. The reason for the contradictory results seen in this work is unknown and require further investigation.

Table 4.12. *Summary of changes to the low energy band edge obtained from XPS valence band narrow scans of CVD doped and un-doped SnO_2 surfaces modified with ODPA and compared to unmodified reference samples.*

Sample	Low energy band edge (eV)	Change to band edge (eV)	Directional change in band bending
Un-doped CVD grown SnO_2 Reference	3.3	-	-
Un-doped CVD grown SnO_2 modified with ODPA	3.3	0.0	None
Doped CVD grown SnO_2 Reference	3.5	-	-
Doped CVD grown SnO_2 modified with ODPA	3.4	-0.1	Upwards

Results described above show the presence of ODPA on both doped and un-doped CVD grown SnO_2 surface after modification. The doped SnO_2 surface appears to be more thoroughly modified evidenced by a greater amount of C and P at the surface. Further evidence is given for this shown by changes to O signal arising from SnO_2. Furthermore, a decrease in the downwards band bending of 0.1 eV is seen for the doped SnO_2 surface after modification not seen for the un-doped modified surface. Due to a lack of Sn-O-P signal for the un-doped modified sample it is believed that ODPA is likely physisorbed to the SnO_2 surface rather than covalently bound. This is consistent with results discussed above for CVD and MBE surfaces modified with F13OPA where it was found that the doped SnO_2 surface had a greater extent of surface modification.

4.3.1.4. Comparison of Laboratory Based XPS Analysis of SnO_2 Surfaces Modified with F13OPA and ODPA

Table 4.13 shows a summary of values for all SnO_2 surfaces modified with F13OPA. Ratio of F:Sn and P:Sn give confidence to doped surfaces being more extensively modified. While an increase is only seen for F CVD and MBE doped surface, the equivalent values seen for P on

all surfaces are within reasonable agreement to the presence of F when accounting for rounding. This is further supported by increased presence of surface O over bulk O for all doped surfaces. This suggest the importance of Sb, not just as dopant, but also as a promoter of the surface modification of SnO_2 surfaces with phosphonic acids. An explanation for this could be due to an increase in surface roughness due to the presence of Sb increasing the surfaces area and active sights availed for modification.[106] Or the rate at which phosphonic acids bond to the surface is increased by the increased presence of free electrons at the surface due to the Sb dopant.[39]

Table 4.13. *Valence band edge measurements and ratios of peak areas of CVD, doped and un-doped and MBE doped SnO_2 surfaces modified with F13OPA obtained from XPS narrow scans.*

Sample	$F_{(total)}$:Sn	P:Sn	Surface $O_{(total)}$:Bulk O	Change to valence band edge (eV)
Un-doped CVD grown SnO_2 F13OPA modified	1.4	0.1	0.8	0.2
Un-doped MBE grown SnO_2 modified with F13OPA	0.8	<0.1	0.4	0.0
Doped CVD grown SnO_2 F13OPA modified	2.0	0.1	1.4	0.1
Doped MBE grown SnO_2 modified with F13OPA	2.4	0.1	1.6	0.5

Changes to the SnO_2 band edge do no follow the same trend. The largest change is seen for the doped MBE modified surface, and the smallest, for the doped CVD modified surface. Although not entirely understood, a possible explanation for this could be related to the SnO_2 growth method used and the resulting organisation of atoms at the SnO_2 surface. For these samples the change in band bending is significantly large for the doped MBE grown sample than for the corresponding CVD grown sample. However repeat experiments are necessary before the generality of this result can be established.

While no trends could be found pertaining to changes to the band bending, these results suggest modification of SnO_2 surfaces with phosphonic acids is only influenced by the presence of the dopant Sb and not the growth method used to produce the SnO_2 substrate.

This is consistent with results seen in chapter 3 where the presence of Sb was seen to show increased modification of SnO_2 surfaces modified with aryl diazoniums salts.

4.3.2. Synchrotron XPS Analysis of Moderately Doped MBE SnO_2 Surfaces Modified with F13OPA, ODPA and PFBPA

Given the results, for SnO_2 surfaces modified with phosphonic acids obtained with the laboratory based XPS instrument, moderately doped SnO_2 samples, grown by MBE, modified with F13OPA, ODPA and PFBPA (figure 4.2) were taken to the Australian Synchrotron for XPS analysis of SnO_2 surface at a much greater surface sensitivity.

4.3.2.1. Moderately Doped MBE SnO_2 Surfaces Modified with F13OPA, ODPA and PFBPA

XPS survey scans and F1s, O1s, C1s, P2p and valence band narrow scan spectra were taken of moderately Sb doped, MBE grown, SnO_2 surfaces modified with F13OPA, ODPA and PFBPA. Measurements were carried out at the Australian Synchrotron by Martin Allen, Roger Reeves, Rodrigo Gazoni, Alexandra McNeill and Jonty Scott of the University of Canterbury.

CA and AFM topographical measurements were also carried on modified surfaces after XPS analysis with results discussed below in the order of CA, AFM and XPS.

4.3.2.1.1. CA and AFM Measurements of Moderately Doped MBE SnO_2 Surfaces Modified with F13OPA, ODPA and PFBPA

Modification of SnO_2 surfaces with F13OPA, ODPA and PFBPA was expected to decrease surface wettability giving an increase in CA. However, results of CA measurements (table 4.14) show no change in surface wettability, within experimental error, this is because unmodified values are very high close to literature values for modified surfaces. This means that CA results neither confirm or deny the presence of a thin film at the surface and thus modification of the SnO_2 surface with phosphonic acids.

Table 4.14. *Summary of results for CA and AFM surface roughness and modification layer thickness for MBE moderately doped unmodified and F13OPA, ODPA and PFBPA modified SnO_2 sample.*

Sample	CA (°)	Literature CA (°)	Roughness (nm)	Thickness (nm)
Moderately doped MBE grown SnO_2 reference	99 ± 2	96	0.4 ± 1	-
Moderately doped MBE grown SnO_2 modified with F13OPA	92 ± 3	108[a]	0.2 ± < 0.1	0.4 ± < 0.1
Moderately doped MBE grown SnO_2 modified with ODPA	96 ± 5	103[b]	1 ± 0.1	1 ± 0.3
Moderately doped MBE grown SnO_2 modified with PFBPA	97 ± 2	≈ 91[c]	1 ± 0.1	0.7 ± < 0.1

[a] reference 107 for F13OPA on ITO.[107] [b] reference 48 for ODPA on ITO.[48] [c] reference 108 for a structurally similar silane derivate on silicon oxide.[108]

The data in table 4.14 shows that except for the F13OPA modified surface, AFM surface roughness measurements show a large increase in surface roughness by ≈ 0.6 nm as compared to the unmodified reference sample. This indicates the presence of a thin film at the surface as a result of modification with phosphonic acids. This increase in surface roughness after modification is consistent with results seen in chapter 3 for SnO_2 surface modified with aryl diazonium salts. This could explain the reduced CA values from expected literature of modified surfaces were increased surface roughness has been shown to increase surface wetability.[70, 109] It is important to note that no direct CA could be found for PFBPA. The CA in table 4.14 is of a structurally similar silane derivative of PFBPA used on native silicon oxide.[108]

(a)

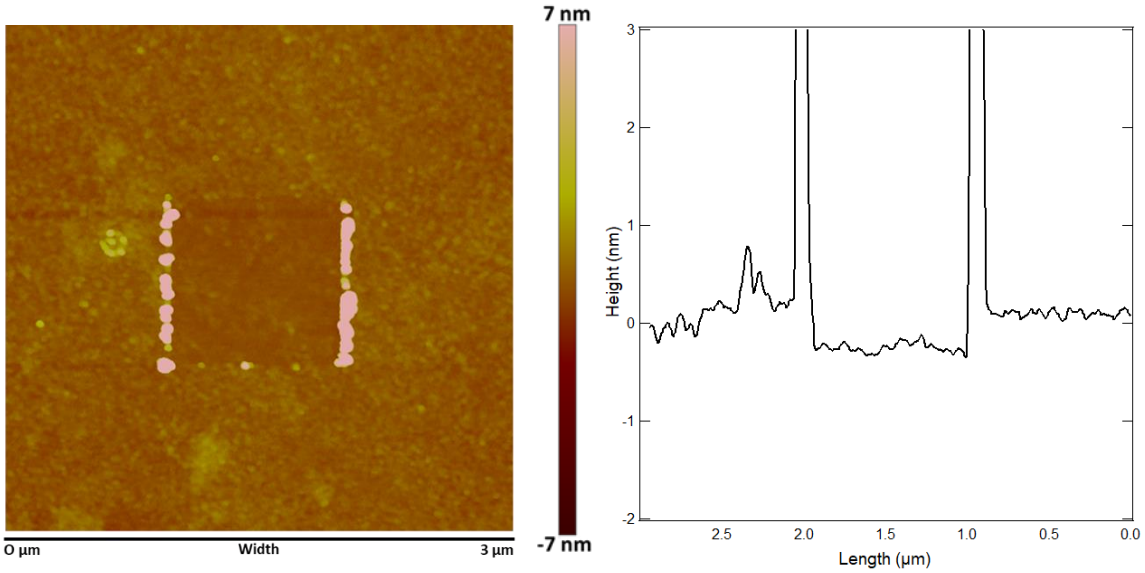
7 nm
-7 nm
O µm
Width
3 µm
Height (nm)
Length (µm)
3
2
1
0
-1
-2
2.5
2.0
1.5
1.0
0.5
0.0

(b)

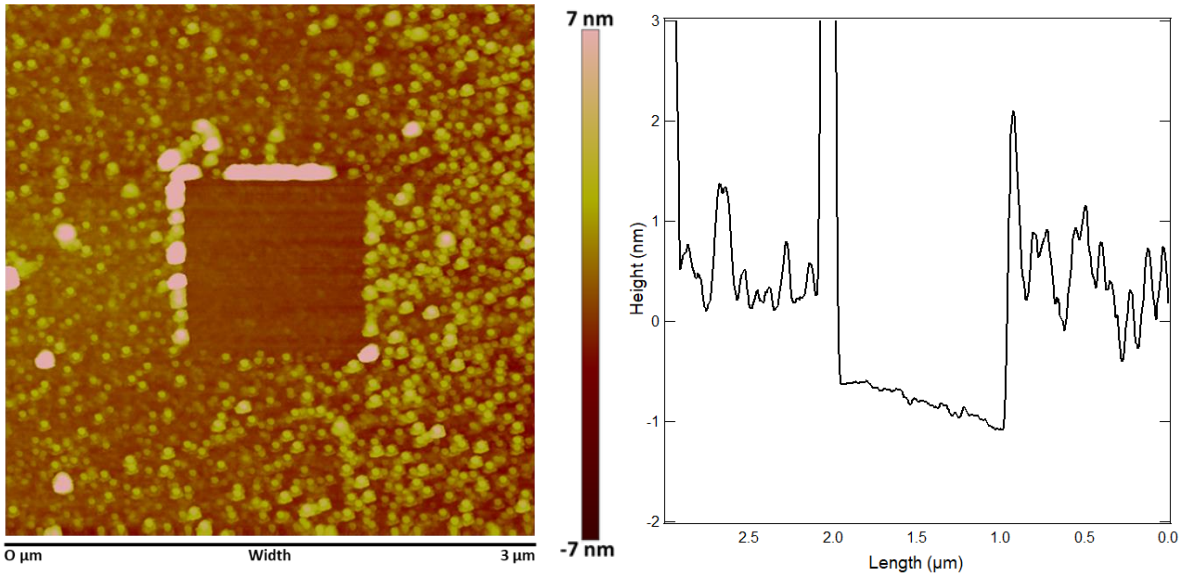
7 nm
-7 nm
O µm
Width
3 µm
Height (nm)
Length (µm)
3
2
1
0
-1
-2
2.5
2.0
1.5
1.0
0.5
0.0

(c)

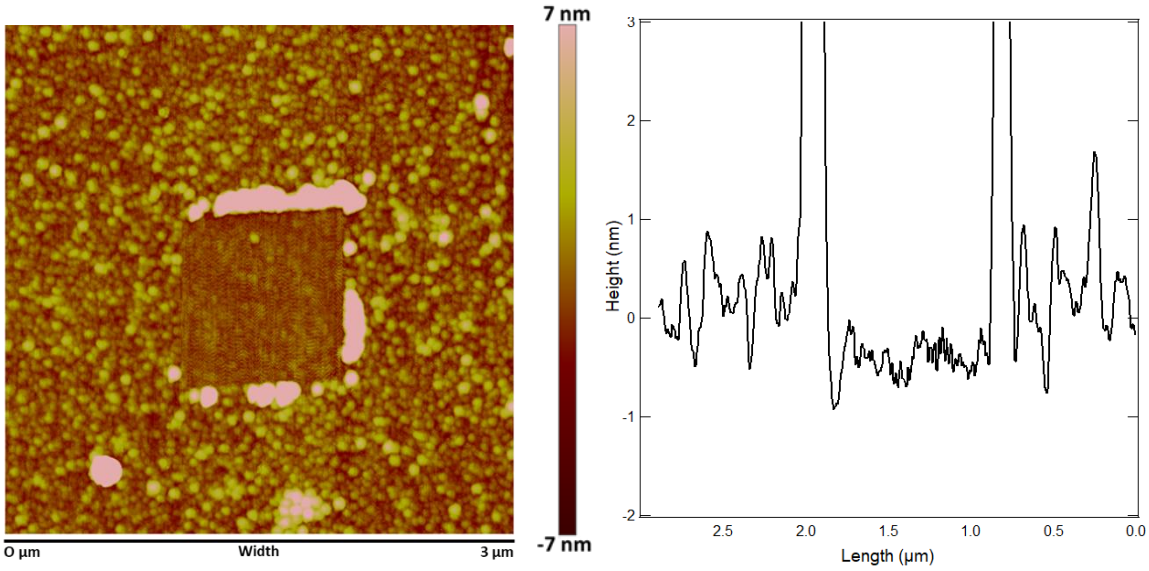

Figure 4.10. *Surface topography measurements taken by AFM showing the modified surfaces after the modification has been removed in a central area. The corresponding depth profiles of the surfaces are also shown. (a) F13OPA modified SnO_2 (b) ODPA modified SnO_2 and (c) PFBPA modified SnO_2.*

AFM topographical images (figure 4.10) reveal the presence of a thin film at the SnO_2 surface. A difference in depth and roughness can be seen between modified and scratched sections of the surfaces. Film thicknesses were measured at 0.1 nm, 0.4 nm and 0.7 nm for F13OPA, ODPA and PFBPA modified surfaces. Figure 4.10(a) of the F13OPA modified surface shows a notable reduction of surface definition compared to the images of the other modified surfaces and those seen in chapter 3. It is suspected to be a feature of the AFM tip not making good contact with the surface and therefore is not a reliable measure of the modified surface.

Literature film thickness values of F13OPA, ODPA and PFBPA give ≈ 1.4 nm (for un-fluorinated octyl phosphonic acid on Au)[110], 1.9 nm[111] and ≈ 1.2 nm (of the silane derivative used on native silicon oxide)[108] respectively. Measured film thicknesses that are smaller than the molecular length of the phosphonic acid are attributed to a combination of degradation of the thin film, were several months had passed before these measurements could be made, film thickness measurements were only collected at one point at the surface not allowing for variation in film thicknesses across surface and increasing statistical certainty and non-lateral organisation of the SAM where phosphonic acid moieties are tilted towards the surface more

than would be expected. The last explanation is likely the biggest contributing factor to the reduced film thickness with evidence for this discussed seen in earlier sections of this chapter.

Nevertheless, results presented above suggest moderately doped, MBE grown SnO_2 surface have been successfully modified with F13OPA, ODPA and PFBPA. Further investigation by XPS is required to make more detailed conclusions.

4.3.2.1.2. XPS Measurements of MBE SnO_2 Surfaces Modified with F13OPA, ODPA and PFBPA

Synchrotron XPS results were expected to yield similar results but with a higher sensitivity to those shown above for surface analysed by laboratory based XPS. F1s, O1s and C1s narrow scans were expected to show the presence of F and CF environments for F13OPA and PFBPA as well as presence of O-P environments for all modified surface.

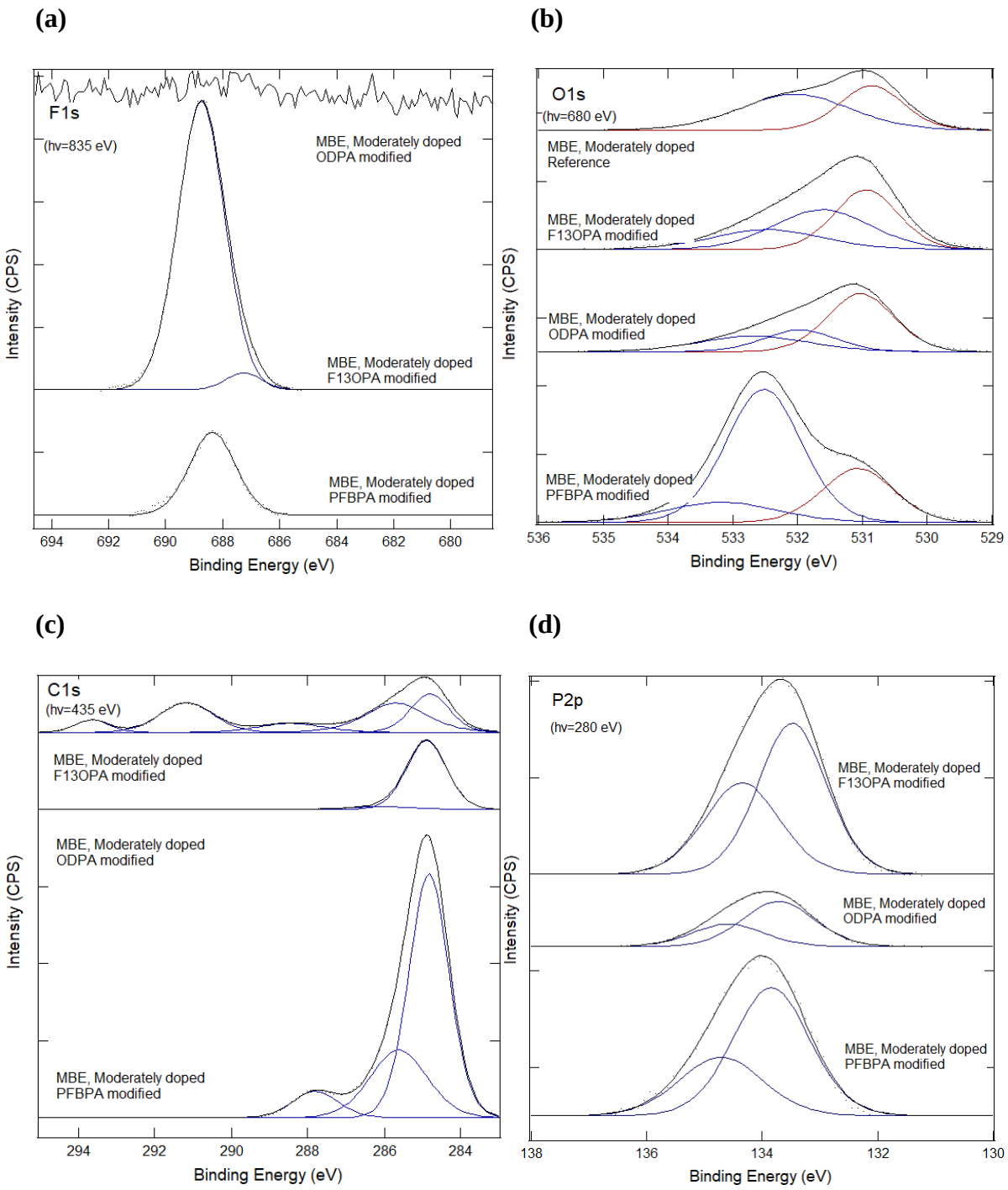

Figure 4.11. *XPS F1s, O1s, C1s and P2p narrow scans, (a), (b), (c) and (d) respectively, of moderately doped MBE SnO_2 surfaces modified with F13OPA, ODPA and PFBPA and their reference samples. (b) Spectrum normalised to the O1s bulk oxygen peaks with bulk O peak highlighted red. (a), (c) and (d) spectra are normalised to the Sn3d 5/2 peak from the XPS survey scan.*

F1s narrow scan show (figure 4.11(a)) shows the presence of F on both F13OPA and PFBPA modified surfaces as expected. The F13OPA modified surface shows two peaks at 688.9 eV

and 687.3 eV assigned to F-C and F-$C_{(aromatic)}$ (table 4.15).[87, 112, 113] While F-$C_{(aromatic)}$ is unexpected for F13OPA modified surfaces it is likely a result of adventitious contamination. The PFBPA surface shows the presence of one peak at 688.0 eV for F-$C_{(aromatic)}$. Given 13 F of F13OPA to five F of PFBPA, the increased presence of F for the F13OPA modified surface is reasonable for a surface that has a similar degree of modification as that of the PFBPA modified surface.

O1s narrow scans of all surfaces show the presence of bulk O of the SnO_2 substrate at ≈ 530.7 eV (figure 4.11(b)). Un-modified reference sample show a surface O peak at 532.0 eV while all modified surfaces show a disappearance of the SnO_2 surface O environments and the appearance of two addition peaks at 532.6 eV and 531.5 eV assigned to Sn-O-P and P-O of the phosphonic acid head group.[100] These two peaks are seen to shift by ≈ 0.3 eV for the PFBPA modified surface which is attributed to electron withdrawing effects of the fluorophenyl ring of the PFBPA. While all three modified surface show a similar presence of Sn-O-P environments, the PFBPA surface shows a marked increase of phosphonic acid P-O groups. An explanation for this is that PFBPA moieties are bound to the surface predominantly in a mono-dentate fashion. This would increase the presence of un-bound P-O environments in relation to P-O-M environments.

Table 4.15. *Assigned peaks seen in XPS narrow scans for MBE moderately doped SnO_2 surfaces modified with F13OPA, ODPA and PFBPA including an unmodified reference sample. (a) F1s; (b) O1s, (c) C1s; (d) P2p. Note, for each element the listed percentages are for each component of that element of REF, F13OPA, ODPA and PFBPA refer to moderately doped, reference, F13OPA modified, ODPA modified and PFBPA modified SnO_2 respectively.*

(a)

Element F1s	Binding Energy (± 0.2 eV)	Assignment	REF (%)	F13OPA (%)	ODPA (%)	PFBPA (%)
	688.9	F-C		95.7	-	
	688.0-687.3	F-$C_{(aromatic)}$ [112, 113]		4.3		100

(b)

Element O1s	Binding Energy (± 0.2 eV)	Assignment	REF (%)	F13OPA (%)	ODPA (%)	PFBPA (%)
	532.6	Sn-O-P	-	22.1	24.0	13.8
	532.0	Surface O	58.1	-	22.0	-
	531.5	P-O	-	39.0	-	62.4
	530.7	Bulk O	41.9	38.9	54.0	23.9

(c)

Element C1s	Binding Energy (± 0.2 eV)	Assignment	REF (%)	F13OPA (%)	ODPA (%)	PFBPA (%)
	293.0	C-F_3		7.0	-	-
	291.2	C-F_2		26.2	-	-
	288.8	π-π^*, Aromatic C		9.9	-	-
	287.8	Aromatic C-F [112]		-	-	8.0
	285.9	C-P		31.3	6.0	26.0

	284.8	C-C, C-H, Adventitious C		25.6	94.0	66.0

(d)

Element P2p	Binding Energy (± 0.2 eV)	Assignment	REF (%)	F13OPA (%)	ODPA (%)	PFBPA (%)
	138.5	Sn	100			
	134.4	P2p $_{1/2}$ [114]	-			
	133.5	P2p $_{3/2}$ [114]	-			

In addition to adventitious C, the C1s narrow scan shows two expected peaks 293.0 eV and 291.2 eV for the F13OPA modified sample showing the presence of CF_3 and CF_2. In contrast the ODPA modified surface shows a loss of nearly all C environments except that of C-C at 284.8 eV. As discussed in section 4.3.1.3, the addition of each ODPA modifier to the surface adds 18 C, accounting for the increase in the C-C environment. The PFBPA modified surface shows the presence of three signals at 284.8 eV, 285.9 eV and 287.8 eV assigned to C-C, C-P and aromatic C-F.[81, 101, 102, 112] The increased presence of C-C environments in relation to aromatic C-F environments is unexpected. It is not known whether this is due to contamination or other factors at the surface.

It is noted that a large presence of adventitious C is seen on all modified surfaces within this chapter except for ODPA modified surfaces. For cleaned surfaces that have then been modified consist primarily of environments relating to the moiety. Research by Kuilong et al.[115] and Hitoshi et al.[116] examined the degradation of THF at various surfaces including Al and Ni at different temperatures where it was found that heating of surfaces containing THF above 45 °C caused THF to degrade forming ether bonds to that surface with an increase in degradation and film formation as temperatures increased to >300 °C (figure 4.12). For the present work, it is proposed that given the use of THF as the modifier solvent and the annealing of SnO_2 surfaces at 150 °C directly after the soaking step, that THF is also becoming covalently bound to the surface. If so, this would explain the large presence of non-phosphonic acid C found on all modified surfaces. For ODPA modified surfaces this would

not be directly seen in the C1s narrow scan were signals pertaining to ODPA would overlap with those of the degraded THF.

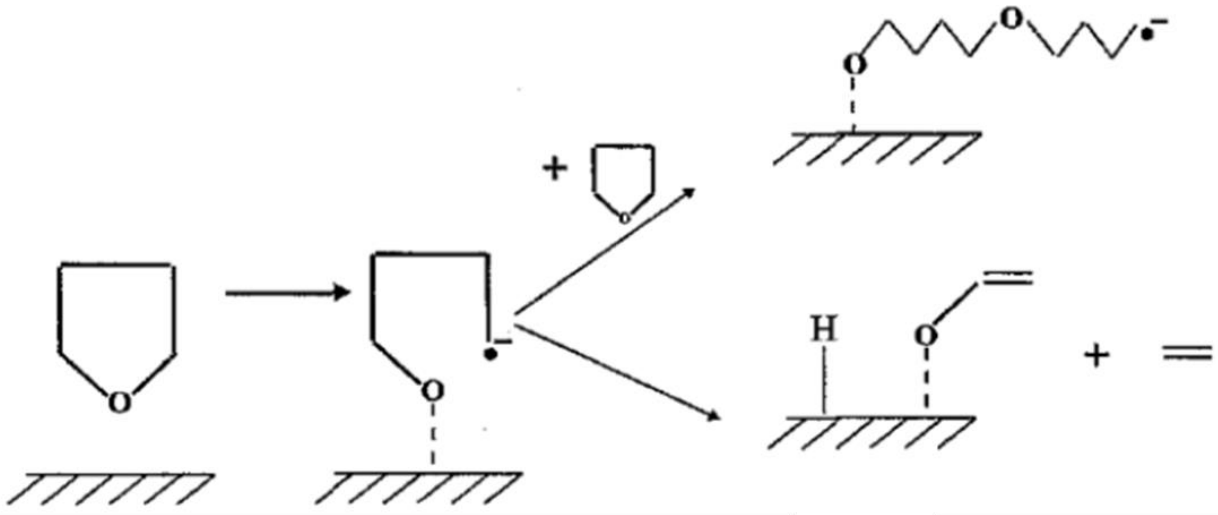

Figure 4.12. *Proposed mechanism for the degradation of THF onto Au surfaces. Figure adapted from reference 115.*[115]

The P2p narrow scans of modified surfaces show two peaks at 134.4 eV and 133.5 eV assigned to spin orbit coupling states of P2p $_{3/2}$ and P2p $_{½}$, respectively originating from the phosphonic acid head groups While P is present on all surfaces, the normalised spectra show that the amount decreases in the order F13OPA>PFBPA>ODPA modifiers.

Table 4.16. *Ratios of peak areas obtained from XPS narrow scans to Sn3d 5/2 peak obtained from the XPS Sn3d narrow scan of that sample for MBE moderately doped SnO_2 surfaces modified with F13OPA, ODPA and PFBPA as well as moderately doped unmodified reference sample*

Sample	$F_{(total)}$:Sn3d	$P_{(total)}$:Sn3d	$C_{(total)}$:Sn3d	Surface $O_{(total)}$:Bulk O
Moderately doped MBE grown SnO_2 Reference	-	-	-	1.3
Moderately doped MBE grown SnO_2 modified with F13OPA	0.7	0.1	0.7	1.7
Moderately doped MBE grown SnO_2 modified with ODPA	-	>0.1	1.1	1.0
Moderately doped MBE grown SnO_2 modified with PFBPA	0.3	0.1	2.7	3.0

Table 4.16 compares elemental ratios for SnO_2 surfaces modified with phosphonic acids. F:Sn ratios for F13OPA and PFBA modified samples suggest similar amounts of modifier on both surfaces, when taking into account 13 F of F13OPA and five F for PFBPA. This is also seen with a ratio of 0.1 for P:Sn on both surfaces. ODPA modified surface shows a smaller P:Sn ratio as well as a smaller $C_{(total)}$:Sn ratio than the fluorinated modifiers. As compared to the unmodified reference sample, modified surfaces show negligible changes to bulk and surface O after modification except for the PFBPA modified surface. These results suggest that all moderately doped, MBE grown SnO_2 surface have been successfully modified with phosphonic acids. ODPA appears to give the lowest surface concentration while F13OPA and PFBPA appear to modify SnO_2 surfaces in similar amounts. The PFBPA surface however is believed to be primarily bound to the surface in a mono-dentate fashion evidenced by the largest presence of surfaces O environments compared to SnO_2 bulk O. It is noted that as in chapter 3 synchrotron XPS data cannot compare different elements as the RSF of each element is unknown.

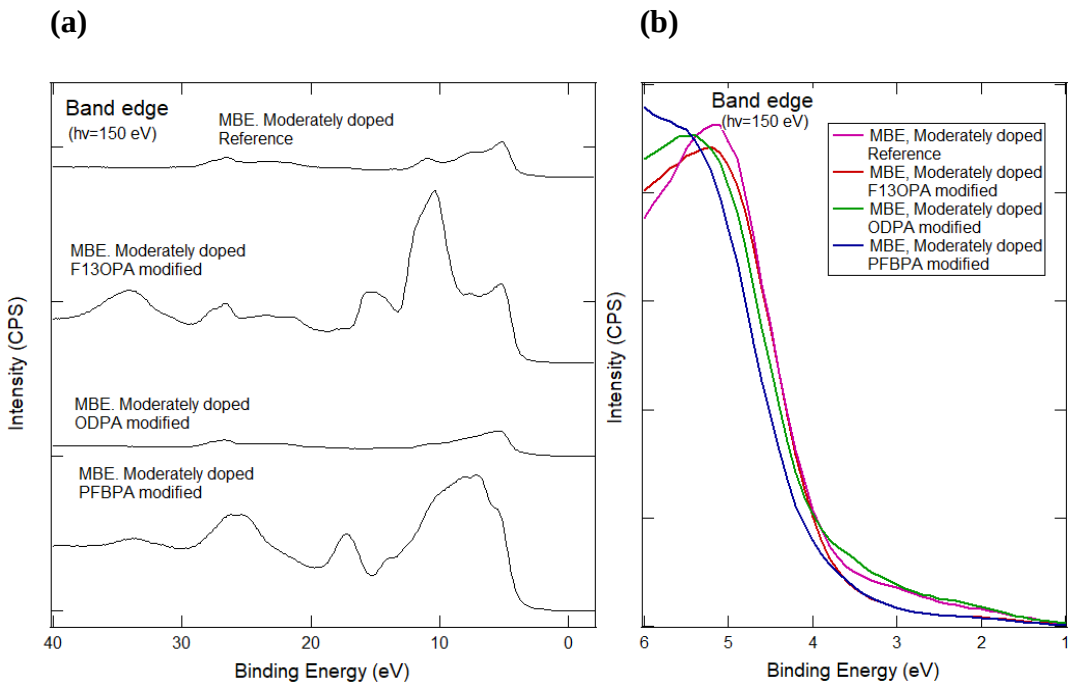

Figure 4.13. *XPS narrow scan of the of the valence band for moderately doped SnO_2 surfaces modified with F13OPA, ODPA and PFBPA and their reference sample. (a), is the full valence band scan. (b) is an overlay of the leading band from the valence band scan.*

XPS measurements of the valence band show distinct changes for all phosphonic acid modified surfaces as compared with the unmodified reference sample (figure 4.13) except for the ODPA modified sample. The F13OPA modified sample shows an increased broadening of the feature at ≈ 10 eV pertaining to C2p states of the F13OPA moiety.[117] The ODPA modified surface shows a decrease in all features and no new features. This is attributed to a low amount of modification as well as being a consequence of normalisation of the spectra to the Sn3d 5/2 peak of the survey scan. Small features at ≈ 26 eV and 17 eV attributed to higher energy Sn electrons are still present as with F13OPA and PFBPA modified surfaces. The PFBPA valence band shows a very broad feature at ≈ 7 eV which is consistent with states pertaining to the phenyl ring as described in chapter 3 for diazonium modified SnO_2 surfaces.

Table 4.17. *Summary of changes to the low energy band edge obtained from XPS valence band narrow scans of moderately doped MBE grown SnO_2 surfaces modified with F13OPA, ODPA and PFBPA and compared to an unmodified reference samples.*

Sample	Low energy band edge (± 0.1 eV)	Change to band edge (eV)	Directional change in band bending
Moderately doped MBE grown SnO_2 Reference	3.7	-	-
Moderately doped MBE grown SnO_2 modified with F13OPA	3.7	0.0	None
Moderately doped MBE grown SnO_2 modified with ODPA	3.8	0.1	Downwards
Moderately doped MBE grown SnO_2 modified with PFBPA	4	0.3	Downwards

Changes to the low energy band edge (figure 4.13(b)) show an increase in the downwards band bending for ODPA and PFBPA modified surface of 0.1 and 0.3 eV respectively (table 4.17). F13OPA modified surface shows no change to the leading edge. While modification with phosphonic acids was expected to increase the downwards band bending this, surprisingly, is not seen for the for the F13OPA modified sample. Although the precise reason for this is unknown, a tentative explanation could be due to degradation of THF at the surface (discussed above) producing a surface thin film of both F13OPA and degraded THF. This mixed SAM could consist of opposing dipoles which would cancel any net effect experienced by the SnO_2 surface.

As discussed in chapter 3 the stability of the phosphonic acids to X-ray was also assessed. F13OPA and PFBPA modified surface underwent a series of scan with an increase flux of X-rays.

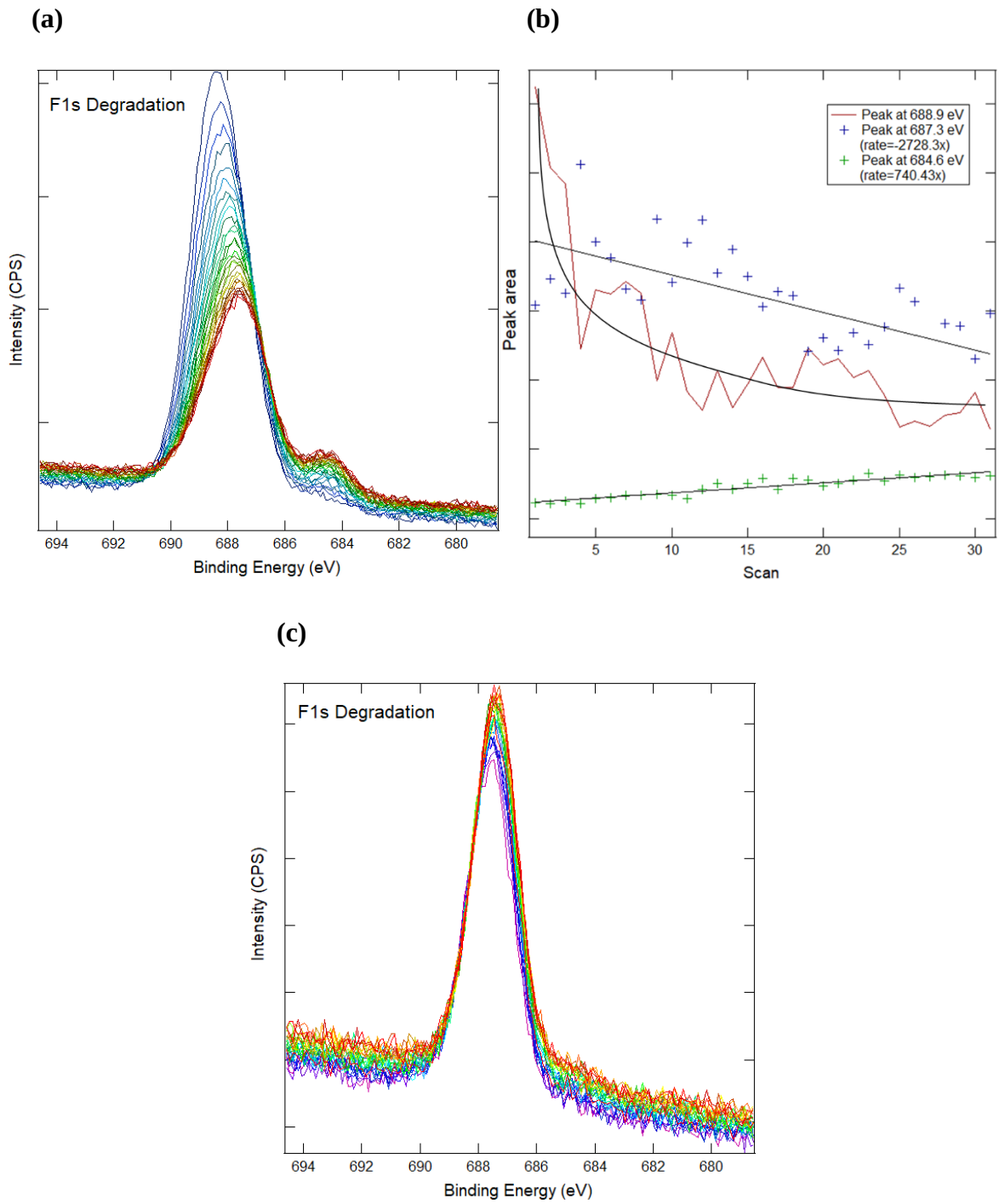

Figure 4.14. *XPS F1s narrow scan series at a higher flux showing the degradation of the moderately doped F13OPA modified SnO_2, its equivalent rates based on peak areas of the scans and the degradation scan of moderately doped PFBPA modified SnO_2, (a), (b) and (c) respectively.*

Figure 4.14(a) shows F1s narrows of the F13OPA modified surface at an increased X-ray flux. Scans show the susceptibility of F13OPA to X-ray degradation. Over a series of 30 scans the peak at 689.0 eV steadily decreases while shifting to lower BE. The feature can be

fitted with two components with peaks at 688.9 eV and 687.3 eV assigned to F-C and F-$C_{(aromatic)}$ respectively.[87, 112, 113] The presence of F bound to aromatic C is assumed to be due to contamination. Another peak appears at 684.6 eV assigned to F-Sn.[105] Figure 4.14(b) shows the rate of appearance/disappearance of assigned F-C peaks. A steady increase of F-Sn is seen while F-C exponentially decreases and F-$C_{(aromatic)}$ only slightly decreases. Results are consistent with a greater stability attributed to F bound to aromatic C. The PFBPA modified surface shows negligible changes in F environment. This gives evidence to a greater stability of PFBPA to X-rays.

Results presented above show the moderately doped, MBE grown SnO_2 surface can be modified with F13OPA, ODPA and PFBPA with a smaller degree of modification for the ODPA modified surface.

4.4. Conclusions

Result have shown that doped and un-doped CVD and MBE grown SnO_2 surfaces can be modified with the phosphonic acids F13OPA, ODPA and PFBPA. A greater degree of surface modification is seen for doped SnO_2 surfaces with no notable preference for surface growth e.g. CVD or MBE. Results do not suggest a preference for surface modification of SnO_2 surfaces grown by different methods. Phosphonic acid surface modification has shown to increase the downwards band bending for almost all modifiers. This suggests that the major factor influencing the band edge is the phosphonic acid head group itself, independent of the phosphonic acid substituents. The degradation of THF on the SnO_2 surface is another possible explanation for the changes seen in the SnO_2 valance band. If THF degradation and surface binding was significant, this could overwhelm any effect of the phosphonic acid on the SnO_2 band bending. Clearly, the influence of THF on the SnO_2 substrate requires a detailed investigation before the effects of the phosphonic acid on electrical, chemical and physical properties of the SnO_2 surface can be understood in detail.

Despite the possible influence of THF, phosphonic acids are clearly a successful candidate for the surface modification of SnO_2 surfaces. Further experimentation should investigate the stability of the phosphonic acid to conditions such as heat, temperature and pressure for their use in devices. Investigation into the controllability of the surface modification is also

required to control factors like SAM packing densities, ordering of the thin films at the surface and degree of covalent modification of the phosphonic acid to the SnO_2 surface.

Chapter 5. Conclusion and Future Work

Results discussed above in chapters 3 and 4 have shown that SnO_2 surfaces can be modified with aryl diazonium salts and phosphonic acids. Surface modification proceeds via covalent bond formation between the modifier and the SnO_2 surface evidenced by XPS. Factors such as the presence of the Sb dopant and the method used for modification have been shown to influence the amount of modifier at the SnO_2 surface. Modification of surfaces with fluorinated compounds are also shown to be susceptible to degradation by X-rays with a reduced stability attributed to aliphatic compounds over aromatic ones. Additional analysis found that after modification, surfaces showed a change to surface roughness and SnO_2 band bending, while investigation of the C1s narrow scan for phosphonic acid modified samples shows possible modification of SnO_2 with THF degradation products resulting from the surface modification annealing step.

For both aryl diazonium salt and phosphonic acid modified surfaces, little changes were seen in surface wettability. For both classes of modifier, experimental CA values were below literature values for that modifier. However, results are still reasonable within experimental uncertainty. The small change to CAs between modified and unmodified surfaces is attributed to the Sb dopant where the presence of Sb was found to greatly increase surface CAs to values similar to those expected for modified surfaces. This has made surface wettability measurement an ineffective measure of surface modification in all cases involving doped SnO_2 surfaces.

AFM surface topographical measurements were used in both tapping and contact modes to good effect. For both classes of modifier, imaging with AFM showed changes in topography of SnO_2 surfaces after modification. Except for the F13OPA modified surface these changes in topography were accompanied by a large increase in surface roughness. AFM in contact mode was also used to scratch away the modification layer at the surface. This revealed film thicknesses consistent with multilayers for aryl diazonium salt modified surfaces. An increase in film thickness was also seen for electrochemical grafting of diazonium salts over spontaneous grafting of SnO_2 surfaces. Film thicknesses measurements of phosphonic acid modified surfaces revealed a thin film less than the expected literature values for each modifier and it was concluded that the film is likely to be horizontally stacked on the SnO_2 surface.

XPS surface measurements gave detailed information about the layers revealing covalent modification of the modifier with the SnO_2 surface and quantitative comparisons of the amounts of modifiers at each surface. Australian Synchrotron XPS investigation of the O1s narrow scan revealed surface modification with aryl diazonium salts produced phenyl films covalently bound through Sn-O-C bonds while phosphonic acid films were covalently bound through Sn-O-P bonds. Additionally, investigation of the SnO_2 valence band found that surfaces modified with aryl diazonium salts with electron withdrawing CF_3 and NO_2 groups, had decreased downwards band bending while surfaces modified with phosphonic acids had increased the downwards band bending. In both cases however, no trend was found between the extent of modification and the extent of band bending.

The amount of modifier at the surface was investigated by comparisons of marker elements found on the modifier such as F for CF3BD, F13OPA and PFBPA, N for aryl diazonium salt modified surfaces and P for phosphonic acid modified surface. Under the same modification conditions, CF3BD and NBD gave similar surface concentrations, whereas the surface concentration of ODPA was less than that of F13OPA and PFBPA. The latter two phosphonic acids gave similar surface amounts. The presence of Sb in the SnO_2 substrate was also found to increase the surface concentration of modifiers at the surface. In the case of aryl diazonium salt modified surfaces, the use of electrochemical grafting over spontaneous grafting was shown to increase the amount of modifier at the surface. The presence of Sb was also shown to increase the formation of azo links in the thin film for spontaneous grafting of SnO_2 surfaces with aryl diazonium salts.

Laboratory based XPS was also used to investigate surfaces modified with phosphonic acids. While this technique was advantaged by having relative sensitivity factor (RSF) for each element allowing for direct comparisons between different elements, it was limited by a decrease in surface sensitivity compared to synchrotron XPS. Investigation of phosphonic acid modified surfaces by this means showed results similar to that of synchrotron XPS, but was also able to directly confirm the presence of the intact modifiers at the surface. Additionally, it was revealed that the degree of modification experienced by the SnO_2 surface was not influenced by the thin film growth method (CVD or MBE).

While direct comparisons between diazonium salt and phosphonic acid modified surfaces cannot be made, results indicate that diazonium salts are more versatile than phosphonic acids for the modification of SnO_2 surfaces. Diazonium salts allow for greater control of the

modification shown by the addition of multilayers at the SnO_2 surface as well as several grafting methods available for modification. Additionally, SnO_2 surface modification with diazonium salts showed a decrease in downwards band bending consistent with electron withdrawing CF_3 and NO_2 groups of the CF3BD and NBD modifiers respectively. It would then be expected that an increase in downwards band bending would be observed by using a diazonium salt with an electron donating substituent. Surface modification with phosphonic acids showed an increase in downwards band bending regardless of the modifier used indicating that the phosphonic acid head group itself influences the electrical properties of SnO_2.

Future work requires repeat of SnO_2 surface modifications and characterisation. With little investigation of the surface modification of SnO_2 surfaces, the results presented in this thesis are therefore considered preliminary results and require repeat experimentation to validate the conclusions presented here.

Concurrent surface modification with THF degradation products for phosphonic acid modified surfaces has been suggested by results presented here. This means that interpretation of results obtained for the modification of SnO_2 surface with phosphonic acids is uncertain. Measured properties such as changes to the valence band, surface wettability and film thickness could be the result of a mixed modification by THF and the phosphonic acid. Thus, this requires careful investigation before further conclusions can be made about SnO_2 surface modification with phosphonic acids.

Future work also needs to investigate the effect of film thickness on factors like the stability of the modification and the effect it has on band bending of the SnO_2 substrate. While film thickness measurements were made during this work, the effect of the film thickness was not investigated. An investigation into different film thicknesses for the same modifier on like surfaces would build up a more detailed understanding of how the surface modification influences the underlying substrate. Additionally, an analysis of this type supported by computational studies, might provide insight into the extent of band bending experienced by the SnO_2 surface which is not well understood.

A thorough investigation into the precise mechanism and bonding experienced by SnO_2 surface with aryl diazonium salts and phosphonic acid needs to be conducted. Although surface modifications of SnO_2 surfaces has been achieved, little data has been collected on the precise way these modification takes place. As such investigation of the type of bonding

(mono, bi and tridentate) of phosphonic acid moieties to the SnO_2 surface, the ordering of the thin films, and how these factors influence physical and electrical properties of the SnO_2 substrate will assist in the controllable use and optimisation of these modifiers in the modification of SnO_2 surfaces for device applications.

Finally, future work requires investigation into the stability of these modifications under different environments. With aims of this research focused on real world application of SnO_2 surfaces in future devices, results have already shown a susceptibility for fluorinated modifiers to degrade in the presence of X-rays. As such, the longevity of any modification of the SnO_2 surface is of strong interest with the usefulness of modification being dependent on its stability over time.

References

1. Batzill, M.; Diebold, U., The Surface and Materials Science of Tin Oxide. *Prog. Surf. Sci.* **2005,** *79* (2-4), 47-154.
2. Pujari, S. P.; Scheres, L.; Marcelis, A. T. M.; Zuilhof, H., Covalent Surface Modification of Oxide Surfaces. *Angew. Chem.-Int. Edit.* **2014,** *53* (25), 6322-6356.
3. Hanson, E. L.; Guo, J.; Koch, N.; Schwartz, J.; Bernasek, S. L., Advanced Surface Modification of Indium Tin Oxide for Improved Charge Injection in Organic Devices. *J. Am. Chem. Soc.* **2005,** *127* (28), 10058-10062.
4. Chockalingam, M.; Darwish, N.; Le Saux, G.; Gooding, J. J., Importance of the Indium Tin Oxide Substrate on the Quality of Self-Assembled Monolayers Formed from Organophosphonic Acids. *Langmuir* **2011,** *27* (6), 2545-2552.
5. Henrich, V. E.; Cox, P. A., *The Surface Science of Metal Oxides*. Cambridge Univ. Press: 1994; p 464 pp.
6. Stavis, C.; Clare, T. L.; Butler, J. E.; Radadia, A. D.; Carr, R.; Zeng, H. J.; King, W. P.; Carlisle, J. A.; Aksimentiev, A.; Bashir, R.; Hamers, R. J., Surface Functionalization of Thin-Film Diamond for Highly Stable and Selective Biological Interfaces. *Proc. Natl. Acad. Sci. U. S. A.* **2011,** *108* (3), 983-988.
7. Melle-Franco, M.; Pacchioni, G.; Chadwick, A. V., Cluster and Periodic Ab Initio Calculations on the Adsorption of CO2 on the SnO2(110) Surface. *Surf. Sci.* **2001,** *478* (1-2), 25-34.
8. Oviedo, J.; Gillan, M. J., First-Principles Study of the Interaction of Oxygen with the Sno(2)(110) Surface. *Surf. Sci.* **2001,** *490* (3), 221-236.
9. Surnev, S.; Ramsey, M. G.; Netzer, F. P., Vanadium Oxide Surface Studies. *Prog. Surf. Sci.* **2003,** *73* (4-8), 117-165.
10. Tsikritzis, D.; Petraki, F.; Kennou, S., An Interface Study of Indium Tin Oxide on Polyethylene Terephthalate with Nickel Phthalocyanine by Photoelectron Spectroscopies: The Effect of Cleaning Pretreatment. *Microelectron. Eng.* **2012,** *90*, 66-68.
11. Barteau, M. A., Organic Reactions at Well-Defined Oxide Surfaces. *Chem. Rev.* **1996,** *96* (4), 1413-1430.
12. Batzill, M.; Katsiev, K.; Diebold, U., Surface Morphologies of SnO2(110). *Surf. Sci.* **2003,** *529* (3), 295-311.
13. Batzill, M.; Burst, J. M.; Diebold, U., Pure and Cobalt-Doped SnO2(101) Films Grown by Molecular Beam Epitaxy on Al2O3. *Thin Solid Films* **2005,** *484* (1-2), 132-139.
14. Kar, A.; Patra, A., Recent Development of Core-Shell SnO2 Nanostructures and Their Potential Applications. *J. Mater. Chem. C* **2014,** *2* (33), 6706-6722.
15. Calloni, A.; Brambilla, A.; Berti, G.; Bussetti, G.; Canesi, E. V.; Binda, M.; Petrozza, A.; Finazzi, M.; Ciccacci, F.; Duo, L., X-Ray Photoemission Spectroscopy Investigation of the Interaction between 4-Mercaptopyridine and the Anatase TiO2 Surface. *Langmuir* **2013,** *29* (26), 8302-8310.
16. Akgul, F. A.; Gumus, C.; Er, A. O.; Farha, A. H.; Akgul, G.; Ufuktepe, Y.; Liu, Z., Structural and Electronic Properties of SnO2. *J. Alloys Compd.* **2013,** *579*, 50-56.
17. Gordon, R. G., Criteria for Choosing Transparent Conductors. *MRS Bull.* **2000,** *25* (8), 52-57.
18. Wang, H. K.; Rogach, A. L., Hierarchical SnO2 Nanostructures: Recent Advances in Design, Synthesis, and Applications. *Chem. Mater.* **2014,** *26* (1), 123-133.
19. Matsubara, I.; Hosono, K.; Murayama, N.; Shin, W.; Izu, N., Organically Hybridized SnO2 Gas Sensors. *Sens. Actuator B-Chem.* **2005,** *108* (1-2), 143-147.
20. Hyodo, T.; Baba, Y.; Wada, K.; Shimizu, Y.; Egashira, M., Hydrogen Sensing Properties of SnO2 Varistors Loaded with SiO2 by Surface Chemical Modification with Diethoxydimethylsilane. *Sens. Actuator B-Chem.* **2000,** *64* (1-3), 175-181.
21. Nardis, S.; Monti, D.; Di Natale, C.; D'Amico, A.; Siciliano, P.; Forleo, A.; Epifani, M.; Taurino, A.; Rella, R.; Paolesse, R., Preparation and Characterization of Cobalt Porphyrin Modified Tin Dioxide Films for Sensor Applications. *Sens. Actuator B-Chem.* **2004,** *103* (1-2), 339-343.

22. Vaezi, M. R., SnO2/ZnO Double-Layer Thin Films: A Novel Economical Preparation and Investigation of Sensitivity and Stability of Double-Layer Gas Sensors. *Mater. Chem. Phys.* **2008,** *110* (1), 89-94.
23. Xu, C. H.; Jiang, Y.; Yi, D. Q.; Sun, S. P.; Yu, Z. M., Environment-Dependent Surface Structures and Stabilities of SnO2 from the First Principles. *J. Appl. Phys.* **2012,** *111* (6), 9.
24. Wada, K.; Egashira, M., Improvement of Gas-Sensing Properties of Sno2 by Surface Chemical Modification with Diethoxydimethylsilane. *Sens. Actuator B-Chem.* **1998,** *53* (3), 147-154.
25. Golovanov, V.; Viitala, M.; Kortelainen, T.; Cramariuc, O.; Rantala, T. T., Stability of Siloxane Couplers on Pure and Fluorine Doped SnO2 (110) Surface: A First Principles Study. *Surf. Sci.* **2010,** *604* (19-20), 1784-1790.
26. Batzill, M., Surface Science Studies of Gas Sensing Materials: SnO2. *Sensors* **2006,** *6* (10), 1345-1366.
27. Das, S.; Jayaraman, V., SnO2: A Comprehensive Review on Structures and Gas Sensors. *Prog. Mater Sci.* **2014,** *66*, 112-255.
28. Verma, S.; Kar, P.; Das, A.; Palit, D. K.; Ghosh, H. N., The Effect of Heavy Atoms on Photoinduced Electron Injection from Nonthermalized and Thermalized Donor States of M-Li-Polypyridyl (M=Ru/Os) Complexes to Nanoparticulate TiO2 Surfaces: An Ultrafast Time-Resolved Absorption Study. *Chem.-Eur. J.* **2010,** *16* (2), 611-619.
29. Szillies, S.; Thissen, P.; Tabatabai, D.; Feil, F.; Furbeth, W.; Fink, N.; Grundmeier, G., Formation and Stability of Organic Acid Monolayers on Magnesium Alloy Az31: The Role of Alkyl Chain Length and Head Group Chemistry. *Appl. Surf. Sci.* **2013,** *283*, 339-347.
30. Brubaker, C. E.; Messersmith, P. B., The Present and Future of Biologically Inspired Adhesive Interfaces and Materials. *Langmuir* **2012,** *28* (4), 2200-2205.
31. Xu, F.; Chen, K. M.; Piner, R. D.; Mirkin, C. A.; Ritchie, J. E.; McDevitt, J. T., Surface Coordination Chemistry of YBa2Cu3O7-Delta. *Langmuir* **1998,** *14* (22), 6505-6511.
32. Chockalingam, M.; Magenau, A.; Parker, S. G.; Parviz, M.; Vivekchand, S. R. C.; Gaus, K.; Gooding, J. J., Biointerfaces on Indium-Tin Oxide Prepared from Organophosphonic Acid Self-Assembled Monolayers. *Langmuir* **2014,** *30* (28), 8509-8515.
33. Tsud, N.; Yoshitake, M., Vacuum Vapour Deposition of Phenylphosphonic Acid on Amorphous Alumina. *Surf. Sci.* **2007,** *601* (14), 3060-3066.
34. ter Maat, J.; Regeling, R.; Yang, M. L.; Mullings, M. N.; Bent, S. F.; Zuilhof, H., Photochemical Covalent Attachment of Alkene-Derived Monolayers onto Hydroxyl-Terminated Silica. *Langmuir* **2009,** *25* (19), 11592-11597.
35. Grandbois, M.; Beyer, M.; Rief, M.; Clausen-Schaumann, H.; Gaub, H. E., How Strong Is a Covalent Bond? *Science* **1999,** *283* (5408), 1727-1730.
36. Chen, R.; Kim, H.; McIntyre, P. C.; Bent, S. F., Investigation of Self-Assembled Monolayer Resists for Hafnium Dioxide Atomic Layer Deposition. *Chem. Mater.* **2005,** *17* (3), 536-544.
37. Kim, B. H.; Lee, D. H.; Kim, J. Y.; Shin, D. O.; Jeong, H. Y.; Hong, S.; Yun, J. M.; Koo, C. M.; Lee, H.; Kim, S. O., Mussel-Inspired Block Copolymer Lithography for Low Surface Energy Materials of Teflon, Graphene, and Gold. *Adv. Mater.* **2011,** *23* (47), 5618-5622.
38. Lee, H.; Dellatore, S. M.; Miller, W. M.; Messersmith, P. B., Mussel-Inspired Surface Chemistry for Multifunctional Coatings. *Science* **2007,** *318* (5849), 426-430.
39. Hotchkiss, P. J.; Jones, S. C.; Paniagua, S. A.; Sharma, A.; Kippelen, B.; Armstrong, N. R.; Marder, S. R., The Modification of Indium Tin Oxide with Phosphonic Acids: Mechanism of Binding, Tuning of Surface Properties, and Potential for Use in Organic Electronic Applications. *Acc. Chem. Res.* **2012,** *45* (3), 337-346.
40. Nie, H. Y.; Walzak, M. J.; McIntyre, N. S., Bilayer and Odd-Numbered Multilayers of Octadecylphosphonic Acid Formed on a Si Substrate Studied by Atomic Force Microscopy. *Langmuir* **2002,** *18* (7), 2955-2958.

41. Brodard-Severac, F.; Guerrero, G.; Maquet, J.; Florian, P.; Gervais, C.; Mutin, P. H., High-Field O-17 MAS NMR Investigation of Phosphonic Acid Monolayers on Titania. *Chem. Mater.* **2008,** *20* (16), 5191-5196.
42. Mutin, P. H.; Guerrero, G.; Vioux, A., Hybrid Materials from Organophosphorus Coupling Molecules. *J. Mater. Chem.* **2005,** *15* (35-36), 3761-3768.
43. Lafond, V.; Gervais, C.; Maquet, J.; Prochnow, D.; Babonneau, F.; Mutin, P. H., O-17 MAS NMR Study of the Bonding Mode of Phosphonate Coupling Molecules in a Titanium Oxo-Alkoxo-Phosphonate and in Titania-Based Hybrid Materials. *Chem. Mater.* **2003,** *15* (21), 4098-4103.
44. Chen, X.; Luais, E.; Darwish, N.; Ciampi, S.; Thordarson, P.; Gooding, J. J., Studies on the Effect of Solvents on Self-Assembled Monolayers Formed from Organophosphonic Acids on Indium Tin Oxide. *Langmuir* **2012,** *28* (25), 9487-9495.
45. Raman, A.; Quinones, R.; Barriger, L.; Eastman, R.; Parsi, A.; Gawalt, E. S., Understanding Organic Film Behavior on Alloy and Metal Oxides. *Langmuir* **2010,** *26* (3), 1747-1754.
46. Herzer, N.; Hoeppener, S.; Schubert, U. S., Fabrication of Patterned Silane Based Self-Assembled Monolayers by Photolithography and Surface Reactions on Silicon-Oxide Substrates. *Chem. Commun.* **2010,** *46* (31), 5634-5652.
47. Sharma, A.; Haldi, A.; Hotchkiss, P. J.; Marder, S. R.; Kippelen, B., Effect of Phosphonic Acid Surface Modifiers on the Work Function of Indium Tin Oxide and on the Charge Injection Barrier into Organic Single-Layer Diodes. *J. Appl. Phys.* **2009,** *105* (7), 6.
48. Paniagua, S. A.; Hotchkiss, P. J.; Jones, S. C.; Marder, S. R.; Mudalige, A.; Marrikar, F. S.; Pemberton, J. E.; Armstrong, N. R., Phosphonic Acid Modification of Indium-Tin Oxide Electrodes: Combined XPS/UPS/Contact Angle Studies. *J. Phys. Chem. C* **2008,** *112* (21), 7809-7817.
49. Putans, B. A.; Bishop, L. M.; Hamers, R. J., Versatile Approach to Formation of Light-Harvesting Complexes on Nanostructured Metal Oxide Surfaces Via "on-Surface" Assembly. *Chem. Mater.* **2014,** *26* (12), 3651-3659.
50. McNeill, A. R.; Hyndman, A. R.; Reeves, R. J.; Downard, A. J.; Allen, M. W., Tuning the Band Bending and Controlling the Surface Reactivity at Polar and Nonpolar Surfaces of ZnO through Phosphonic Acid Binding. *ACS Appl. Mater. Interfaces* **2016,** *8* (45), 31392-31402.
51. Hotchkiss, P. J.; Li, H.; Paramonov, P. B.; Paniagua, S. A.; Jones, S. C.; Armstrong, N. R.; Bredas, J. L.; Marder, S. R., Modification of the Surface Properties of Indium Tin Oxide with Benzylphosphonic Acids: A Joint Experimental and Theoretical Study. *Adv. Mater.* **2009,** *21* (44), 4496-+.
52. Ferri, V.; Costa, E.; Biancardo, M.; Argazzi, R.; Bignozzi, C. A., Electrochromic Properties of Mixed Valence Binuclear Ruthenium Complexes Adsorbed on Nanocrystalline SnO2 Films. *Inorg. Chim. Acta* **2007,** *360* (3), 1131-1137.
53. Gheonea, R.; Mak, C.; Crasmareanu, E. C.; Simulescu, V.; Plesu, N.; Ilia, G., Surface Modification of SnO2 with Phosphonic Acids. *J. Chem.* **2017**, 7.
54. Holland, G. P.; Sharma, R.; Agola, J. O.; Amin, S.; Solomon, V. C.; Singh, P.; Buttry, D. A.; Yarger, J. L., NMR Characterization of Phosphonic Acid Capped SnO2 Nanoparticles. *Chem. Mater.* **2007,** *19* (10), 2519-2526.
55. Delamar, M.; Hitmi, R.; Pinson, J.; Saveant, J. M., Covalent Modification of Carbon Surfaces by Grafting of Functionalized Aryl Radicals Produced from Electrochemical Reduction of Diazonium Salts. *J. Am. Chem. Soc.* **1992,** *114* (14), 5883-5884.
56. Belanger, D.; Pinson, J., Electrografting: A Powerful Method for Surface Modification. *Chem. Soc. Rev.* **2011,** *40* (7), 3995-4048.
57. Adenier, A.; Cabet-Deliry, E.; Chausse, A.; Griveau, S.; Mercier, F.; Pinson, J.; Vautrin-Ul, C., Grafting of Nitrophenyl Groups on Carbon and Metallic Surfaces without Electrochemical Induction. *Chem. Mater.* **2005,** *17* (3), 491-501.
58. Combellas, C.; Delamar, M.; Kanoufi, F.; Pinson, J.; Podvorica, F. I., Spontaneous Grafting of Iron Surfaces by Reduction of Aryldiazonium Salts in Acidic or Neutral Aqueous Solution. Application to the Protection of Iron against Corrosion. *Chem. Mater.* **2005,** *17* (15), 3968-3975.

59. Mesnage, A.; Magied, M. A.; Simon, P.; Herlin-Boime, N.; Jegou, P.; Deniau, G.; Palacin, S., Grafting Polymers to Titania Nanoparticles by Radical Polymerization Initiated by Diazonium Salt. *J. Mater. Sci.* **2011,** *46* (19), 6332-6338.
60. Maldonado, S.; Smith, T. J.; Williams, R. D.; Morin, S.; Barton, E.; Stevenson, K. J., Surface Modification of Indium Tin Oxide Via Electrochemical Reduction of Aryldiazonium Cations. *Langmuir* **2006,** *22* (6), 2884-2891.
61. Drevet, R.; Dragoe, D.; Barthes-Labrousse, M. G.; Chausse, A.; Andrieux, M., XPS-Nanocharacterization of Organic Layers Electrochemically Grafted on the Surface of SnO2 Thin Films to Produce a New Hybrid Material Coating. *Appl. Surf. Sci.* **2016,** *384*, 442-448.
62. Dunker, M. F. W.; Starkey, E. B.; Jenkins, G. L., The Preparation of Some Organic Mercurials from Diazonium Borofluorides. *J. Am. Chem. Soc.* **1936,** *58*, 2308-2309.
63. Downard, A. J., Electrochemically Assisted Covalent Modification of Carbon Electrodes. *Electroanalysis* **2000,** *12* (14), 1085-1096.
64. Lund, T.; Nguyen, P. T.; Ruhland, T., Electrochemical Grafting of TiO2-Based Photo-Anodes and Its Effect in Dye-Sensitized Solar Cells. *J. Electroanal. Chem.* **2015,** *758*, 85-92.
65. Bell, K. J.; Brooksby, P. A.; Polson, M. I. J.; Downard, A. J., Evidence for Covalent Bonding of Aryl Groups to MnO2 Nanorods from Diazonium-Based Grafting. *Chem. Commun.* **2014,** *50* (89), 13687-13690.
66. Schlesinger, R.; Xu, Y.; Hofmann, O. T.; Winkler, S.; Frisch, J.; Niederhausen, J.; Vollmer, A.; Blumstengel, S.; Henneberger, F.; Rinke, P.; Scheffler, M.; Koch, N., Controlling the Work Function of ZnO and the Energy-Level Alignment at the Interface to Organic Semiconductors with a Molecular Electron Acceptor. *Phys. Rev. B* **2013,** *87* (15), 5.
67. Hunger, R.; Jaegermann, W.; Merson, A.; Shapira, Y.; Pettenkofer, C.; Rappich, J., Electronic Structure of Methoxy-, Bromo-, and Nitrobenzene Grafted onto Si(111). *J. Phys. Chem. B* **2006,** *110* (31), 15432-15441.
68. McNeill, A. R.; Bell, K. J.; Hyndman, A. R.; Gazoni, R. M.; Reeves, R. J.; Downard, A. J.; Allen, M. W., From Accumulation to Depletion: Removing the Downward Band Bending and 2-Dimensional Electron Gas at ZnO Surfaces Using Grafted Aryl Layers. *Unpublished work* **2017**.
69. Allongue, P.; de Villeneuve, C. H.; Cherouvrier, G.; Cortes, R.; Bernard, M. C., Phenyl Layers on H-Si(111) by Electrochemical Reduction of Diazonium Salts: Monolayer Versus Multilayer Formation. *J. Electroanal. Chem.* **2003,** *550*, 161-174.
70. Purkayastha, D. D.; Brahma, R.; Krishna, M. G.; Madhurima, V., Effects of Metal Doping on Photoinduced Hydrophilicity of SnO2 Thin Films. *Bull. Mater. Sci.* **2015,** *38* (1), 203-208.
71. Tessier, L.; Deniau, G.; Charleux, B.; Palacin, S., Surface Electroinitiated Emulsion Polymerization (Seep): A Mechanistic Approach. *Chem. Mater.* **2009,** *21* (18), 4261-4274.
72. Hurley, B. L.; McCreery, R. L., Covalent Bonding of Organic Molecules to Cu and Al Alloy 2024 T3 Surfaces Via Diazonium Ion Reduction. *J. Electrochem. Soc.* **2004,** *151* (5), B252-B259.
73. Distefano, G.; Guerra, M.; Jones, D.; Modelli, A.; Colonna, F. P., Experimental and Theoretical-Study of Intense Shake-up Structures in the XPS Spectra of Nitrobenzenes and Nitrosobenzenes. *Chem. Phys.* **1980,** *52* (3), 389-398.
74. Roodenko, K.; Gensch, M.; Rappich, J.; Hinrichs, K.; Esser, N.; Hunger, R., Time-Resolved Synchrotron XPS Monitoring of Irradiation-Induced Nitrobenzene Reduction for Chemical Lithography. *J. Phys. Chem. B* **2007,** *111* (26), 7541-7549.
75. Szczuko, D.; Werner, J.; Oswald, S.; Behr, G.; Wetzig, K., XPS Investigations of Surface Segregation of Doping Elements in SnO2. *Appl. Surf. Sci.* **2001,** *179* (1-4), 301-306.
76. Stuckert, E. P.; Fisher, E. R., Ar/O-2 and H2O Plasma Surface Modification of SnO2 Nanomaterials to Increase Surface Oxidation. *Sens. Actuator B-Chem.* **2015,** *208*, 379-388.
77. Kwoka, M.; Ottaviano, L.; Passacantando, M.; Santucci, S.; Czempik, G.; Szuber, J., XPS Study of the Surface Chemistry of L-Cvd Sno2 Thin Films after Oxidation. *Thin Solid Films* **2005,** *490* (1), 36-42.

78. Kumar, S. N.; Bouyssoux, G.; Gaillard, F., Electronic and Structural Characterization of Electrochemically Synthesized Conducting Polyaniline from XPS Studies. *Surf. Interface Anal.* **1990,** *15* (9), 531-536.
79. Doppelt, P.; Hallais, G.; Pinson, J.; Podvorica, F.; Verneyre, S., Surface Modification of Conducting Substrates. Existence of Azo Bonds in the Structure of Organic Layers Obtained from Diazonium Salts. *Chem. Mater.* **2007,** *19* (18), 4570-4575.
80. Biniak, S.; Szymanski, G.; Siedlewski, J.; Swiatkowski, A., The Characterization of Activated Carbons with Oxygen and Nitrogen Surface Groups. *Carbon* **1997,** *35* (12), 1799-1810.
81. Ilangovan, G.; Pillai, K. C., Electrochemical and XPS Characterization of Glassy Carbon Electrode Surface Effects on the Preparation of a Monomeric Molybdate(Vi)-Modified Electrode. *Langmuir* **1997,** *13* (3), 566-575.
82. Sherwood, P. M. A., Valence-Band Spectra of Tin Oxides Interpreted by X-Alpha Calculations. *Phys. Rev. B* **1990,** *41* (14), 10151-10154.
83. Nagata, T.; Bierwagen, O.; White, M. E.; Tsai, M. Y.; Speck, J. S., Study of the Au Schottky Contact Formation on Oxygen Plasma Treated N-Type SnO2 (101) Thin Films. *J. Appl. Phys.* **2010,** *107* (3), 7.
84. Themlin, J. M.; Chtaib, M.; Henrard, L.; Lambin, P.; Darville, J.; Gilles, J. M., Characterization of Tin Oxides by X-Ray-Photoemission Spectroscopy. *Phys. Rev. B* **1992,** *46* (4), 2460-2466.
85. Casademont, H.; Fillaud, L.; Lefevre, X.; Jousselme, B.; Derycke, V., Electrografted Fluorinated Organic Ultrathin Film as Efficient Gate Dielectric in MoS2 Transistors. *J. Phys. Chem. C* **2016,** *120* (17), 9506-9510.
86. Li, H.; Huang, C. Y.; Zhang, L.; Lou, W. Q., Fabrication of Superhydrophobic Surface on Zinc Substrate by 3-Trifluoromethylbenzene Diazonium Tetrafluoroborate Salts. *Appl. Surf. Sci.* **2014,** *314*, 906-909.
87. Ferraria, A. M.; da Silva, J. D. L.; do Rego, A. M. B., XPS Studies of Directly Fluorinated Hdpe: Problems and Solutions. *Polymer* **2003,** *44* (23), 7241-7249.
88. Fujimoto, H.; Mabuchi, A.; Maeda, T.; Matsumura, Y.; Watanabe, N.; Touhara, H., New Fluorine-Carbon Compound Prepared by the Direct Fluorination of Mesophase Pitch. *Carbon* **1992,** *30* (6), 851-857.
89. Brooksby, P. A.; Downard, A. J., Electrochemical and Atomic Force Microscopy Study of Carbon Surface Modification Via Diazonium Reduction in Aqueous and Acetonitrile Solutions. *Langmuir* **2004,** *20* (12), 5038-5045.
90. Srinivasan, V.; Walton, R. A., X-Ray Photoelectron-Spectra of Inorganic Molecules .20. Observations Concerning Sulfur 2p Binding-Energies in Metal-Complexes of Thiourea. *Inorg. Chim. Acta* **1977,** *25* (2), L85-L86.
91. Briggs, D.; Beamson, G., Primary and Secondary Oxygen-Induced C1s Binding-Energy Shifts in X-Ray Photoelectron-Spectroscopy of Polymers. *Anal. Chem.* **1992,** *64* (15), 1729-1736.
92. Barber, M.; Connor, J. A.; Guest, M. F.; Hillier, I. H.; Schwarz, M., Bonding in Some Donor-Acceptor Complexes Involving Boron-Trifluoride - Study by Means of ESCA and Molecular-Orbital Calculations. *Journal of the Chemical Society-Faraday Transactions Ii* **1973,** (4), 551-558.
93. Clark, D. T.; Woolsey, I. S.; Robinson, S. D.; Laing, K. R.; Wingfield, J. N., Complexes of Platinum Metals .8. Electron-Spectroscopy for Chemical-Analysis Studies of Some Nitrosyl, Aryldiazo, and Aryldiimine Derivatives of Ruthenium, Osmium, Rhodium, and Iridium. *Inorg. Chem.* **1977,** *16* (5), 1201-1206.
94. Seki, K.; Hayashi, N.; Oji, H.; Ito, E.; Ouchi, Y.; Ishii, H., Electronic Structure of Organic/Metal Interfaces. *Thin Solid Films* **2001,** *393* (1-2), 298-303.
95. Hayashi, N.; Ishii, H.; Ouchi, Y.; Seki, K., Examination of Band Bending at Buckminsterfullerene (C-60)/Metal Interfaces by the Kelvin Probe Method. *J. Appl. Phys.* **2002,** *92* (7), 3784-3793.
96. Hoffmann, M. W. G.; Prades, J. D.; Mayrhofer, L.; Hernandez-Ramirez, F.; Jarvi, T. T.; Moseler, M.; Waag, A.; Shen, H., Highly Selective Sam-Nanowire Hybrid NO2 Sensor: Insight into

Charge Transfer Dynamics and Alignment of Frontier Molecular Orbitals. *Adv. Funct. Mater.* **2014,** *24* (5), 595-602.
97. Li, H.; Paramonov, P.; Bredas, J. L., Theoretical Study of the Surface Modification of Indium Tin Oxide with Trifluorophenyl Phosphonic Acid Molecules: Impact of Coverage Density and Binding Geometry. *J. Mater. Chem.* **2010,** *20* (13), 2630-2637.
98. Schulmeyer, T.; Paniagua, S. A.; Veneman, P. A.; Jones, S. C.; Hotchkiss, P. J.; Mudalige, A.; Pemberton, J. E.; Marder, S. R.; Armstrong, N. R., Modification of Batio3 Thin Films: Adjustment of the Effective Surface Work Function. *J. Mater. Chem.* **2007,** *17* (43), 4563-4570.
99. Frantz, R.; Durand, J. O.; Lanneau, G. F.; Jumas, J. C.; Olivier-Fourcade, J.; Cretin, M.; Persin, M., Studies of Phosphonic Acids Containing a Pi-Conjugated Ferrocenyl Unit Grafted on Metal Oxides - Mossbauer and Electrochemical Behaviour. *Eur. J. Inorg. Chem.* **2002,** (5), 1088-1093.
100. Adolphi, B.; Jahne, E.; Busch, G.; Cai, X. D., Characterization of the Adsorption of Omega-(Thiophene-3-Yl Alkyl) Phosphonic Acid on Metal Oxides with Ar-XPS. *Anal. Bioanal. Chem.* **2004,** *379* (4), 646-652.
101. Viornery, C.; Chevolot, Y.; Leonard, D.; Aronsson, B. O.; Pechy, P.; Mathieu, H. J.; Descouts, P.; Gratzel, M., Surface Modification of Titanium with Phosphonic Acid to Improve Bone Bonding: Characterization by XPS and ToF-SIMS. *Langmuir* **2002,** *18* (7), 2582-2589.
102. Davies, P. R.; Newton, N. G., The Chemisorption of Organophosphorus Compounds at an Al(111) Surface. *Appl. Surf. Sci.* **2001,** *181* (3-4), 296-306.
103. Vanattekum, P.; Trooster, J. M., Bulk-Plasmon-Loss and Surface-Plasmon-Loss Intensities in Photoelectron, Auger, and Electron-Energy-Loss Spectra of Mg Metal. *Phys. Rev. B* **1979,** *20* (6), 2335-2340.
104. Gawalt, E. S.; Lu, G.; Bernasek, S. L.; Schwartz, J., Enhanced Bonding of Alkanephosphonic Acids to Oxidized Titanium Using Surface-Bound Alkoxyzirconium Complex Interfaces. *Langmuir* **1999,** *15* (26), 8929-8933.
105. Shuttleworth, D., Preparation of Metal-Polymer Dispersions by Plasma Techniques - an ESCA Investigation. *J. Phys. Chem.* **1980,** *84* (12), 1629-1634.
106. Gazoni, R. M., *Unpublished work* **2018**.
107. Sharma, A.; Kippelen, B.; Hotchkiss, P. J.; Marder, S. R., Stabilization of the Work Function of Indium Tin Oxide Using Organic Surface Modifiers in Organic Light-Emitting Diodes. *Appl. Phys. Lett.* **2008,** *93* (16), 3.
108. Patrone, L.; Gadenne, V.; Desbief, S., Single and Binary Self-Assembled Mono Layers of Phenyl- and Pentafluorophenyl-Based Silane Species, and Their Phase Separation with Octadecyltrichlorosilane. *Langmuir* **2010,** *26* (22), 17111-17118.
109. Stambouli, V.; Labeau, M.; Matko, I.; Chenevier, B.; Renault, O.; Guiducci, C.; Chaudouet, P.; Roussel, H.; Nibkin, D.; Dupuis, E., Development and Functionalisation of Sb Doped SnO2 Thin Films for DNA Biochip Applications. *Sens. Actuator B-Chem.* **2006,** *113* (2), 1025-1033.
110. Niegelhell, K.; Leimgruber, S.; Griesser, T.; Brandl, C.; Chernev, B.; Schennach, R.; Trimmel, G.; Spirk, S., Adsorption Studies of Organophosphonic Acids on Differently Activated Gold Surfaces. *Langmuir* **2016,** *32* (6), 1550-1559.
111. Nie, H. Y.; McIntyre, N. S.; Lau, W. M.; Feng, J. M., Optical Properties of an Octadecylphosphonic Acid Self-Assembled Monolayer on a Silicon Wafer. *Thin Solid Films* **2008,** *517* (2), 814-818.
112. Quinones, R.; Shoup, D.; Behnke, G.; Peck, C.; Agarwal, S.; Gupta, R. K.; Fagan, J. W.; Mueller, K. T.; Iuliucci, R. J.; Wang, Q., Study of Perfluorophosphonic Acid Surface Modifications on Zinc Oxide Nanoparticles. *Materials* **2017,** *10* (12), 16.
113. Hoste, S.; Vandevondel, D. F.; Vanderkelen, G. P., XPS Spectra of Organometallic Phenyl Compounds of P, as, Sb and Bi. *J. Electron. Spectrosc. Relat. Phenom.* **1979,** *17* (3), 191-195.
114. Textor, M.; Ruiz, L.; Hofer, R.; Rossi, A.; Feldman, K.; Hahner, G.; Spencer, N. D., Structural Chemistry of Self-Assembled Monolayers of Octadecylphosphoric Acid on Tantalum Oxide Surfaces. *Langmuir* **2000,** *16* (7), 3257-3271.

115. Wang, K. L.; Ross, P. N., XPS and UPS Characterization of the Reactions of Al(111) with Tetrahydrofuran and Propylene Carbonate. *Surf. Sci.* **1996,** *365* (3), 753-768.
116. Ota, H.; Sakata, Y.; Wang, X. M.; Sasahara, J.; Yasukawa, E., Characterization of Lithium Electrode in Lithium Imides/Ethylene Carbonate and Cyclic Ether Electrolytes - Li. Surface Chemistry. *J. Electrochem. Soc.* **2004,** *151* (3), A437-A446.
117. Lock, E. H.; Petrovykh, D. Y.; Mack, P.; Carney, T.; White, R. G.; Walton, S. G.; Fernsler, R. F., Surface Composition, Chemistry, and Structure of Polystyrene Modified by Electron-Beam-Generated Plasma. *Langmuir* **2010,** *26* (11), 8857-8868.